Multi-TASTE

TECHNICAL ASSISTANCE TO MULTI-MISSION VALIDATION BY SOUNDERS, SPECTROMETERS AND RADIOMETERS

ANNUAL REPORT #2

OCTOBER 2009 – OCTOBER 2010

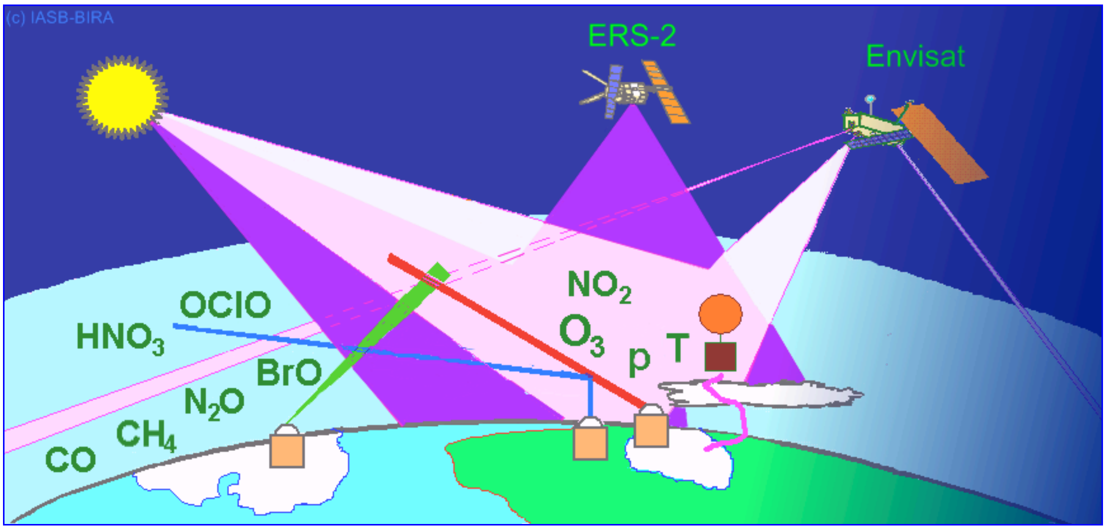

reference / *référence*	TN-IASB-TASTE2-AR2
issue / *édition*	1
revision / *révision*	0
date of issue / *date d'édition*	16 December 2010
status / *état*	final
document type / *type de document*	Project Report

aeronomie.be

NIWA
Taihoro Nukurangi

Université de Liège

UNIVERSITÄT BREMEN

iup

INTA

[this page intentionally left blank]

title / *titre*	Multi-TASTE Annual Report #2 / October 2009 – October 2010
reference / *référence*	TN-IASB-TASTE2-AR2
date of issue / *date d'édition*	16 December 2010
issue / *édition*	1
revision / *révision*	0
status / *état*	final
document type / *type de document*	Project Report
ESA contract Nr / *contrat ESA No*	21819/08/I-OL

prepared by / *préparé par* — D. Hubert and J.-C. Lambert

contributeurs / *contributors* — O. Aulamo, A. Bazureau, T. Blumenstock, J. P. Burrows, M. De Mazière, P. Demoulin, I. De Smedt, B. Dils, C. Fayt, S. Godin-Beekmann, J. Granville, M. Gil, F. Goutail, F. Hase, F. Hendrick, C. Hermans, D. Hubert, P. V. Johnston, R. Kivi, G. Kopp, K. Kreher, E. Kyrö, J.-C. Lambert, E. Mahieu, M. Marchand, S. Mikuteit, M. Navarro Comas, J. Notholt, A. Pazmiño, D. Pieroux, G. Pinardi, J-P. Pommereau, O. Puentedura, A. Richter, A. Thomas, S. Vandenbussche, M. Van Roozendael, T. Warneke, F. Wittrock, S. Wood, and M. Yela Gonzalez

external contributors / *contributeurs externes* — H. Claude, H. De Backer, V. Dorokhov, P. Eriksen, G. Held, T. Leblanc, I. S. McDermid, S. Oltmans, T. Portafaix, H. K. Roscoe, J. D. Shanklin, J. Stähelin, K. Stebel, W. Steinbrecht, R. Stubi, and G. Vaughan

NDACC teams contributing ground-based correlative measurements

Acronym	***Organisation***	***Country***
BAS-NERC	British Antarctic Survey – National Environment Research Council	United Kingdom
BIRA-IASB	Belgian Institute for Space Aeronomy	Belgium
CAO	Central Aerological Observatory	Russia
CNRS/LATMOS	CNRS, Laboratoire Atmosphères, Milieux, Observations Spatiales	France
DMI	Danish Meteorological Institute	Denmark
DWD	Deutsche Wetterdienst – Hohenpeissenberg	Germany
FMI-ARC	Finnish Meteorological Institute – Arctic Research Centre	Finland
IFE/IUP	Institut für Umweltphysik/Fernerkundung, University of Bremen	Germany
IMK/FZK	FZK/Institut für Meteorologie und Klimaforschung, U. Karlsruhe	Germany
INTA	Instituto Nacional de Técnica Aeroespacial	Spain
IPMet/UNESP	Instituto de Pesquisas Meteorológicas, Universidade Estadual Paulista	Brazil
JPL	Jet Propulsion Laboratory/California Institute of Technology	USA
KMI-IRM	Royal Meteorological Institute of Belgium	Belgium
KSNU	Geophysical Laboratory, Kyrgyz State National University	Kyrgyzstan
MeteoSwiss	MeteoSwiss, Aerological Station of Payerne	Switzerland
NILU	Norwegian Institute for Air Research	Norway
NIWA	National Institute of Water and Atmospheric Research	New Zealand
NOAA/ESRL	NOAA Earth System Research Laboratory	USA
U. Manchester	University of Manchester and University of Wales	United Kingdom
U. Réunion/LACY	Université de la Réunion	France

document change record / *historique du document*

Issue	***Rev.***	***Date***	***Section***	***Description of Change***
0		30/08/2010	all	Creation of this document
1		26/11/2010		Draft for review
1		10/12/2010		Final version

[this page intentionally left blank]

CONTENTS

[this page intentionally left blank]

I INTRODUCTION

Multi-TASTE provides ESA with Multi-mission Technical Assistance To Envisat and TPM validation by sounders, spectrometers and radiometers. It supports long-term validation activities of ESA in the evolving context of the GEOSS and GMES implementation. The scope of the former TASTE project (2004-2008), focusing on stratospheric species measured by Envisat, has broadened in Multi-TASTE to consider also multi-mission validation, as well as new validation needs for tropospheric and climate measurements. It paves the way to multi-mission validation tasks of ESA Climate Change Initiative projects (CCI) and gives QA grounds for future Sentinel missions.

Validation support is given by an international consortium gathering complementary expertise in remote sensing and satellite validation, all involved in the Network for the Detection of Atmospheric Composition Change (NDACC), namely: BIRA-IASB (Uccle, Belgium), CNRS/LATMOS (Verrières-le-Buisson/Paris, France), FMI-ARC (Sodankylä, Finland), IFE/IUP (Bremen, Germany), FZK/IMK (Karlsruhe, Germany), INTA (Torrejón de Ardoz, Spain), NIWA (Lauder, New Zealand), and ULg (Liège, Belgium), and their collaborators. Main tasks relate to: (a) the collection of ground-based correlative observations acquired by NDACC-certified instruments, the monitoring and verification of those data sets, and their delivery to the Envisat Cal/Val Data Centre (EVDC) operated at NILU on behalf of ESA; (b) geophysical validation studies of atmospheric composition (level-2) data products from Envisat and Third Party Missions based on comparisons with correlative data sets; (c) support to ESA for the development of validation strategies, among others in the GEO-CEOS context; and (d) the valorisation of the validation results and of the expertise through the Envisat Quality Working Groups (QWGs) and more open scientific events.

The present document reports on activities carried out during the second term of the Multi-TASTE project (ESA contract No.21819/08/I-OL), from October 2009 to October 2010. **Section II** reviews the acquisition and collection of correlative data records relevant to Envisat and TPM validation. Monthly data statistics on data delivered to the Envisat Validation Data Centre (EVDC) in the framework of Multi-TASTE are given in **Annexe 2** (or **Section V**), from 2006 to 2010. **Section III** gives an overview of the validation work performed during the reporting period, to which members of the consortium have contributed. It summarises the quality status of latest Envisat data versions and it includes delta validation results of major processor upgrades for MIPAS and SCIAMACHY, progress with multi-mission validation of ozone sounders, and support to algorithm development activities performed within the Envisat QWGs. **Annexe 1** (or **Section IV**) lists relevant meetings, peer-reviewed publications and conference proceedings, which constitute tangible deliverables of the project, as well as other relevant presentations. At last, the content of the correlative database contributed by the project is described in **Annexe 2** (hereafter **Section V**).

II CORRELATIVE MEASUREMENTS

II.1 Overview

The following correlative measurements have been collected from NDACC stations and delivered by project partners to the Envisat Validation Data Centre operated at NILU on behalf of ESA:

- O_3 vertical column data measured by Differential Optical Absorption (DOAS/SAOZ) visible spectrometers (hereafter VIS), by Dobson and Brewer ultraviolet spectrophotometers, and by Fourier Transform infrared spectrometers (FTIR);
- O_3 vertical profile data measured by balloon-borne electrochemical ozonesondes (O_3S) and by millimetre wave radiometers (MWR);
- NO_2 vertical column data measured by DOAS/SAOZ visible spectrometers;
- BrO and OClO column data measured by DOAS ultraviolet spectrometers;
- NO_2, BrO and HCHO tropospheric data measured by MAX-DOAS instruments;
- O_3, NO_2, CO, CH_4, HNO_3 and N_2O column data measured by FTIR spectrometers;
- O_3, CO, CH_4, HNO_3 and N_2O vertical profile data measured by FTIR spectrometers.

Beyond original plans, the following correlative measurements have been collected and delivered as well:

- H_2O, HCHO and ClO column data measured by FTIR spectrometers;
- HCl, HCHO and NO_2 vertical (profile) by FTIR spectrometers;
- H_2O profile data measured by MW radiometers;
- pressure and temperature profile data measured by the PTU radiosondes to which electrochemical ozonesondes are coupled.

Correlative measurements have been collected at the geographical locations identified in Figure 1 and listed in Annexe 2 (Section V). They address major atmospheric regimes in the polar and middle latitudes of both hemispheres and in the tropics.

In addition to the correlative measurements freshly acquired in the timeframe of the project, Multi-TASTE, as an extension of TASTE, collects updated and upgraded data since the beginning of the Envisat mission to bridge the gap between the Commissioning Phase validation of Envisat (2002-2003) and the main and long-term validation of Envisat (from 2004 onwards). The project relies on quality standards and data formats in application within the NDACC, for which all contributing instruments are certified. It is fortunate that, while the NDACC remains committed to its original goal, that is, monitoring changes in the stratosphere with an emphasis on the long-term evolution of the ozone layer, its priorities have broadened considerably to encompass issues such as the detection of trends in overall atmospheric composition and understanding their impacts on the stratosphere and troposphere, and establishing links between climate change and atmospheric composition. Multi-TASTE benefits from new NDACC capabilities and expertise as they develop in the time frame of the project. A clear illustration of this benefit is the availability at EVDC of correlative data not foreseen in the original Multi-TASTE proposal.

Collected data records for which suitable variables and metadata exist, have been converted into the agreed HDF 4.1.3 data format and uploaded to EVDC. Collected data sets for which suitable variables and metadata do not exist have been collected by the groups, distributed to interested Envisat partners in other formats, and used for Envisat validation, although not submitted to the Envisat Cal/Val database. A few ground-based data products still in development at the beginning of the project, like NO_2 and BrO profiles from UVVIS measurements, have now been consolidated at pilot stations and used for Envisat validation.

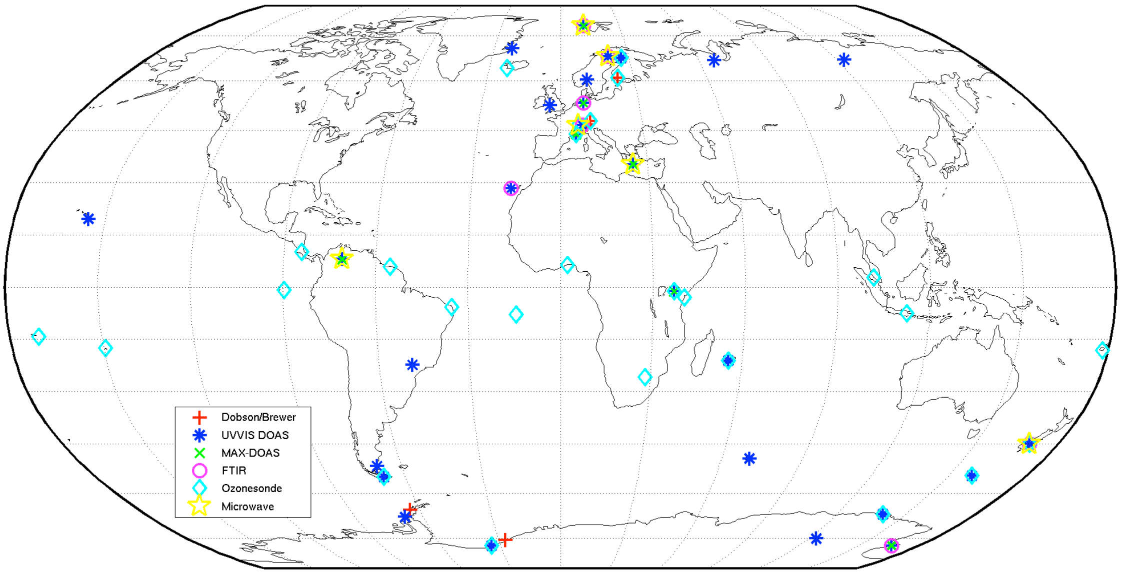

Figure 1: Ground-based instrumentation contributing to Multi-TASTE validation studies in 2008-2010: Dobson and Brewer UV spectrophotometers operating at selected NDACC stations, NDACC-certified DOAS UV-visible spectrometers, MAX-DOAS UV-visible spectrometers, balloon-borne ozonesondes (including the SHADOZ contributing network), NDACC FTIR spectrometers, and NDACC millimetre wave radiometers.

Upload Status Tables in Annexe 2 (Section V) display, year after year, an estimate of the number of measurement days a month that have been uploaded to EVDC. Nearly all instruments worked nominally and for a majority of them correlative data acquired directly by members of the consortium were uploaded within a few months after data acquisition. Uploads of data acquired partly by third parties, sometimes on a best effort basis, or acquired at very remote locations, are sometimes experiencing larger delays, but it must be pointed out that most of those delayed data sets had already made available to Envisat validation through other means. Details by partner and station are given hereafter in the following section.

II.2 Status of data acquisition and uploads

II.2.1 BIRA-IASB

Vertical column measurements of ozone, NO_2 and BrO, and slant column measurements of OClO acquired by the DOAS UV-visible spectrometer operated by IASB-BIRA at Harestua, Norway, as well as ozone and NO_2 vertical column data measured at the Jungfraujoch with the SAOZ spectrometer, have been converted to monthly HDF files and the data transferred every month on the Cal/Val database until August 2010.

The Bruker 120M FTIR instrument at Saint-Denis, Reunion Island, has been operated on a campaign basis from August to October 2004 and from May to end of October 2007. It is now operating quasi-continuously since end of May 2009. A serious instrument failure occurred from March 8th to April 21st 2010. A Bruker 125HR FTIR instrument is being prepared for installation at Reunion Island in September 2010, to be fully operational by summer 2011 at latest.

The FTIR data for Saint-Denis have been made available in HDF AVDC/NDACC format via the NDACC database for CH_4 (2004 and 2007), CO (2004 and 2007), N_2O (2004 and 2007) and HCl (2004, 2007 and 2009); and via the local database at BIRA-IASB for HNO_3 (2007). The data could not be uploaded to the Cal/Val database due to the unfortunate incompatibility of the AVDC/NDACC and NILU's HDF formats.

II.2.2 CNRS/LATMOS

During the second year of Multi-TASTE, the CNRS team has performed all measurements indicated in WP3100-a. The real time SAOZ columns (O_3 and NO_2) have been converted to monthly HDF files and the data transferred every month on the Cal/Val database until August 2010.

Since August 2009, 30 ozonesondes have been launched at Dumont d'Urville, and 52 from Observatoire de Haute-Provence. The PTU sonde of the ozonesondes has changed from Vaisala to Model sondes for both stations, respectively since 2007 and 2008. As the format is not the same, the conversion software has been rewritten and the data can now be directly archived in NASA Ames format. CNRS is trying to organise an automatic conversion of NASA Ames format to HDF but due to lack of manpower, it is not done yet. The OHP profiles until August 2009 are on the NDACC data base (in ASCII). The Dumont d'Urville profiles until July 2010 are ready to be transferred to the NDACC data base (in ASCII).

The CNRS team has started a systematic comparison of ozone and NO_2 long term series with various satellites, TOMS Nimbus, Meteor, EP TOMS, GOME, SCIAMACHY, OMI-TOMS, OMI-DOAS and GOME-2. As during the previous winters since 2005, a mobile SAOZ has been installed at Eureka/Canada for the winter 2010 ACE validation campaign.

II.2.3 FMI-ARC

Brewer observations have been continuous (sun elevation permitting) and soundings have been made on regular basis in Sodankylä (Arctic Finland) and Marambio (Antarctic Peninsula) and during winter campaigns in Jokioinen. Data have been acquired, collected, converted into HDF 4.1.3 format and uploaded to the Envisat Cal/Val database.

Preliminary comparisons between ground-based and satellite data have been carried out to determine systematic and random differences. A Brewer Intercomparison Campaign will take place in Sodankylä in spring 2011. A large number of ozonesondes was flown in January-March 2010 during the LAPBIAT Atmospheric Sounding Campaign in Sodankylä. These additional sondes were also made available for Cal/Val purposes.

The new FTIR system has been operated on regular basis in Sodankylä; it is based on Bruker IFS 125 HR with A547N Solar Tracker. Our FTIR participated in GOSAT validation activities since May 2009. A limited data set of comparisons has been collected since then.

Data from the reference water vapour hygrometer was used in the validation of retrieval of water vapour vertical distributions in the upper troposphere and the lower stratosphere from SCIAMACHY limb measurements [Rozanov et al., 2010].

II.2.4 IFE

FTIR and microwave measurements at Ny-Ålesund (Spitsbergen) and Bremen (Germany)

The Multi-TASTE funding was essential to continue with the FTIR and microwave observations planned in WP 3100-d. At Ny-Ålesund ozone profiles have been continuously measured with the microwave instrument since 2008, except for short maintenance breaks. For Ny-Ålesund and Bremen respectively 27 and 36 FTIR measurement days have been added to the database. The submission of the HDF data is planned by the end of the year. This depends, however, on the finalisation of the latest asc2hdf package.

UV/VIS DOAS measurements at Ny-Ålesund, Bremen, Mérida, Heraklion and Nairobi

Over the period summer 2009 to summer 2010, ground-based MAX-DOAS measurements were performed by IUP Bremen at the stations of Ny-Ålesund, Bremen, Nairobi and Heraklion. In addition, the Bremen campaign instrument participated in two campaigns, the Cabauw Intercomparison Campaign of Nitrogen Dioxide measuring Instruments (CINDI) in the Netherlands and the TRANSBROM campaign between Japan and Australia. The Mérida station has not provided measurements for technical and logistical reasons.

The instrument in Mérida had to be removed in June 2010 from the measurement location as access via the cable car is no longer deemed to be safe and will therefore not be possible for at least two years until the cable car has been refurbished. The instrument has been brought to Bremen for testing and upgrading and will be located to another measurement site as soon as an appropriate arrangement could be made. The data set available (until March 2008) has been uploaded to the data base (total columns of NO_2 and ozone).

The instrument in Nairobi has been offline for most of the time (about 50 measurement days in 2009 and 2010) as result of lack of local support and problems with stability of electrical power supply. Another problem was the quite often very slow internet connection to Kenya which prevents simple checks of the data acquisition software. It is currently being investigated whether the instrument can be relocated to another location in Nairobi or elsewhere in Africa, the latter solution is preferred. In any case it will have to be brought back to Bremen for repair and upgrading before it can be brought back into the BREDOM network.

In Heraklion (Iraklion), frequent interruptions of power supply and internet connections have led to substantial data gaps, in particular in 2010. In addition the visible channel was most probably damaged during a thunderstorm event in August 2009. In total we were able to perform measurements on 240 days in the UV and on 130 days in the visible wavelength range since beginning of 2009. It is currently planned to move the instrument from Heraklion to Athens where maintenance and access will be simpler. The existing data from the instrument could not yet be uploaded to the Cal/Val database as there is not yet an entry for this measurement location. We have contacted the responsible people at NILU to solve this problem as soon as possible.

Stratospheric columns of NO_2 and O_3 have been submitted whenever possible to the NILU database for all locations. For Ny-Ålesund the whole ozone and NO_2 time series since 2003 has been reanalyzed following the new NDACC recommendations and even more important using one single Fraunhofer spectrum as background for each year. This has led to a much more consistent data set (see e.g.

Figure 2). Stratospheric BrO and OClO columns have been analyzed but are not yet in the Cal/Val database. For Ny-Ålesund and Nairobi these data are available as part of the EU project GEOMON (ftp://ftp.nilu.no/pub/GEOmon/activity4_StratosphericOzone). In Bremen, the quality of the BrO column is affected by strong tropospheric NO_2 pollution which has a spectral interference with the BrO retrieval.

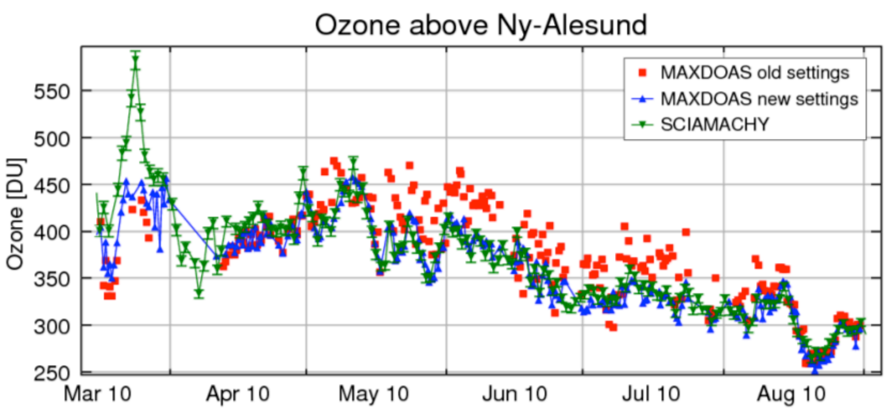

Figure 2: Comparison of MAX-DOAS ozone data with SCIAMACHY time series in 2010. With the new data set (available for all years since 2003) a much better agreement with satellite overpass data is obtained.

Tropospheric columns and profiles of NO_2 and HCHO have been derived for the measurements in Bremen, Nairobi and Heraklion, but due to formatting issues are not yet on the Cal/Val database (see next paragraph). But again they are available using the link to public ftp server as part from the GEOMON project.

Table 1: Overview on the data acquisition at the IUP Bremen stations. Red colour indicates no measurements, green colour data already submitted to the Cal/Val data base, orange data that have been taken and analyzed but are not yet on the database, blue are available from the GEOMON ftp server.

Station	Lat.	Instrument	Species	C/P	Institute
Ny-Ålesund	79°N	MAX-DOAS MAX-DOAS	O3, NO2,BrO, OClO (NO_2, BrO)	C TC	IFE / AWI
Bremen	53°N	MAX-DOAS MAX-DOAS	O3, NO2,BrO,(OClO) NO_2, HCHO	C Trop. C	IFE
Heraklion	35°N	MAX-DOAS MAX-DOAS	O3, NO2,BrO NO2, HCHO	C Trop. C	IFE
Mérida	8°N	MAX-DOAS MAX-DOAS	O_3, NO_2, BrO (HCHO, NO2)	C Trop. C	IFE
Nairobi	1°S	MAX-DOAS MAX-DOAS	O3, NO2, BrO NO2, HCHO	C Trop. C	IFE

As part of the European project GEOMON we agreed on a common HDF data format for future uploads of enhanced MAX-DOAS data products (e.g. trace gas profiles, tropospheric columns). To avoid double work in the future we defined our HDF-files according to the current NASA-AVDC (and NDACC) standard. NILU currently does not support this standard with their ESA-CDB (which includes the Envisat Cal/Val database) system. So, as long as NILU is not supporting this version, we decided to put the data to the GEOMON ftp-server. This has already been done for some of the data (see above). For the rest it will be done in time (October 2010).

ENVISAT validation activities since summer 2009 include the comparison of operational and scientific retrievals of OClO, SO_2, NO_2, H_2O columns from measurements of the SCIAMACHY instrument; the validation of SCIAMACHY OClO retrievals with ground-based MAX-DOAS observations in Ny-Ålesund, Summit, and Bremen [Oetjen et al., 2009]; the validation of SCIAMACHY tropospheric NO_2-columns using the ground-based MAX-DOAS measurements collected during the DANDELIONS and CINDI campaigns and the validation of SCIAMACHY O_3, NO_2, and BrO retrievals using the ship-borne MAX-DOAS measurements taken during the TRANSBROM cruise. Contributions to the delta validation of the SCIAMACHY processor upgrade SGP 5.01 include the detailed verification of nearly all SCIAMACHY products using scientific retrievals developed by the IUP Bremen and the submission of ground-based observations for the pole-to-pole validation of O_3 and NO_2 columns

II.2.5 IMK

Measurements at Kiruna (Sweden) and Izaña (Tenerife Island) have been performed as planned in WP 3100-e. In 2009 Kiruna measurements have been performed on 42 days of observation. In 2009 Izaña measurements have been performed on 101 days of observation. The Kiruna instrument had a failure of the scanner motor in May 2009. Although the scanner motor was replaced by a new one as soon as possible some days of observation have been missed.

Data recorded until middle of 2009 are in the Cal/Val database. Data of all FTIR species listed in WP 3100-e (O_3, N_2O, CO, CH_4, NO_2, HNO_3) are uploaded in the NDACC database. The new data analysis harmonisation approach as well as format harmonization (HDF format) within NDACC has been applied for the entire data set from the beginning of the measurement up to the end of 2009. These data files are freely available.

Kiruna data have been used to compare with HDO/H2O data from SCIAMACHY [Frankenberg et al., 2009]. MIPAS and ACE validation papers have been published in 2009 [Payan et al., 2009; Dupuy et al., 2009].

II.2.6 INTA

For UV-Visible measurements at Izaña, measurements of NO_2 and O_3 are going on as planned in WP 3100-f. Quality controlled data have been submitted in HDF format at Cal/Val database until July 2010. We detected degradation in the instrument from middle 2006. Data have been corrected and a new version has been uploaded to the database. On February 2010 the instrument has been replaced by a new one, after a few months working together for inter-comparison purposes. The new instrument (RASAS-II) participated in the CINDI campaign in June-July 2009. Noise in the BrO detector increased during 2009. Replacement of the instrument is planned by the end of 2010. Measurements of BrO are ongoing, but not yet analyzed.

At Marambio, measurements of NO_2 are going on as planned. Quality controlled data have been submitted in HDF format to the Cal/Val database until July 2010. In February 2010, the instrument was changed to a new housing. The sealed insulator used in the new container caused some problems with water filtrations and ice inside the instrument until beginning of March, when it was carefully sealed by a new insulator. Due to this change of emplacement of the instrument, as well as its repairs and cleanliness, it has been necessary to change reference to the analysis of the data in two occasions.

At Belgrano, measurements of NO_2 are going on as planned. Quality controlled data have been submitted in HDF format at Cal/Val database until April 2010. Measurements from August will be analyzed after the Antarctic spring, and then a new reference spectrum will be chosen for the DOAS retrieval.

At Ushuaia, measurements of NO_2 are going on as planned. Quality controlled data have been submitted in HDF format at Cal/Val database until July 2010.

For ozone soundings, at Belgrano, Keflavik and Ushuaia, measurements of vertical ozone profiles are going on as planned. Quality controlled data have been submitted in HDF format at Cal/Val database until July 2010 for these stations.

II.2.7 NIWA

The overall status of the NIWA measurements is good and we have not experienced any serious problems with instrumentation, logistics or manpower since the previous annual report.

The only exception are the UV-visible measurements made at Kiruna, Sweden, which stopped in March 2010 due to instrument failure. This DOAS instrument has been working fine until the end of February 2010. The measurements stopped early March 2010 because of computer failure. Additionally, the spectrometer had already previously shown some signs of fatigue and we are currently negotiating the replacement or withdrawal of the instrument. The UV-visible measurements made at Mauna Loa, Hawaii, were processed routinely until 29 February 2008 (the data has also been submitted to the database until then) when the instrument failed and was found to be un-repairable. A new array detector spectrometer to measure both NO_2 and BrO (330 – 450 nm region measurements) simultaneously was installed on 28 April 2009 and has been operating since. The data processing is currently still under investigation and data submission to the Cal/Val database is expected to commence soon again. Total UV-visible DOAS column data have been submitted up to the end of July 2010 for the following stations: Lauder, Macquarie Island and Arrival Heights.

As part of our contribution to Multi-TASTE, we have further developed our capability to retrieve profile information from MAX-DOAS measurements. This retrieval technique includes a forward model (full spherical Monte Carlo radiative transfer model called NIMO (NIWA Monte Carlo)) describing the relation between DSCDs and the to-be-retrieved trace gas concentration profile and an optimal estimation routine allowing us to choose the most likely possible set of profiles consistent with the measured DSCDs. The retrieval has been tested using MAX-DOAS measurements of NO_2 from the CINDI campaign in Cabauw and the retrieved profiles for the lower troposphere and boundary layer are comparable to the profiles retrieved by other participating groups. The retrieval has also been performed on measurements of BrO from Antarctica and enhanced boundary layer BrO concentrations were retrieved on days when BrO was observed in the DSCDs. Two publications will be submitted shortly to ensure that the retrieval technique can be referenced with a peer-reviewed publication before the results are submitted to the Cal/Val database.

For FTIR measurements (O_3, N_2O, CH_4, HNO_3, CO and HCl) in New Zealand and in Antarctica, data have been submitted to the Cal/Val database as planned and the data sets are all up to date, July 2010 inclusive. Partial stratospheric and tropospheric columns are submitted for CH_4 and NO_2. The HDF profile format for NDACC submissions has been developed and if it can be confirmed that the Cal/Val format is preferably the same or very similar then submission of profiles can be started. The data will be prepared according to the recommendations and guidelines within the FTIR working group and submitted as soon as these discussions have been completed.

The ozonesonde data for Lauder has been updated until the end of August 2010. There are still approximately 12 flights during the last 12 months that need to be processed and submitted; this will be done before the end of 2010.

The Lauder and Arrival Heights Dobson have also been updated until the end of July 2010.

Section II.4 describes the work carried out by NIWA on "Techniques for analysing ground-based UV-visible long-term BrO and NO_2 observations for satellite validation and trend analysis", presented at the COSPAR 2010 meeting.

II.2.8 ULg

The FTIR instruments at Jungfraujoch have been working nominally during the reporting period. All available FTIR profile data (after QA/QC checks) for January 2002 until April 2010 inclusive are catalogued, for CH_4, CO, HNO_3 and N_2O. Data archiving is ongoing nominally, the temporary HDF FTIR template is satisfactory. However, harmonization with the NDACC template is eagerly awaited.

Since summer 2009, CO FTIR profile data from the Jungfraujoch have been included in a validation study of five years of SCIAMACHY measurements (IMLM) [de Laat et al., 2010]. Also, CH4 data products have been included in comparisons with model and SCIAMACHY products [Dils et al, 2010].

II.3 Quality assurance of correlative data

A large part of the contributing instruments are part of the NDACC, a major contributor to WMO's Global Atmosphere Watch programme (GAW). The NDACC Data Protocol is structured to ensure excellent data quality while providing ready data access. It recognises that, in order to produce a verifiable data product, sufficient time is needed to collect, reduce, calibrate, test, analyse, and inter-compare the streams of preliminary analyses at every NDACC site. Among others, seasonal analyses may be required for observations from both individual and multiple sites and it is expected that such a procedure shall yield the verifiable product referred to as "NDACC data" within a two-year period after acquisition. The faster data availability required by Multi-TASTE validation activities implies that limited time only is available to recalibration, state-of-the-art processing or simply quality verification. Therefore we have developed and implemented verification procedures to check first-order quality/consistency of the fresh fast-delivery data collected in the frame of the project.

The quite large number of contributing instruments and stations implies the use of automated routines flagging non-standard events, which can be looked at more carefully once detected. The first step consists in scanning the data files in order to identify clearly aberrant data, e.g. negative species concentration values, impossible sunlight measurements during polar night, or sunrise NO_2 columns exceeding systematically sunset NO_2 columns. At ground stations where long enough time-series are available in the NDACC data archive and/or the WOUDC (for ozone data), the second step of the verification procedure consists in comparing fresh data to climatological means and standard deviations that we calculate on low-pass filtered time-series starting, if possible, in 1995. Column values deviating from the climatological mean by more than 2σ and 3σ are pointed out. Trains of consecutive values falling out of the $\pm 3\sigma$ interval are looked at carefully to determine whether such persistent deviations may be due to data quality issues, to natural atmospheric variability, or to unexpected atmospheric features like the 2002 Antarctic vortex split. Single values falling out of the ±3σ interval without belonging to a justifiable 2σ train are flagged accordingly but not rejected systematically since they could be associated e.g. to real events of extreme variability or to tropospheric pollution episodes enhanced by multiple scattering within clouds. For newer stations with shorter time-series, consistency checks are based on data already stored at NILU Cal/Val, acquired by other instruments at nearly collocated stations, or even by the same instrument. Results are reported in a log file. The climatological verification method is illustrated in the *TASTE Progress Report January-October 2004* issued in November 2004, available on the ESA website.

II.4 Techniques for analysing ground-based UV-visible long-term BrO and NO_2 observations for satellite validation and trend analysis

At the COSPAR Assembly 2010 NIWA presented examples of UV-visible DOAS data sets analysed using several different techniques. The resulting data sets are employed for satellite validation and trend analysis.

Zenith sky DOAS measurements
The observed DOAS slant columns are converted into total vertical columns using either air mass factors or a profile retrieval method. The latter is more sophisticated and can be used to obtain both profile information and partial and total vertical columns, e.g. [Schofield et al., 2004a; Schofield et al., 2004b; Hendrick et al., 2007; Hendrick et al., 2009]. Figures 3-4 show examples where measurements made at Lauder (45°S), New Zealand have been used for a comparison with satellite data [Hendrick et al., 2009; Salawitch et al., 2010].

Combination of zenith sky and direct sun measurements
The combination can also be used in a retrieval algorithm [Schofield et al., 2004a] to gain profile information. In this case the zenith sky observations provide predominantly the information on the stratospheric partial column and the direct sun observations on the tropospheric contribution. This has been discussed previously for observations made at Lauder and Arrival Heights, Antarctica [Schofield et al., 2004b, Schofield et al., 2006].

MAX-DOAS (Multi-Axis Differential Optical Absorption Spectroscopy) measurements
These are used for the retrieval of trace gas profiles in the lower troposphere, e.g. to measure pollution (relevant for trace gases such as NO_2) or bromine explosion events (relevant for BrO at high latitudes) in the boundary layer or lower troposphere. These time series can then be used for a comparison with satellite data directly or to remove the partial column measured by MAX-DOAS from the total column amount. Figure 5 shows an example of NO_2 profiles measured during CINDI on two *golden days* in June 2009. The profile retrieval algorithm applied here has been developed by PhD student Timothy Hay [Hay, 2010].

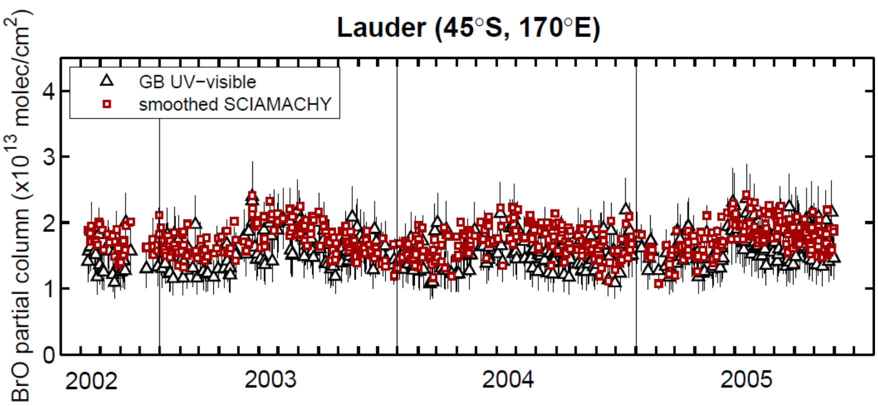

Figure 3: Comparison of the 15–27 km BrO partial columns calculated from the smoothed SCIAMACHY limb and ground-based UV-visible measurements at Lauder, New Zealand for 2002–2005 [Hendrick et al., 2009]. The mean relative difference is between both data sets is +11 ± 16%. About 10% of this offset is explained by the fact that different BrO cross sections have been used in the SCIAMACHY and ground-based UV-visible retrievals.

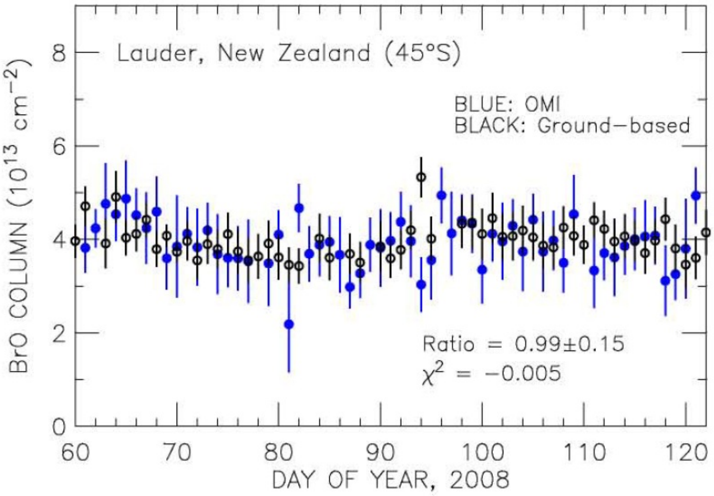

Figure 4: Comparison of BrO vertical columns measured by OMI during March and April 2008 over Lauder, New Zealand, with ground-based BrO measurements [Salawitch et al., 2010]. The total column BrO is inferred from vertical profiles retrievals [Hendrick et al., 2007]. The agreement is also very good: within 15% with no detectable bias.

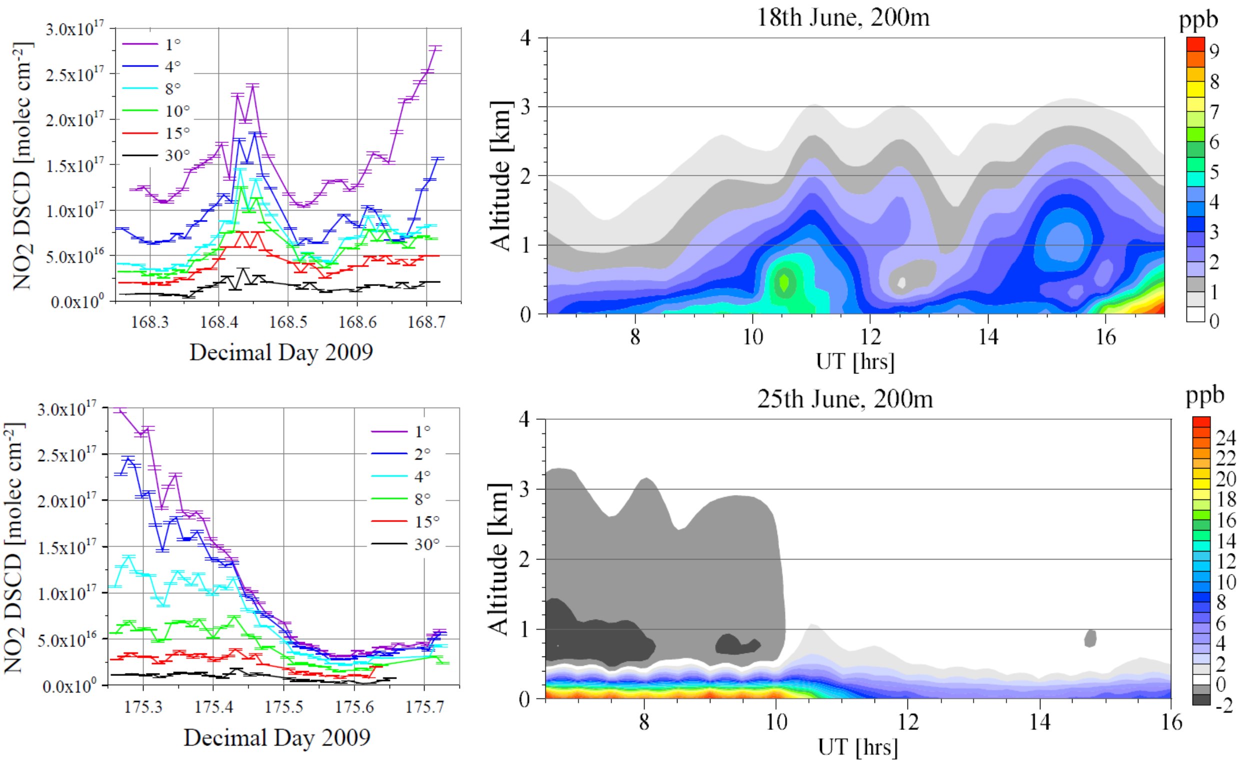

Figure 5: MAX-DOAS differential slant column densities (DSCDs) measured by the NIWA instrument and the corresponding NO2 profiles retrieved at 30 minute intervals for two days with ideal weather conditions are displayed. The contour plots show the NO2 mixing ratio profiles for the 200m layer retrievals.

The same retrieval algorithm has also been applied to MAX-DOAS observations made at Ross Island, Antarctica during a measurement campaign using a mobile Max-DOAS instrument. In general, the observations show that the retrieved BrO was concentrated within the layer from the surface to 50 m.

II.5 References

de Laat et al., 2010, full reference in Section IV.2.

Duchatelet et al., 2010, full reference in Section IV.6.

Dupuy et al., 2009, full reference in Section IV.2.

Frankenberg et al., 2009, full reference in Section IV.2.

Hay, T., MAX-DOAS measurements of bromine explosion events in McMurdo Sound, Antarctica, PhD thesis, submitted 2010.

Hendrick, F., Van Roozendael, M., Chipperfield, M. P., Dorf, M., Goutail, F., Yang, X., Fayt, C., Hermans, C., Pfeilsticker, K., Pommereau, J.-P., Pyle, J. A., Theys, N., and De Mazière, M.: Retrieval of stratospheric and tropospheric BrO profiles and columns using ground-based zenith-sky DOAS observations at Harestua, 60° N, Atmos. Chem. Phys., 7, 4869-4885, doi:10.5194/acp-7-4869-2007, 2007.

Hendrick, F., Rozanov, A., Johnston, P. V., Bovensmann, H., De Mazière, M., Fayt, C., Hermans, C., Kreher, K., Lotz, W., Sinnhuber, B.-M., Theys, N., Thomas, A., Burrows, J. P., and Van Roozendael, M.: Multi-year comparison of stratospheric BrO vertical profiles retrieved from SCIAMACHY limb and ground-based UV-visible measurements, Atmos. Meas. Tech., 2, 273-285, doi:10.5194/amt-2-273-2009, 2009.

Mahieu et al., 2010, full reference in SectionIV.5.

Lejeune et al., 2010, full reference in Section IV.6.

Li et al., 2009, full reference in Section IV.2.

Payan, et al., 2009, full reference in Section IV.2.

Rozanov et al., 2010, full reference in Section IV.2.

Salawitch et al., 2010, full reference in Section IV.2.

Schofield, R., Connor, B. J., Kreher, K., Johnston, P. V., Rodgers, C. D., The retrieval of profile and chemical information from ground-based UV-visible spectroscopic measurements, Journal of Quantitative Spectroscopy and Radiative Transfer 86 (2), 115-131, 2004a.

Schofield, R., Kreher, K., Connor, B.J., Johnston, P.V., Thomas, A., Shooter, D., Chipperfield, M.P., Rodgers, C.D. and Mount, G.H., Retrieved tropospheric and stratospheric BrO columns over Lauder, New Zealand, J. Geophys. Res., 109, doi:10.1029/2003JD004463, 2004b.

Schofield, R., Johnston, P. V., Thomas, A., Kreher, K., Connor, B. J., Wood, S., Shooter, D., Chipperfield, M. P., Richter, A., von Glasow, R., Rodgers, C. D., Tropospheric and stratospheric BrO columns over Arrival Heights, Antarctica, 2002, Journal of Geophysical Research - Atmospheres 111 (D22), 2006.

III VALIDATION ACTIVITIES

During the reporting period, the Multi-TASTE consortium was tasked to validate Envisat data products generated routinely, to support algorithm development activities carried out by the Envisat Quality Working Groups (QWG), namely by organising and carrying out the delta validation of MIPAS and SCIAMACHY processor upgrades, and to assess the quality of new SCIAMACHY level-2 data products. Envisat data products were generated both by Processing and Archiving Centres (PAC) operated at/on behalf of ESA, and by scientific institutes with their homemade retrieval software tools. Within Multi-TASTE, validation was carried out both independently by individual partners using their own methods, and by IASB-BIRA using a common method for all stations. This dual approach fostered constructive discussions and yielded a consolidated appreciation of Envisat data quality. Details of the studies fall beyond the scope of this report but they can be found in the reports and publications listed in Section IV (Annexe 1). Detailed quality assessments as well as feedback were provided to ESA and the Envisat QWGs. Where relevant, validation studies based on correlative data collected within Multi-TASTE were augmented with similar data collected from archives of the NDACC, WOUDC and SHADOZ programmes. This section gives an overview of validation work achieved during this second year of Multi-TASTE and summarises the main achievements for the latest data versions.

III.1 Envisat GOMOS

During the reporting period no improved version of GOMOS Prototype Processor v6.0cf / IPF 5.00 was made available to the validation teams. Therefore the Multi-TASTE partners took the opportunity to consolidate the previous validation results, and to start a systematic multi-validation of limb sounders reported hereafter in Section III.5.1 on Multi-Mission studies.

III.1.1 Validation of ozone profile [IPF 5.00 / Prototype 6.0cf]

Monthly statistics of the agreement between Envisat GOMOS Prototype Processor v6.0cf / IPF 5.00 ozone profile data and correlative measurements from ozonesonde stations contributing to the Multi-TASTE project are provided as an electronic annex.

The results are detailed in Section III.5.1 on Multi-Mission studies.

III.1.2 Validation of temperature profile [IPF 5.00 / Prototype 6.0cf]

Current versions of the GOMOS processor prototype, v6.0cf, and of its operational implementation, IPF 5.00, include the retrieval of High Resolution Temperature Profile (HRTP) data. Preliminary validation studies have shown that, as for the ozone profile data, only dark limb HRTP data are of suitable quality for scientific use. The occultation obliquity also impacts the validity altitude range and the accuracy of HRTP data (GOMOS Product Handbook, http://envisat.esa.int/handbooks/gomos). For vertical occultations, the validity range of HRTP profiles is 18-35 km (depending on the scintillation strength) while it is 20-30 km for oblique occultations. The lowest bias (about 1 to 2K) is obtained for vertical (or close to vertical) occultations.

We present here an update of comparisons between GOMOS HRTP data (from August 2002 to September 2009) and correlative temperature profile data recorded by 70 radiosondes launched on board the ozonesonde balloons and by 10 temperature lidars. The co-location criteria were chosen as the best compromise between a sufficient amount of comparison points and a sufficient co-location of the probed air masses: a maximum distance of 500 km between the ground-based station and the GOMOS tangent point, and a maximum time difference of 12h for radiosondes and 6h for temperature lidars. Reducing the spatial coincidence criteria reduces strongly the amount of collocations and limits the statistical relevance of the results.

We first excluded unreliable correlative and satellite measurements from the analysis. For the correlative data we based ourselves on the evolution in altitude, pressure and temperature to reject individual measurement points. Likewise, GOMOS data points with a temperature retrieval error larger than 500% were rejected, and, when more than five grid points satisfied this condition, the entire profile was removed. For this work, we only selected the dark limb and dark straylight data (PCD_ILLUM = 0 or 3), but did not filter the GOMOS data with respect to the obliquity of the occultation. The correlative profiles were box-averaged to the satellite resolution, before all data (satellite and ground-based) were linearly interpolated to a common altitude grid between 15-35km.

Monthly statistics of the agreement between Envisat GOMOS Prototype Processor v6.0cf / IPF 5.00 temperature profile data and correlative measurements from radiosonde stations contributing to the Multi-TASTE project are provided as an electronic annex.

The absence of significant time-dependencies permitted the statistical study of the vertical structure of the differences between pairs of co-located profiles, which is presented in Figure 6 for the ground-based measurements at Ny-Ålesund (Svalbard), Uccle (Belgium) and Marambio (Antarctica). The plot shows the median (solid) and 68% inter-percentile (dashed) of the absolute temperature differences between GOMOS and correlative measurements. These results are representative for the other ground-based stations.

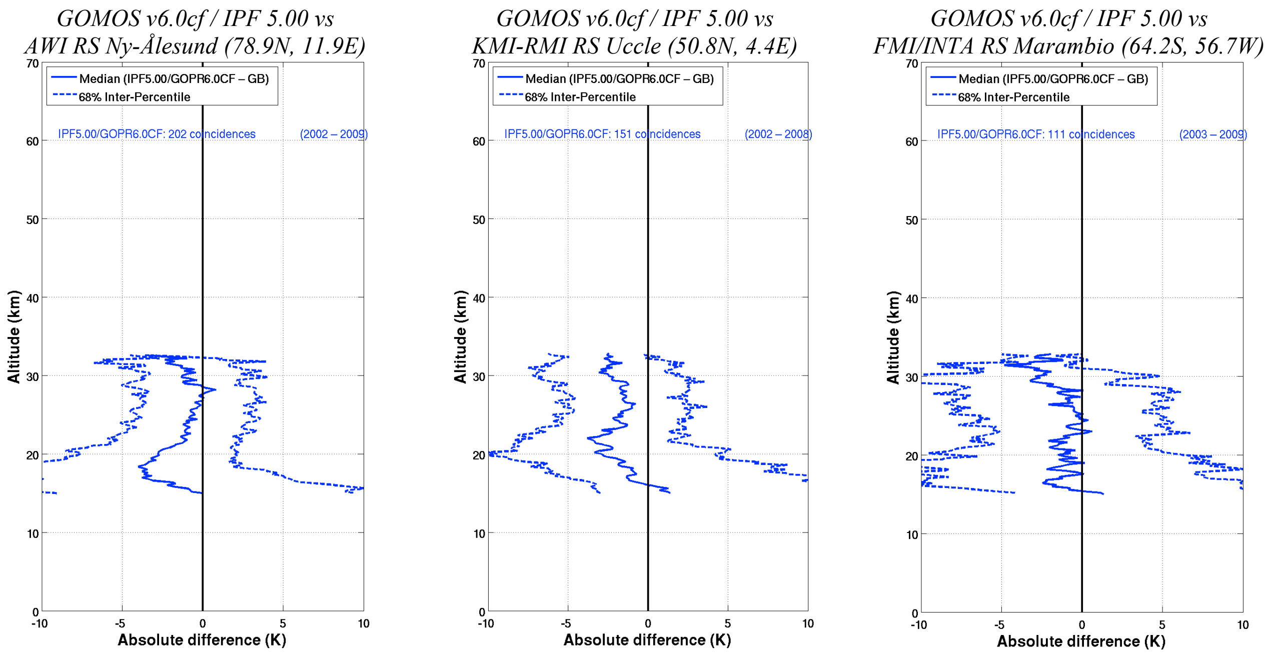

Figure 6: Vertical dependence of median (solid) and 68% inter-percentile (dashed) of the absolute temperature differences between GOMOS Prototype Processor 6.0cf / IPF 5.00 and three radiosondes.

Due to the long-term stability and the similarity of the results for stations close in latitude, we computed the multi-year median of the absolute differences for all co-located ozone profiles within 5° latitude bands, see Figure 7 for radiosonde stations (the lidar stations led to similar results).

This analysis update confirms the conclusions of the previous report. In the tropics and at mid-latitudes, a negative bias of -2 to -3K is observed from 20 km up to the burst point of the balloon. At high northern and southern latitudes, the median of the differences seems to vary linearly with altitude. There is a negative bias of about -3K at 15-20 km, which diminishes with increasing altitude. From about 25-30 km altitude, the median bias is close to 0K. Above 30 km, the differences increase again to reach about -2 to -3K in median. The half 68% inter-percentile is of about 4K in the stratosphere at all latitudes. In the UTLS, absolute differences increase to more than 10K in some cases and are much noisier; the half 68% inter-percentile exceeds 10K.

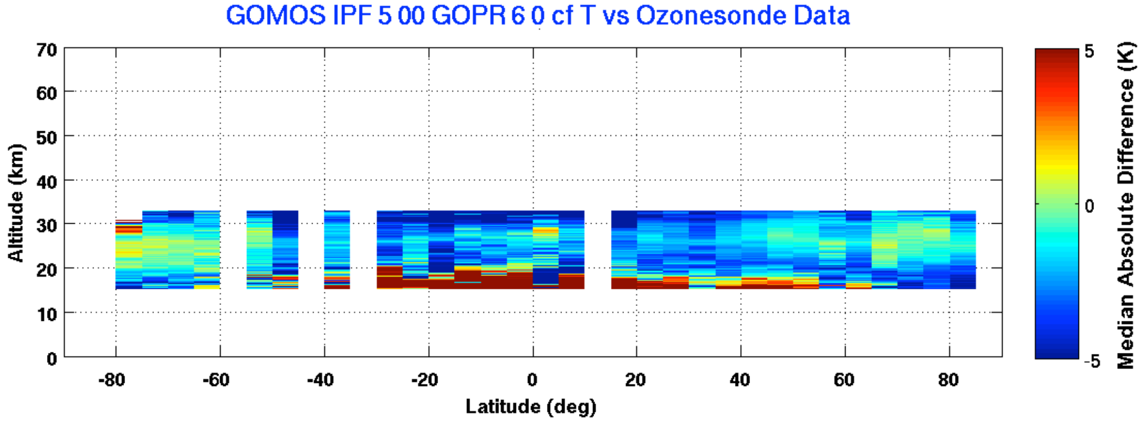

Figure 7: Median absolute temperature difference between GOMOS Prototype Processor 6.0cf / IPF 5.00 and radiosonde data as a function of altitude and latitude.

III.2 Envisat MIPAS

During the reporting period a data set processed with the improved version of the MIPAS processor, IPF 5.04, was provided to the validation teams. This processor retrieves geophysical observables from optimized resolution data, which allows, for the first time, to process the complete mission. Before establishing this processor as the next operational baseline, the IPF 5.04 data were subjected to a validation process by the various Multi-TASTE partners. The initial results were presented at the MIPAS Quality Working Group meeting #23 at KIT in June 2010. In parallel, the validation results of the previous processor IPF 4.61/4.62 (which handles full resolution data only) were consolidated and a systematic multi-validation of limb sounders was started (the latter is reported in Section III.5.1 on Multi-Mission studies).

III.2.1 History of instrument operations and processor upgrades

MIPAS operated at full resolution from July 2002 to March 2004, when the interferometer experienced a major anomaly. In January 2005 instrument operations were resumed in an optimized resolution mode with reduced spectral but finer vertical sampling. The complete set of full resolution spectra was processed with the operational processor IPF 4.61/4.62 and has been available since several years. The newest Level 1b-2 processor, IPF 5.04, permits the production of profiles for both resolution modes. This allowed the restart of the operational processing at the ESA Ground segment on 10th June 2010 for near real-time production (ESRIN, Kiruna) and on 21st June 2010 for offline production (D-PAC).

The following changes and improvements were implemented in the new L1b-L2 processor IPF 5.04 (which is fully aligned with its scientific prototype ORM 1):

- The instrument misalignment matrix is now partly taken into account, which reduces the observed offset and gradient of the difference between engineering and true tangent altitudes of the previous L1b processor. (Pressure remains the recommended altitude proxy.)
- A-posteriori regularisation to compensate for the ill-conditioned situation due to the finer vertical measurement grid in the optimized resolution mode. It is applied for the main target parameters (temperature, O_3, HNO_3, CH_4, N_2O and NO_2), except for H_2O and pressure.
- Inclusion of the averaging kernel matrix of the regularized profile in the output Level 2 product
- Computation of conditioning parameter (information about the stability of the matrix inversion)
- Bug correction in continuum derivatives and T/VMR derivatives
- Update of the partitioning functions of HNO3
- Option for more accurate FOV convolution, which impacts H_2O profiles near the tropopause

It is important to keep in mind that the full resolution and optimized resolution retrievals are characterized by different measurement scenarios, different L1 files, different L2 algorithms and different microwindows.

III.2.2 Validation of temperature profile [IPF 4.61 and IPF 5.04]

We present the results of comparisons between full resolution IPF 4.61 (4465 orbits, July 2002 - March 2004) and optimized resolution IPF 5.04 (4048 orbits, January 2005 - December 2008) MIPAS temperature profiles and a data set of correlative temperature profiles provided by PTU radiosondes and lidars operating in the NDACC, SHADOZ and GAW networks. We found that the profiles in both MIPAS data sets co-located with profiles recorded at 47 radiosonde and 7 lidar stations. Since the two MIPAS data sets are disjoint, we could not perform a profile-by-profile comparison of both processor versions, instead it was done on a statistical basis. The co-location criteria were chosen as the best compromise between a sufficient amount of comparison points and a sufficient co-location of the probed air masses. First, a maximum distance of 500 km between the ground-based station and the MIPAS tangent point for the scan at 30km altitude, and, second, a maximum time difference of 6h (for both day-time radiosonde and night-time lidar data). Tightening the spatial criteria reduces the amount of co-locations strongly and hence limits the statistical relevance of the results. MIPAS data points with a temperature retrieval error larger than 500% were rejected, and, when more than five grid points satisfied this condition, the entire profile was removed. The correlative profiles were then box-averaged to the satellite resolution. And finally all data (satellite and ground-based) were linearly interpolated to a common pressure grid between 450-0.06 hPa. We remind the reader that the retrieval grid is finer for IPF 5.04 than for IPF 4.61, due to the finer vertical sampling in the optimized resolution mode.

Monthly statistics of the agreement between MIPAS IPF 4.61 and IPF 5.04 temperature profile data and radiosonde measurements from stations contributing to the Multi-TASTE project are provided as an electronic annex.

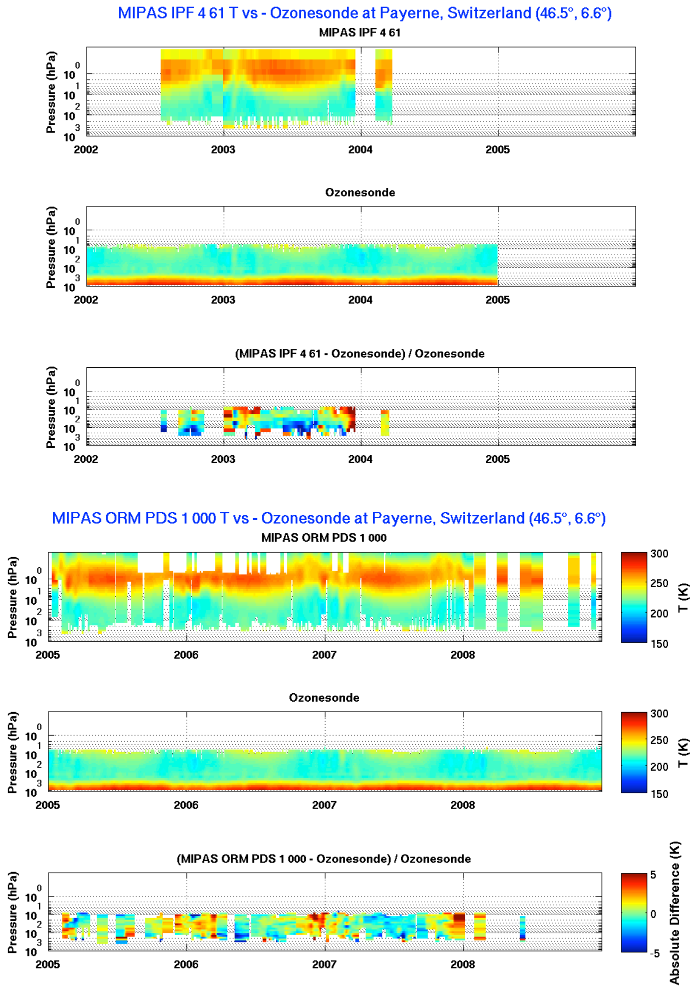

Figure 8: Time series of the vertical temperature profile as retrieved by MIPAS (top panels) and by the MCH radiosondes launched at Payerne (centre). The bottom panels show the absolute temperature difference between the co-located profiles. Both MIPAS processor versions are shown: IPF 4.61 (left) and IPF 5.04 (right).

Figure 8 illustrates the first part of the validation study, which consisted of the visual inspection and the statistical study of temperature profile time series at each station. The figure shows the time series of temperature profiles at the MCH radiosonde station at Payerne, Switzerland. The objective is to identify possible global features, cyclic errors and long-term drifts. The top and central panels show the profiles as retrieved respectively by the MIPAS processors (left: IPF 4.61; right: IPF 5.04) and by the ground-based measurements, while the bottom panel presents their absolute difference, calculated as satellite-ground. For a better visibility a one-month running mean was applied to all time series. The empty areas P < 1 hPa for the IPF 5.04 time series in 2005-2006 correspond to UTLS-1 measurement mode periods. This mode has a maximum scan altitude of 51.5 km, opposed to 68 km in the nominal measurement mode.

The Payerne time series shown Figure 8 is typical for all ground stations: the qualitative temporal and vertical behaviour of IPF 5.04 and IPF 4.61 is in agreement with the correlative data for a wide range of atmospheric phenomena. No significant global or seasonal features were observed. A robust linear regression analysis indicated drifts (at 95% confidence level) at some stations at some altitudes, e.g. at Payerne at 110 hPa (see Figure 9), but the time series are too short and hence the results too noisy to provide conclusive statements.

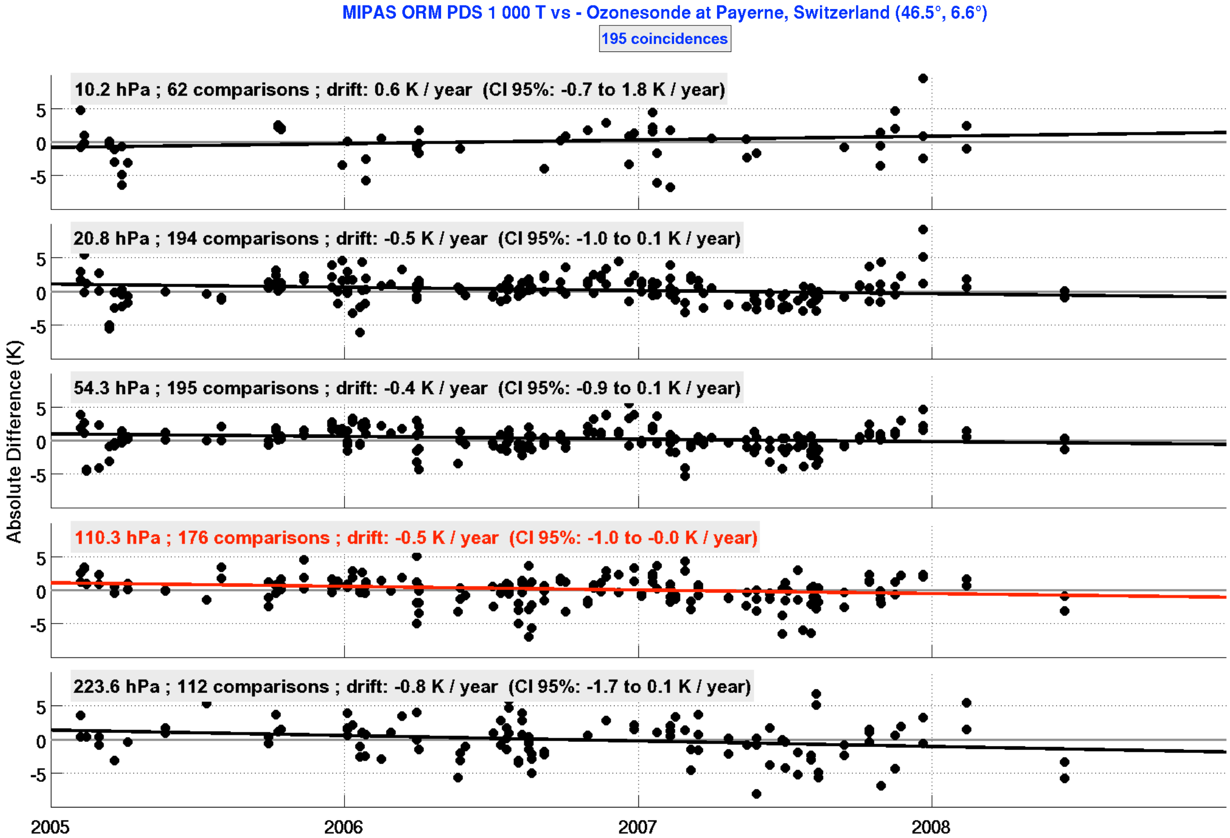

Figure 9: Time series of absolute temperature differences between MIPAS IPF 5.04 and MCH radiosonde data at Payerne, Switzerland at selected pressure levels. A linear regression was fitted to the data when more than 20 co-located pairs were found and the spread in their relative differences was less than 30%. Black lines are not significant, red lines are significant at 95% confidence level. The annual slope and 95% confidence interval are indicated in each subplot.

In most cases the absence of significant dependences on time permitted the statistical study of the vertical structure of the absolute temperature differences between pairs of co-located profiles. This was done for each ground station;

Figure 10 presents the results at the station of Sodankylä, Finland. The left panel shows the median (solid) and 68% inter-percentile (dashed) of the absolute differences between MIPAS and radiosonde measurements for IPF 5.04 (blue) and IPF 4.61 (red). The right panel shows the median absolute precision (dashed) and bias (solid) for MIPAS (blue, red) and for the correlative data (grey). Three additional stations (Hohenpeißenberg, Lauder and Belgrano) are shown in Figure 11; these results are representative for the other ground-based stations.

Between 10 hPa (≈ 30 km) and 100-200 hPa (≈ 16-11 km), the IPF 5.04 temperature profiles underestimate the correlative data by 1-2 K, almost independent of altitude and latitude. At these altitudes the comparisons are similar for both processors, except at polar latitudes where the bias of the previous processor is less pronounced (cf.

Figure 10 and Figure 11, right). However, below the tropopause (>100-200 hPa) the IPF 5.04 cold bias gradually increases and reaches -5 K at the bottom of the profile. The vertical analysis of IPF 4.61 did not indicate such a gradually increasing disagreement.

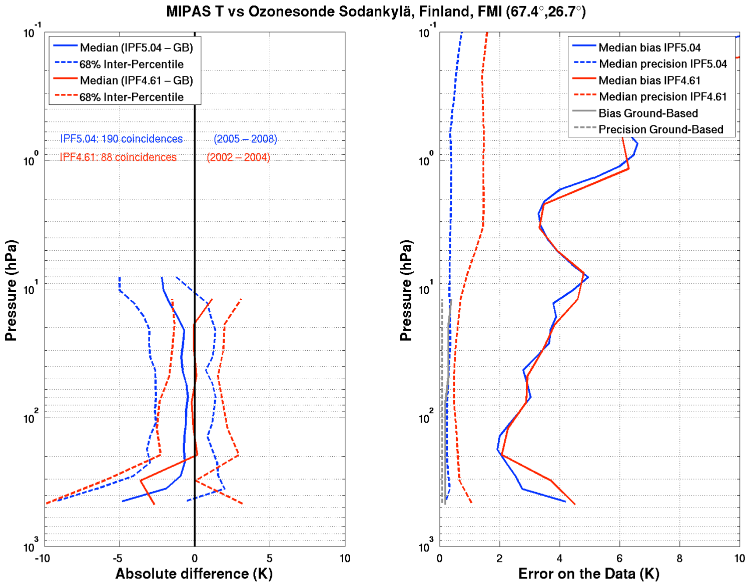

Figure 10 – left: vertical dependence of median (solid) and 68% inter-percentile (dashed) of the absolute temperature differences between both MIPAS processors (red, blue) and FMI radiosonde data at Sodankylä, Finland. Right panel: median absolute precision (dashed) and bias (solid) for MIPAS and correlative data.

MIPAS IPF 4.61 & IPF 5.04 vs DWD RS Hohenpeißenberg (47.8N, 11.0E) | *MIPAS IPF 4.61 & IPF 5.04 vs NIWA RS Lauder (45.0S, 169.7W)* | *MIPAS IPF 4.61 & IPF 5.04 vs FMI/INTA RS Belgrano (77.9S, 34.6W)*

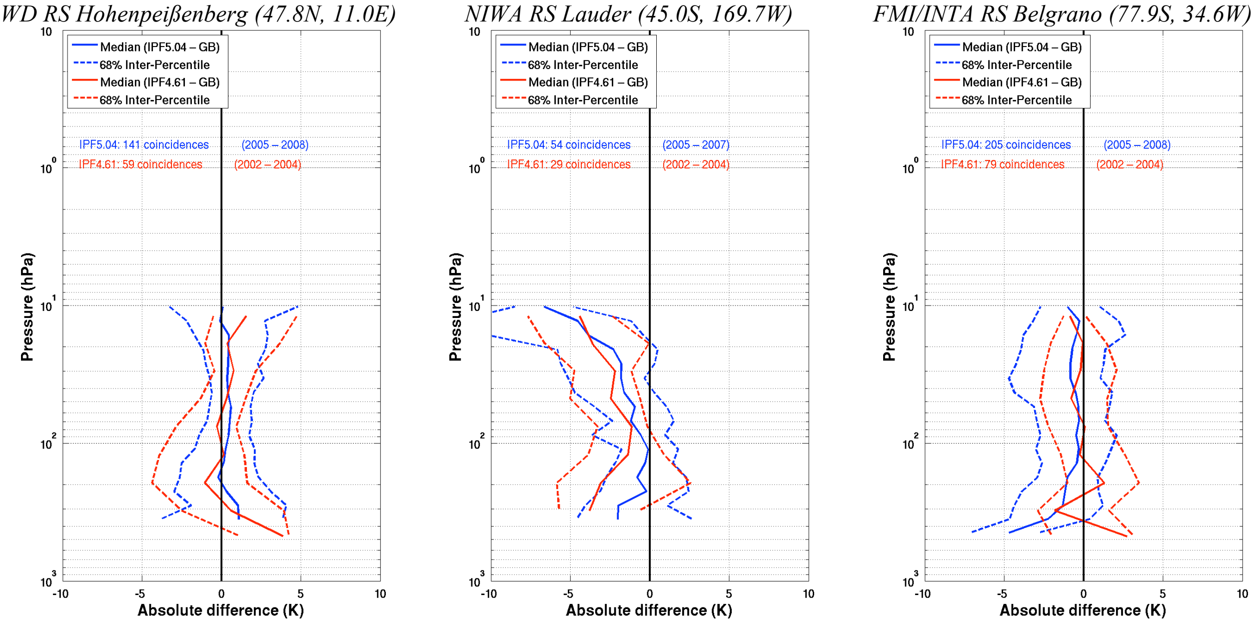

Figure 11: Vertical dependence of median (solid) and 68% inter-percentile (dashed) of the absolute temperature differences between both MIPAS processors (red, blue) and correlative data at three radiosonde stations.

The precision of the MIPAS L2 algorithms has decreased from 0.4-0.8 K (IPF 4.61) to 0.2-0.5 K (IPF 5.04). However, after combination with the 0.1 K precision of the correlative measurements, this is significantly smaller than the observed 2-4 K half 68% inter-percentiles of the comparisons. Previous studies [Ridolfi et al., 2007] drew a similar conclusion for IPF 4.61; insufficient cloud-flagging and spatial smoothing errors were suggested contributions to the unexplained random error component. Apart from the -5 K underestimation at the bottom of the profiles, the observed bias of the comparisons is consistent with MIPAS systematic error, which is around 2-3 K and up to 5 K at polar latitudes.

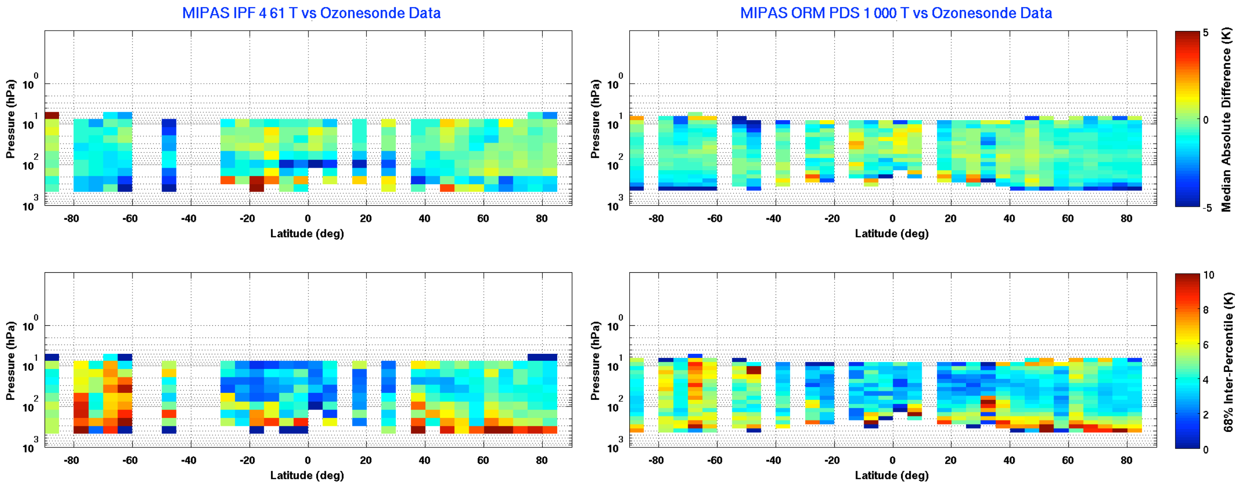

Figure 12: Median (top) and half 68% inter-percentile (bottom) of the absolute difference between MIPAS and radiosonde data as a function of pressure and latitude; for IPF 4.61 (left) and IPF 5.04 (right).

Given the long-term stability and the similarity of the results for stations close in latitude, we derived multi-year and zonal statistics; see Figure 7 for radiosonde stations (the lidar stations led to similar results). The medians (top) and half 68% inter-percentiles (bottom) of the absolute differences are computed for all co-located temperature profiles within 5° latitude bands. The results are shown for both IPF 4.61 (left panels) and IPF 5.04 (right).

Summary

Our previous conclusions are confirmed by Figure 7. There is no significant change in the comparison bias or spread above the tropopause, except at polar latitudes where IPF 5.04 produces <0.5 K colder values than its predecessor. In general, both versions of MIPAS profiles show a cold bias of not more than 1-2 K; they are of good quality.

Below the tropopause we found an increasing cold bias for IPF 5.04, but not for IPF 4.61. It reaches -5 K at the bottom of the profile. Since this can not be fully ascribed to the systematic error of the comparison, we recommend that the quantitative use and interpretation of MIPAS IPF 5.04 temperature data below the tropopause should be done with caution. The IPF 4.61 temperature profiles on the other hand seem more reliable in this region of the atmosphere.

III.2.3 Validation of ozone profile [IPF 4.61/4.62 and IPF 5.04]

We present the results of comparisons between full resolution IPF 4.61/4.62 (7011 orbits, July 2002 - March 2004) and optimized resolution IPF 5.04 (4048 orbits, January 2005 - December 2008) MIPAS ozone profiles and a data set of correlative ozone profiles provided by ozonesondes and lidars operating in the NDACC, SHADOZ and GAW networks. At 49 ozonesonde and 9 lidar stations we found co-located profiles for the two MIPAS data sets. Since the two MIPAS data sets are disjoint, we could not perform a profile-by-profile comparison of both processor versions, instead it was done on a statistical basis. We refer the reader to Section III.5.1 where the IPF 4.61/4.62 validation is put in the context of multi-mission studies.

The co-location criteria were chosen as the best compromise between a sufficient amount of comparison points and a sufficient co-location of the probed air masses. First, a maximum distance of 500 km between the ground-based station and the MIPAS tangent point, and, second, a maximum time difference of 6h (for both day-time ozonesonde and night-time lidar data). Tightening the spatial criteria reduces the amount of co-locations strongly and hence limits the statistical relevance of the results. MIPAS data points with an ozone VMR error larger than 500% were rejected, and, when more than five grid points satisfied this condition, the entire profile was removed. The correlative profiles were then box-averaged to the resolution of MIPAS. And finally all data (satellite and ground-based) were linearly interpolated to a common pressure grid between 450-0.06 hPa. We remind the reader that the retrieval grid is finer for IPF 5.04 than for IPF 4.61, due to the finer vertical sampling in the optimized resolution mode.

Monthly statistics of the agreement between MIPAS IPF 4.61/4.62 and IPF 5.04 ozone profile data and correlative measurements from ozonesonde stations contributing to the Multi-TASTE project are provided as an electronic annex.

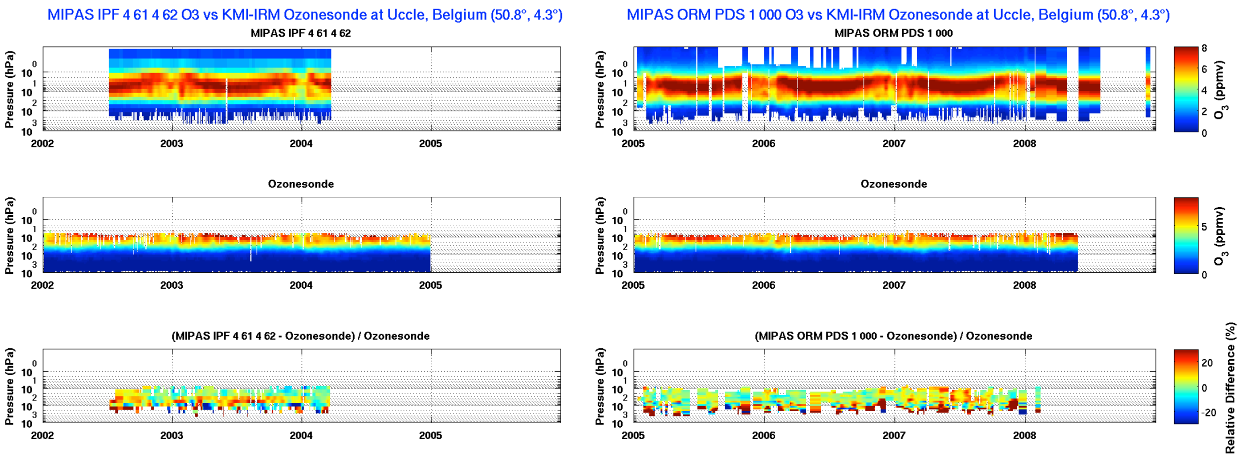

Figure 13: Time series of the vertical profile of ozone volume mixing ratio as retrieved by MIPAS (top panels) and by the ozonesondes launched at the KMI-IRM station Uccle (centre). The bottom panels show the relative difference between the co-located profiles. Both MIPAS processor versions are shown: IPF 4.61/4.62 (left) and IPF 5.04 (right).

Figure 13 illustrates the first part of the validation study, which consisted of the visual inspection and the statistical study of the ozone profile time series at each ground station. The figure shows the time series of ozone VMR profiles at the ozonesonde station of Uccle, Belgium. The objective is to identify possible global features, cyclic errors and long-term drifts. The top and central panels show the profiles as retrieved respectively by the MIPAS processors (left: IPF 4.61/4.62; right: IPF 5.04) and by the ground-based measurements, while the bottom panel presents their relative difference, calculated as (satellite-ground)/ground. For a better visibility a one-month running mean was applied to all time series. The empty areas P < 1 hPa for the IPF 5.04 time series in 2005-2006 correspond to UTLS-1 measurement mode periods. This mode has a maximum scan altitude of 51.5 km, opposed to 68 km in the nominal measurement mode.

The Uccle time series shown above is typical for all ground stations: the qualitative temporal and vertical behaviour of IPF 5.04 and IPF 4.61/4.62 is in agreement with the correlative data for a wide range of atmospheric phenomena. Besides a positive bias during Antarctic ozone hole events, no significant global or seasonal features were observed. A robust linear regression analysis indicated drifts (at 95% confidence level) at some stations at some altitudes, e.g. at Uccle at 54 hPa (see
Figure 14), but the time series are too short and hence the results too noisy to provide conclusive statements.

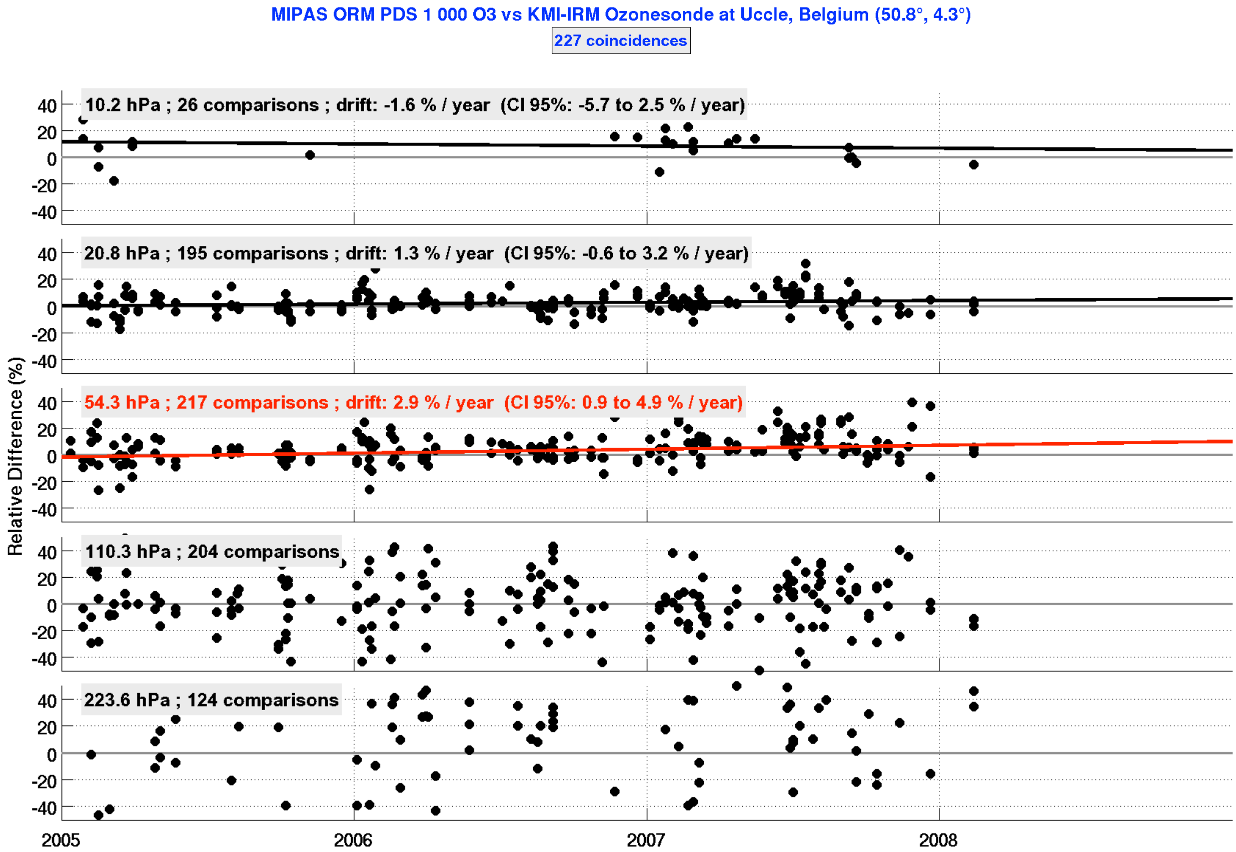

Figure 14: Time series of relative differences between MIPAS IPF 5.04 and KMI-IRM ozonesonde data at Uccle, Belgium at selected pressure levels. A linear regression was fitted to the data when more than 20 co-located pairs were found and the spread in their relative differences was less than 30%. Black lines are not significant, red lines are significant at 95% confidence level. The annual slope and 95% confidence interval are indicated in each subplot.

The absence of significant time-dependencies permitted the statistical study of the vertical structure of the relative differences between pairs of co-located profiles. This was done for each ground station;

Figure 15 presents the results at the station of Sodankylä, Finland. The left panel shows the median (solid) and 68% inter-percentile (dashed) of the relative differences between MIPAS and ozonesonde measurements for IPF 5.04 (blue) and IPF 4.61/4.62 (red). The right panel shows the median relative precision (dashed) and bias (solid) for MIPAS (blue, red) and for the correlative data (grey). Three additional stations (Hohenpeißsenberg, Paramaribo and Belgrano) are shown in Figure 16; these results are representative for the other ground-based stations.

In the stratosphere, between 10 hPa (≈ 30 km) and 50-100 hPa (≈ 20-15 km), the IPF 5.04 ozone profiles are within ±5% of the correlative data, almost independent of altitude and latitude. The exception is a 20-30% overestimation of Antarctic ozone hole events. The comparisons for the latest and the older processor are very similar in the stratosphere; and the latter are in agreement with those of previous validation studies (see Section III.5.1). In the Upper Troposphere Lower Stratosphere (p >50-100 hPa), IPF 5.04 overestimates ground-based measurements by 20% to 50%. Such a positive bias, although of smaller magnitude, has been reported for the previous processor as well [Cortesi et al., 2007].

The precision of the MIPAS L2 algorithms has improved from 5-10% to 2-5%. After combination with the 5-7% precision of the correlative measurements, this is in agreement with the generally observed 5-10% half 68% inter-percentiles of the comparisons. The analysis of systematic errors has not been updated; so they remain around 5-15%.

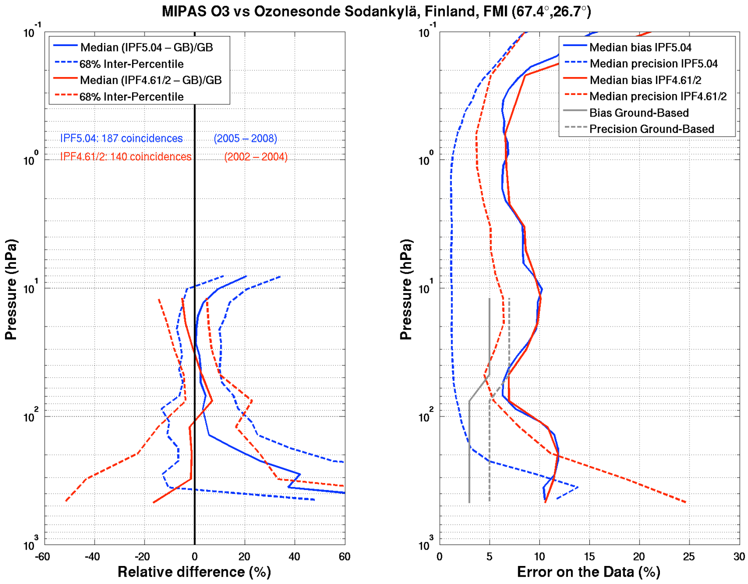

Figure 15 – left: vertical dependence of median (solid) and 68% inter-percentile (dashed) of the relative differences between both MIPAS processors (red, blue) and FMI ozonesonde data at Sodankylä, Finland. Right panel: median relative precision (dashed) and bias (solid) for MIPAS and correlative data.

MIPAS IPF 4.61/4.62 & IPF 5.04 vs DWD O3S Hohenpeißenberg (47.8N, 11.0E)

MIPAS IPF 4.61/4.62 & IPF 5.04 vs KNMI O3S Paramaribo (5.8N, 55.2W)

MIPAS IPF 4.61/4.62 & IPF 5.04 vs FMI/INTA O3S Belgrano (77.9S, 34.6W)

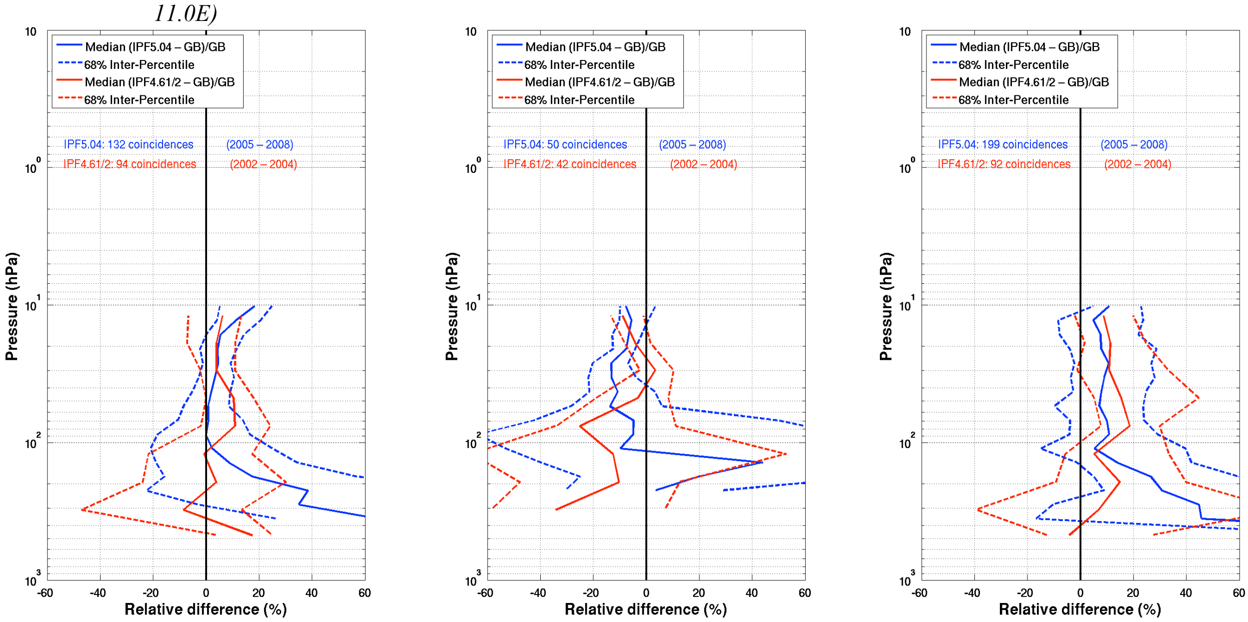

Figure 16: Vertical dependence of median (solid) and 68% inter-percentile (dashed) of the relative ozone VMR differences between both MIPAS processors (red, blue) and correlative data at three ozonesonde stations.

Given the long-term stability and the similarity of the results for stations close in latitude, we derived multi-year and zonal statistics; see Figure 17 for ozonesonde stations (the lidar stations led to similar results). The medians (top) and half 68% inter-percentiles (bottom) of the relative differences are computed for all co-located ozone profiles within 5° latitude bands. The results are shown for both IPF 4.61/4.62 (left panels) and IPF 5.04 (right).

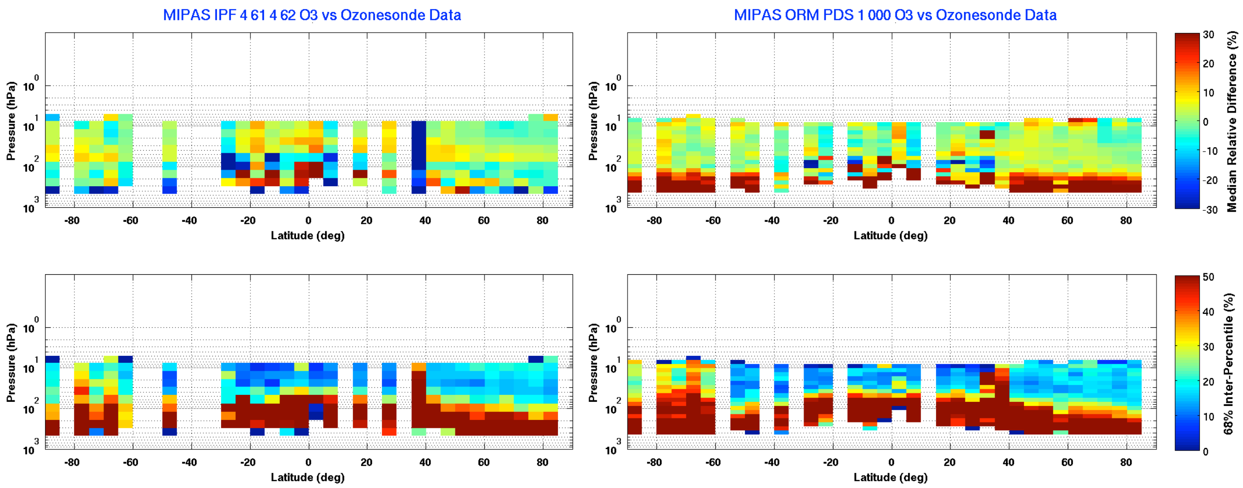

Figure 17: Median (top) and half 68% inter-percentile (bottom) of the relative difference between MIPAS and ozonesonde data as a function of pressure and latitude; for IPF 4.61/4.62 (left) and IPF 5.04 (right).

<u>Summary</u>
Our previous conclusions are confirmed by Figure 17. There is no significant change in the comparison bias or spread in the stratosphere. Apart from a 20-30% positive bias during Antarctic ozone hole events, both versions of MIPAS ozone profiles are generally within ±5% from correlative data; they are of good quality.

In the UTLS IPF 5.04 produces a much larger overestimation (20-50%) of the correlative data than its predecessor. The large positive bias at the bottom of the profile can only partly be ascribed to the combined systematic error of the comparison and to the higher natural variability of the probed air masses. Hence, we recommend that the quantitative use and interpretation of MIPAS IPF 5.04 ozone data in this region of the atmosphere should be done with caution. This remark is also valid for MIPAS IPF 4.61/4.62 ozone data, as these show a positive bias at low altitudes as well.

III.2.4 Validation of CH_4, N_2O and HNO_3 profiles [IPF 5.04]

CH_4, N_2O and HNO_3 profile data from the MIPAS prototype processor IPF 5.04 have been validated against ground-based FTIR data at Jungfraujoch, Kiruna and St Denis at Ile de La Réunion. We compared ground-based and MIPAS data, coinciding within ±6 h in time and 500 km in distance.

For methane (CH_4) a small underestimation was observed for IPF 5.04, typically smaller than 10% in the altitude range 20-50 km. The previous processor IPF 4.61 slightly overestimated the CH_4 ground-based data [Payan et al., 2009].

For nitrous oxide (N_2O) the preliminary comparison results for IPF 5.04 look very close to what was reported for IPF 4.61 [Payan et al., 2009], with differences between the MIPAS and the ground-based data close to zero, except for Kiruna at altitudes above 25 km where the N_2O volume mixing ratio becomes very small.

The preliminary nitric acid (HNO_3) validation results show discrepancies up to 50%, which is worse than the validation results of the previous processor IPF 4.61/4.62 [Wang et al., 2007]. However, we have to compare the relevant partial column differences more precisely, taking into account the limited number of degrees of freedom in the ground-based profile data (i.e. very coarse vertical resolution). This work remains to be done.

III.3 Envisat SCIAMACHY

During the reporting period a data set processed with the improved versions of the SCIAMACHY L1b and L2 processors, SGP 7.03/5.01, was provided to the validation teams. This processor contains several major corrections and introduces new trace gas retrievals as well. Before establishing this processor as the next operational baseline, the SGP 5.01 data were subjected to a validation process by the various Multi-TASTE partners. The initial results were presented at the SCIAMACHY Quality Working Group meeting at ESA-ESRIN in June 2010 and at the SCIAVALIG Quick Look Validation meeting at BIRA-IASB in September 2010. In parallel, the validation results of the previous processor SGP 3.01 were consolidated and a systematic multi-validation of limb sounders was started (the latter is reported in Section III.5.1 on Multi-Mission studies).

III.3.1 The new SGP 7.03 Level 1b and SGP 5.01 Level 2 operational processors

The new versions of SCIAMACHY's Level-0-to-1b and Level-1b-to-2 operational processors were activated on 4th February 2010 at the near real-time processing centres and five days later at the D-PAC offline processing centre. The new Level-0-to-1b processor, IPF 7.03, introduces a new limb state in the mesosphere (with scan altitudes between 60 and 150 km) and offers improved stray light correction for spectral channel 2. With respect to its predecessor SGP 3.01, the new Level-1b-to-2 processor, SGP 5.01, includes substantial updates and upgrades:

- M-factor correction, impacting nadir O_3 retrievals and AAI retrievals
- Change of NO_2 retrievals now using not radiometrically calibrated data
- New AAI algorithm
- Improvements of cloud fraction retrieval
- New forward model in limb retrievals using Picard iteration
- Optimized settings for limb profile retrieval of NO_2 and O_3
- Usage of the Limb Cloud Flag in O_3 profile retrieval
- Update of the usage of aerosols in O_3 profile retrieval
- Reduction of the step size of the vertical retrieval grid from 3.5 km to 1.75 km between 14-42km

Several new trace gas data products are introduced too:

- Nadir products: SO_2 total column for normal and volcanic conditions, BrO total column, OClO slant column, H_2O total column and CO total column.
- Limb products: BrO profiles and cloud flags for PSC and tropospheric clouds.

The data quality of the various trace gas data products must be evaluated before establishing IPF 7.03 and SGP 5.01 as the new operational processors. The BIRA-IASB validation team identified and delivered to DLR the list of all SCIAMACHY orbits that co-located in space and time with measurements in the correlative data set between 2002 and 2010. Due to reprocessing time constraints, a total of 1900 orbits (mainly during 2002, 2003 and 2006) were processed with IPF 7.03 and SGP 5.01 and made available to the validation teams.

III.3.2 Delta-validation of nadir ozone column [SGP 5.01]

SCIAMACHY ozone column data sets available for delta validation of SGP upgrades have been compared to correlative data sets provided by ground-based networks of Dobson and Brewer spectrophotometers and of DOAS/SAOZ UV-visible spectrometers associated with WMO's Global Atmosphere Watch (GAW). Both SGP 3.01 and SGP 5.01 generate ozone column data generally consistent with GAW ground-based data records. As shown in Figure 18 where SGP data are compared statistically to the Dobson and Brewer networks, differences between the two SGP versions are small, usually in the form of a bias smaller than 0.6% on an average. With SGP 3.01 a negative drift in ozone column values had been noticed at numerous but not all stations. Although slightly different, this drift seems to persist with the current SGP 5.01 data set available for delta validation. The introduction of the degradation correction improves on the drift in the tropics, but not on mid to high latitudes. Differences between SGP 5.01 and ground-based networks increase at large Solar Zenith Angle (SZA) and at low ozone column values as measured during the Antarctic ozone hole, as illustrated in Figure 19 at two Antarctic stations.

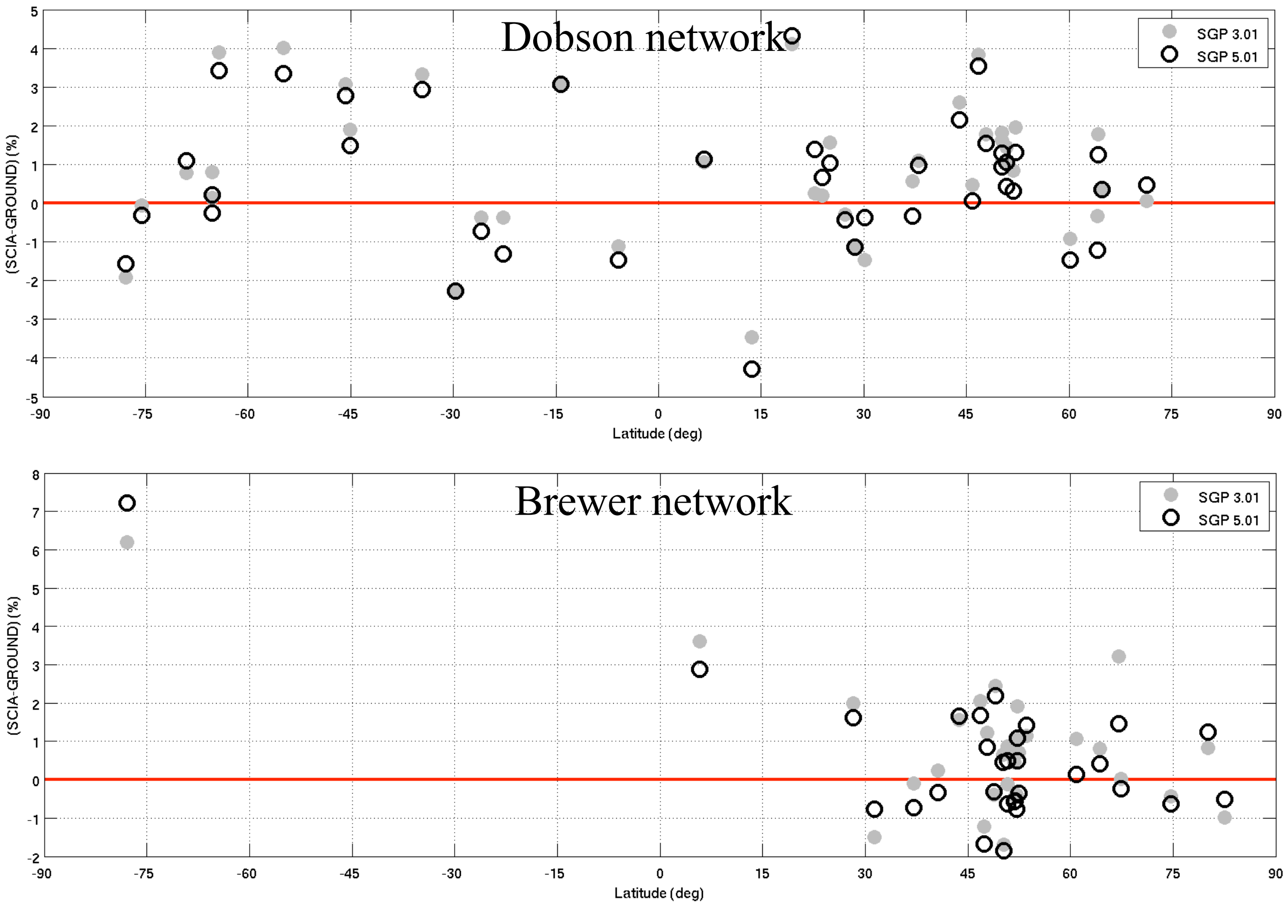

Figure 18: Mean percent relative difference between SCIAMACHY SGP (3.01 and 5.01) and ground-based total ozone measured from pole to pole by the Dobson (top) and Brewer (bottom) networks.

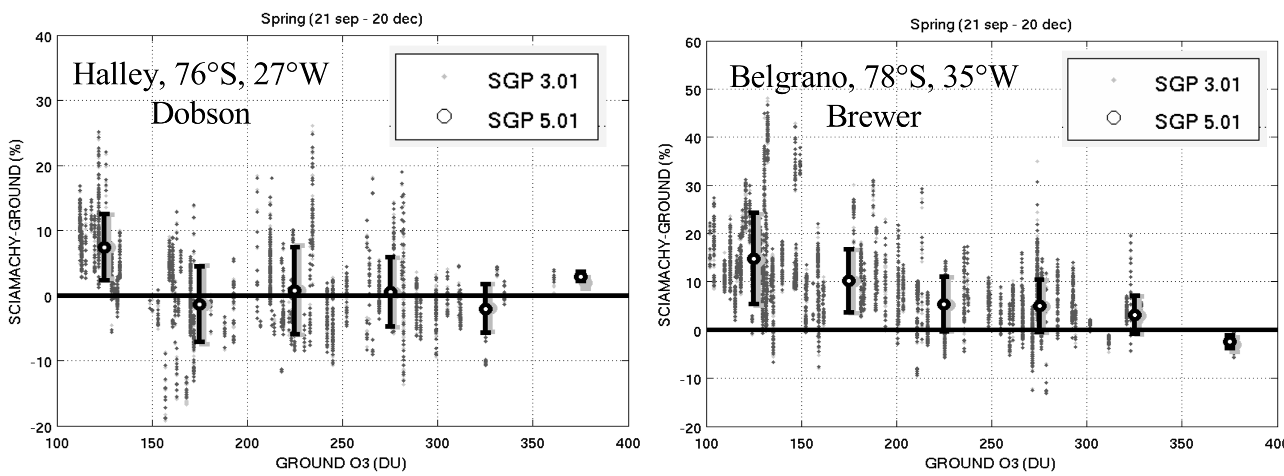

Figure 19: Percent relative difference between SCIAMACHY SGP (3.01 and 5.01) and ground-based total ozone measured in the Antarctic ozone hole at Halley by the BAS-NERC Dobson (left) and at Belgrano by the INTA Brewer (right), as a function of the ground-based total ozone value.

III.3.3 Delta-validation of nadir nitrogen dioxide [SGP 5.01]

SGP 3.01 and SGP 5.01 generate NO_2 column data mutually consistent and also with NDACC/UV-visible and GOME GDP 4.1 data records. As shown in Figure 20, where SGP data are compared statistically to the NDACC/UV-visible network, SGP 3.01 usually is lower than SGP 5.01 by a few 10^{13} to 10^{14} molec.cm^{-2}, a value close to the detection limit of UV-visible spectrometers. SCIAMACHY SGP 5.01 is low biased wrt NDACC and GOME GDP 4.1 in the Southern Hemisphere, by about 5 10^{14} molec.cm^{-2}. This negative bias exhibits a seasonal cycle, as illustrated in Figure 20.

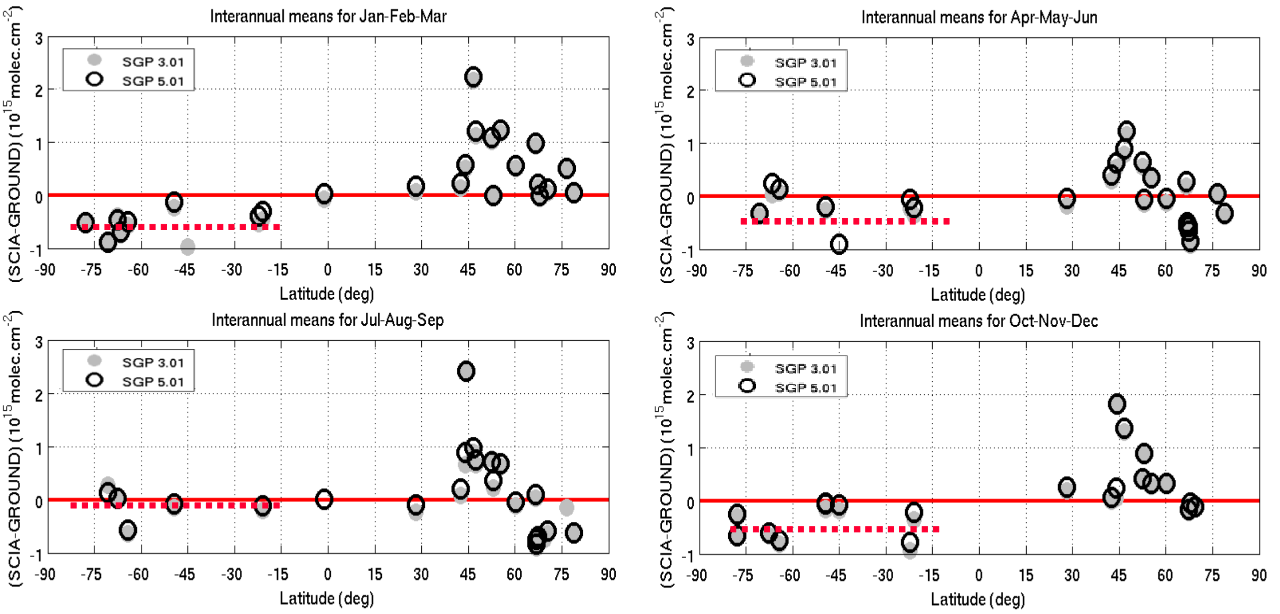

Figure 20: Mean absolute difference between SCIAMACHY SGP (3.01 and 5.01) and ground-based total NO_2 measured from pole to pole by NDACC UV-visible spectrometers. Results are presented by season.

III.3.4 Validation of nadir methane column [IMAP, WFMD]

The validation of the SCIAMACHY scientific data products for CH_4, from the algorithms IMAP v4.9 and WFM-DOAS v1.0/C, has been finalized. The data set used for the validation is the FTIR data set generated in the EU project HYMN (http://www.knmi.nl/samenw/hymn); which came to an end by the end of 2009. This data set includes the FTIR data from all HYMN FTIR partners with in addition data from a few non-European stations, making it a quasi-global dataset including 15 stations worldwide. Within HYMN, the data have been made more consistent among each other by constraining the retrieval parameters [Sussmann et al., 2009], making it most suitable for a coordinated network-based satellite validation.

The most important validation results are the following:

- The precision of SCIAMACHY XCH4 from IMAP v4.9 and WFM-DOAS v1.0 has strongly improved since 2005 (WFM-DOAS v0.41).
- Due to this improvement it is now possible to retrieve via a relatively small 200 km pixel selection radius realistic values on the day-to-day variability of XCH4.
- There is a high bias of SCIAMACHY IMAP v4.9 and WFM-DOAS v1.0 of 2 to 2.5% relative to the global FTIR data set.
- There is no significant latitudinal dependency of the bias.
- Still no significant correlation of the annual cycles between FTIR and SCIA can be found. Comparisons of the seasonality of XCH4 between the FTIR and the SCIAMACHY WFM-DOAS and IMAP data, show that IMAP-DOAS has a similar amplitude as FTIR but with a noticeable phase shift while WFM-DOAS exhibits an even stronger seasonality but also exhibits a much larger scatter (see e.g. at Jungfraujoch in Figure 21). Fitting a simple sloped sinus function through the model, FTIR and SCIAMACHY data confirms these observations (see Table 2).

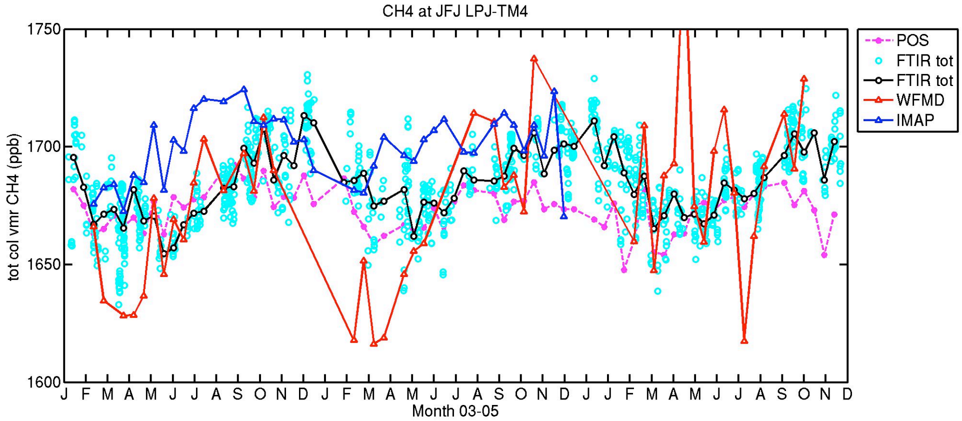

Figure 21: Biweekly median FTIR, model TM4-LPJ (POS) and SCIAMACHY time series of CH4 total columns at Jungfraujoch, Germany.

Table 2: Amplitudes (in ppb) for the CH_4 total column FTIR and SCIAMACHY data. Note that extreme WFMD values due to unreliable fits are excluded from the table.

	NYA	THU	KIR	HAR	BRE	ZUG	JFJ	TOR	IZA	WOL	MEAN
FTIR	11,6	40,2	5,7	10,5	18,2	14,0	16,9	21,1	6,0	16,5	**16,1**
IMAP	19,6	18,4	10,3	15,1	14,3	12,0	17,4	5,0	12,6	4,7	**12,9**
WFMD	-	-	-	30,3	-	20,9	23,8	27,3	25,2	16,2	**23,9**

III.3.5 Delta-validation of nadir carbon monoxide column [SGP 5.01]

The CO column data from the new SCIAMACHY operational processor baseline SGP 7.03/5.01 have been evaluated and compared to ground-based FTIR data at Ny-Ålesund, Bremen and Jungfraujoch.

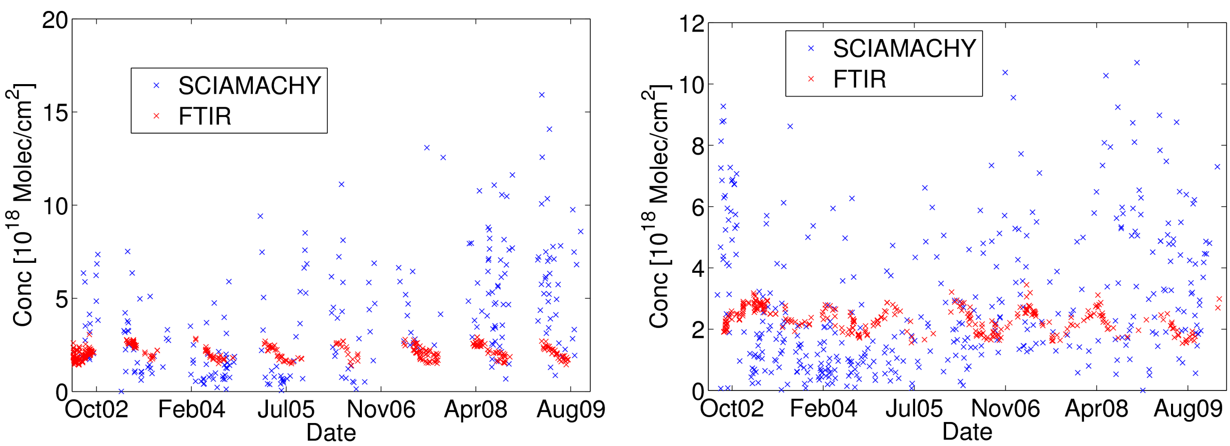

Figure 22: Comparison of the daily mean time series of the CO total column between SCIAMACHY SGP 5.01 and the FTIR stations Ny-Ålesund, Spitsbergen (left) and Bremen, Germany (right).

The SGP 5.01 CO total column data set suffers from a large amount of extreme outliers, zeros and negative values. Even after the elimination of these noisy data, no seasonal cycle is visible for SGP 5.01. Figure 22 presents the comparisons of the daily mean at the FTIR sites of Ny-Ålesund and Bremen. The CO column data are both inadequate in precision and accuracy.

III.3.6 Delta-validation of nadir bromine monoxide column [SGP 5.01]

The new nadir BrO column product has been validated against UV-visible measurements at Harestua, Norway. The latter were retrieved by applying an OEM-based profiling technique to sunrise zenith-sky BrO slant column density measurements [Hendrick et al., 2007; Hendrick et al., 2009]. The ground-based measurements were compared to data from SCIAMACHY when it passed within 300 km from the station. The correlative data were photochemically converted to the satellite overpass time.

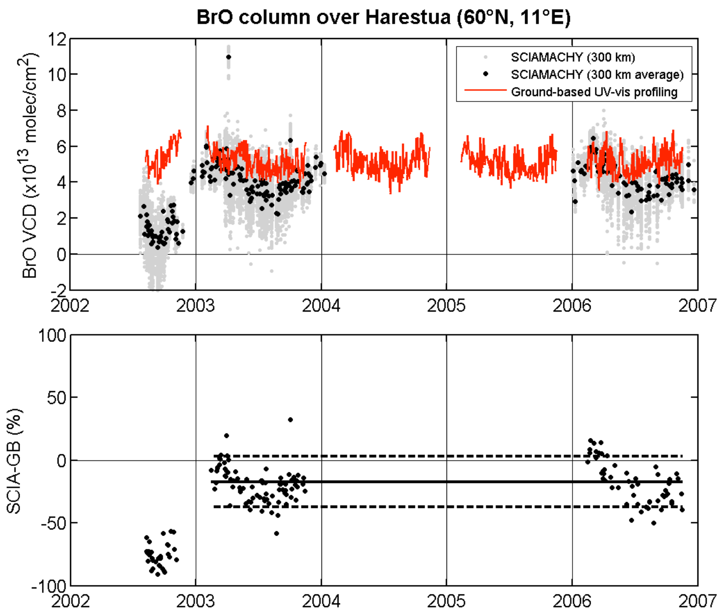

Figure 23: Time series of the BrO column (top) and the relative difference (bottom) between SCIAMACHY SGP 5.01 and correlative data at Harestua, Norway.

Figure 23 shows that the SGP 5.01 BrO column data have a stronger seasonality than the correlative measurements. For 2003 and 2006 the mean agreement, -17 ± 20%, is reasonably good. In 2002 SCIAMACHY has a significant low bias and even produces negative column values.

III.3.7 Validation of limb ozone profile [SGP 3.01]

Monthly statistics of the agreement between Envisat SCIAMACHY SGP 3.01 limb ozone profile data and correlative measurements from ozonesonde stations contributing to the Multi-TASTE project are provided as an electronic annex.

The results are detailed in Section III.5.1 on Multi-Mission studies.

III.3.8 Delta-validation of limb ozone profile [SGP 5.01]

We present the results of comparisons between SCIAMACHY limb ozone profile data (July 2002 to January 2010) and a large data set of correlative ozone profiles provided by ozonesondes and lidars operating in the NDACC, SHADOZ and GAW networks. We found that the SGP 5.01 profiles in the validation data set, which was described in Section III.3.1, co-located with profiles recorded at 48 ozonesonde and 9 lidar stations. For each SGP 5.01 profile the corresponding SGP 3.01 retrieval data was extracted as well, which allows a direct comparison between both processor versions.

The co-location criteria were chosen as the best compromise between a sufficient amount of comparison points and a sufficient co-location of the probed air masses. First, a maximum distance of 500 km between the ground-based station and the SCIAMACHY tangent point, and, second, a maximum time difference of 12h. Tightening the spatial criteria reduces the amount of co-locations strongly and hence limits the statistical relevance of the results.

We first excluded unreliable correlative and satellite measurements from the analysis. For the correlative data we based ourselves on the evolution in altitude, pressure, temperature and ozone number density to reject individual measurement points. Likewise, SCIAMACHY data points with an ozone density error larger than 500% were rejected, and, when more than five grid points satisfied this condition, the entire profile was removed. The correlative profiles were then box-averaged to the resolution of SCIAMACHY. And finally all data (satellite and ground-based) were linearly interpolated to a common altitude grid between 14 and 100 km. We remind the reader that this grid is coarser between 14 and 42 km for SGP 3.01, as explained in Section III.3.1.

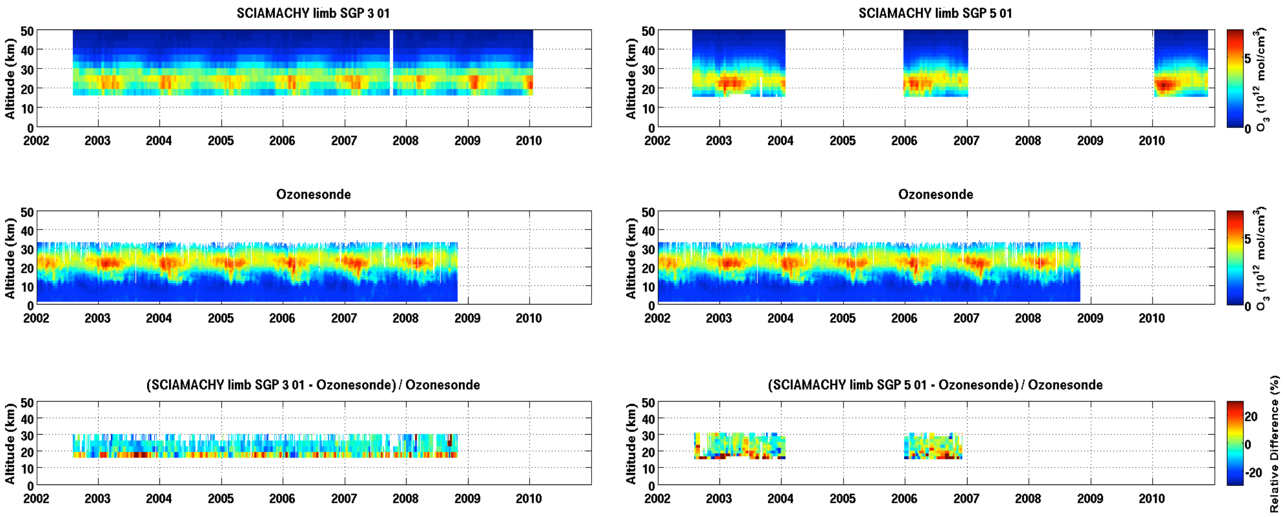

Figure 24: Time series of the ozone number density profile as measured by SCIAMACHY (top) and by the ozonesondes launched by RMI at the NDACC station in Uccle (centre). The bottom panels show the relative difference between the co-located profiles. Both SCIAMACHY processor versions are shown: SGP 3.01 (left) and SGP 5.01 (right).

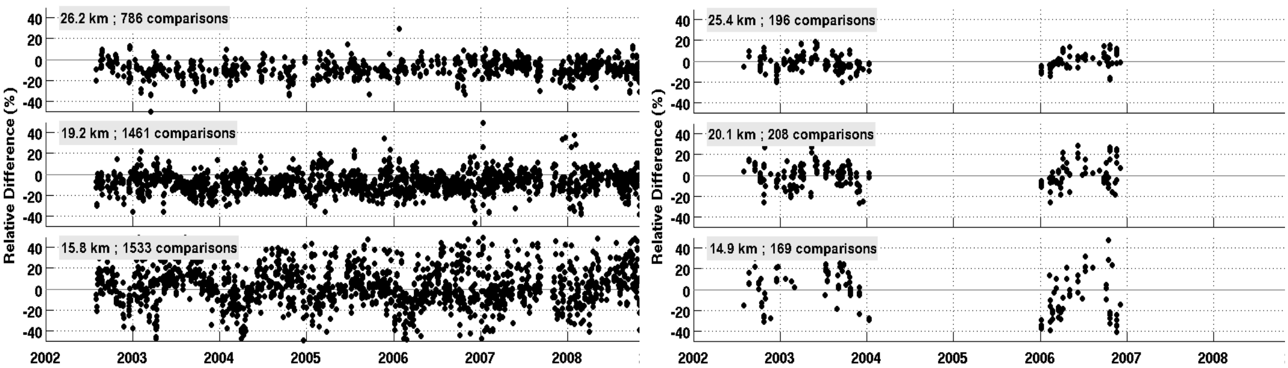

Figure 25: Time series of the relative difference between SCIAMACHY limb and co-located ozone profiles measured by RMI ozonesondes at Uccle, at various altitude levels. SGP 3.01 (left) and SGP 5.01 (right).

Figure 24 and Figure 25 illustrate the first part of the validation study, that is, the visual inspection and the statistical study of the individual time series at each station. The objective is to identify possible global features, cyclic errors and long-term drifts. Upper and central panels show the ozone profile as retrieved by the SCIAMACHY processors (left: SGP 3.01, right: SGP 5.01] and measured by ozonesondes launched by RMI at Uccle, respectively, while the bottom panel presents their relative difference, calculated as (satellite-ground)/ground. For a better visibility a one-month running mean is applied to all three time series.

The time series in Uccle shown in Figure 24 is representative of all ground stations: the qualitative temporal and vertical behaviour of SGP 3.01 and SGP 5.01 is in agreement with the correlative data for a wide range of atmospheric phenomena. Some hints of the existence of a seasonal cycle or drifts were observed, similar to the SGP 3.01 data at various stations (see Section III.5.1), but the validation data set is too small to be conclusive statistically. Such investigation will only be possible once the full data set has been reprocessed.

The absence of significant time-dependencies permitted the statistical study of the vertical structure of the relative differences between pairs of co-located profiles. This was done for each ground station; Figure 26 presents the results at the station of Uccle. The left panel shows the median (solid) and 68% inter-percentile (dashed) of the relative differences between SCIAMACHY and ozonesonde measurements for SGP 5.01 (blue) and SGP 3.01 (red). The right panel shows the median relative precision (dashed) and bias (solid) for SCIAMACHY (blue, red) and for the correlative data (grey). Unfortunately SCIAMACHY's bias is currently not reported. Three additional stations (Sodankylä, Payerne and Belgrano) are shown in Figure 27; these results are representative for the other ground-based stations.

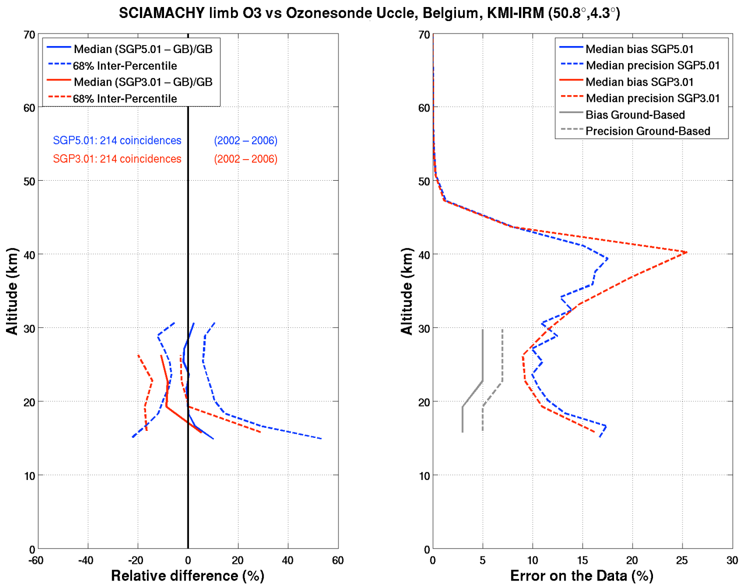

Figure 26 – left: vertical dependence of median (solid) and 68% inter-percentile (dashed) of the relative ozone number density differences between both SCIAMACHY processors (red, blue) and KMI-RMI ozonesonde data at Uccle, Belgium. Right panel: median relative precision (dashed) and bias (solid) for SCIAMACHY and correlative data. SCIAMACHY's systematic error has yet to be reported.

SCIAMACHY SGP 3.01 & SGP 5.01 vs FMI O3S Sodankylä (67.4N, 26.7E)

SCIAMACHY SGP 3.01 & SGP 5.01 vs MCH O3S Payerne (46.5N, 6.6W)

SCIAMACHY SGP 3.01 & SGP 5.01 vs FMI/INTA O3S Belgrano (77.9S, 34.6W)

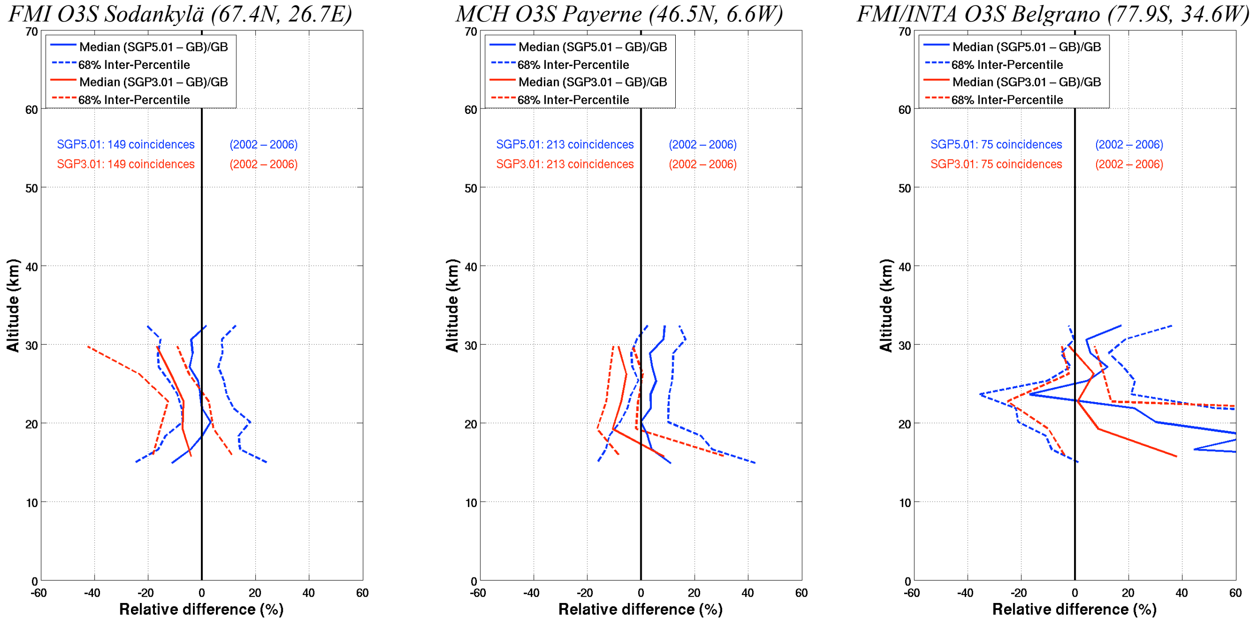

Figure 27: Vertical dependence of median (solid) and 68% inter-percentile (dashed) of the ozone number density differences between both SCIAMACHY processors (red, blue) and correlative data at three ozonesonde stations.

For high northern latitudes 50°-90°N the median agreement is ±(5-10)% between 19-25 km. Outside this altitude range, SGP 5.01 systematically underestimates the correlative data by 5-10%. For this latitude range the current version improves over SGP 3.01, which had an almost systematic 10% negative bias for all latitudes and altitudes (see Section III.5.1). At other latitudes the comparisons for SGP 5.01 seem not worse than for its predecessor, but a significant improvement is probably not present. At mid and low northern latitudes the median bias for SGP 5.01 is around ±10%. In the southern hemisphere the disagreement becomes larger, ±(20-30)%.

The precisions of both algorithms are very similar, between 10-15% depending on altitude. These values are in good agreement with the observed 10% half 68% inter-percentiles of the comparisons. An interesting observation is that the SGP 5.01 precision between 20-35 km shows an oscillating behaviour at most stations.

We would like to mention that, due to the restricted size of the validation data set, the previous quantitative conclusions should be treated with care. For some stations, especially in the southern hemisphere, few (<20) co-located profiles were found and some were recorded during challenging atmospheric conditions. It is clear that in this situation the comparison results will not be representative for the station. However, the results of our study were very similar for stations in the same latitude band, which provides some statistical strength. A larger data set will provide more robust quantitative conclusions.

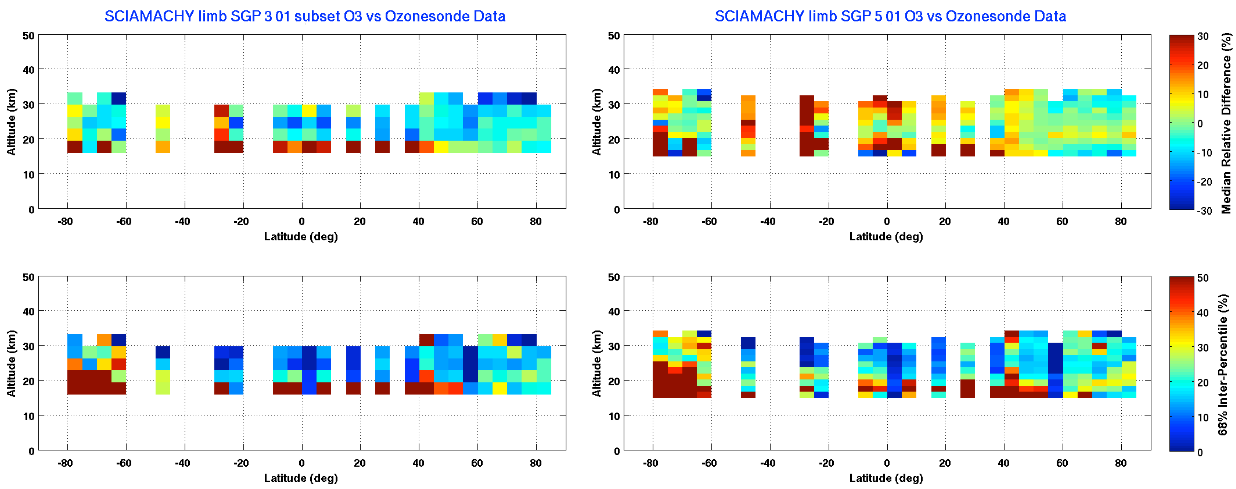

Figure 28: Median (top) and half 68% inter-percentile (bottom) of the relative difference between SCIAMACHY and ozonesonde data as a function of altitude and latitude; for SGP 3.01 (left) and SGP 5.01 (right).

Given the long-term stability and the similarity of the results for stations close in latitude, we derived multi-year and zonal statistics; see Figure 28 for ozonesonde stations (the lidar stations led to similar results). The medians (top) and half 68% inter-percentiles (bottom) of the relative differences are computed for all co-located ozone profiles within 5° latitude bands. The results are shown for both SGP 3.01 (left panel) and SGP 5.01 (right).

The previously reported improvement with respect to SGP 3.01 is clear at northern high latitudes between 19 and 25 km. In the tropics the bias seems larger than for SGP 3.01. In the southern hemisphere no clear improvement or deterioration is visible.

III.3.9 Validation of limb bromine monoxide profile [SGP 5.01]

The new limb BrO profile product has been validated against UV-visible measurements at Harestua, Norway. The latter were retrieved by applying an OEM-based profiling technique to sunrise zenith-sky BrO slant column density measurements [Hendrick et al., 2007; Hendrick et al., 2009].

The SGP 5.01 profiles were smoothed with the ground-based averaging kernels, due to the worse vertical resolution of the UV-visible data. Before comparing the SCIAMACHY and ground-based profiles that colocate within 500 km, the latter were photochemically converted to the solar zenith angle at the tangent point. For the 398 found coincidences, only the altitude range 15-27 km were considered, where the measurement response is maximal for the ground-based data.

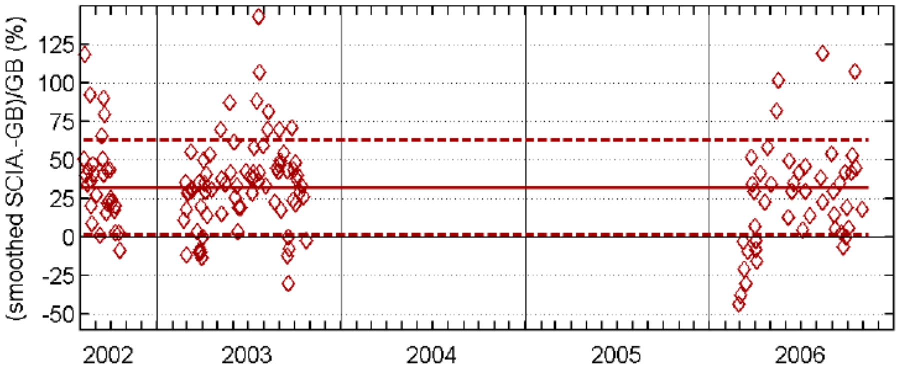

Figure 29: Time series of the relative difference of the 15-27 km BrO partial columns between SCIAMACHY SGP 5.01 and UV-visible data at Harestua, Norway.

Figure 29 presents the time series of the relative differences of the 15-27 km partial BrO columns. The operational SGP 5.01 data overestimate the correlative data, with a mean bias of 32% and an accuracy of 31%. The operational processor performs worse than the scientific processor of IUP-Bremen, which produces a positive mean bias of 4.5% with accuracy 19%.

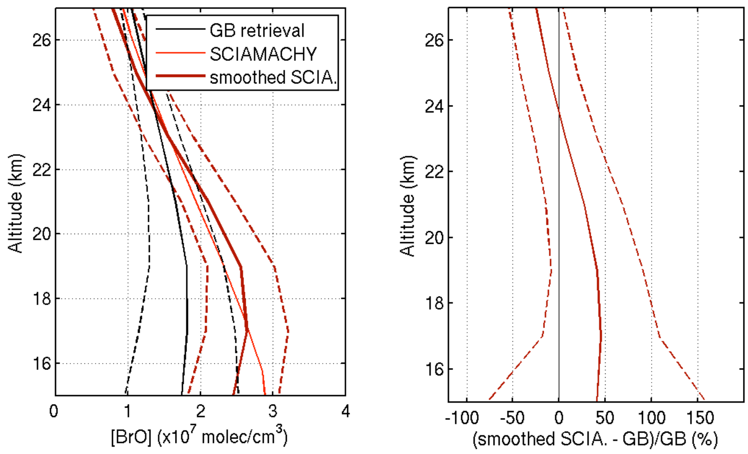

Figure 30 - left: Mean (solid) and 1σ standard deviation (dashed) of the UV-visible and SCIAMACHY SGP 5.01 profiles at Harestua, Norway. Right: vertical dependence of the relative difference of the smoothed SGP 5.01 and correlative data.

Figure 30 (left) shows the mean and spread of the correlative and SCIAMACHY profiles in the 15-27 km altitude range; the right panel presents the relative differences. There is a significantly large positive bias (up to 50%) between 15 and 21 km.

III.4 Third Party Missions: ACE-FTS and GOSAT TANSO

III.4.1 SCISAT-1 ACE FTS

Since the massive ACE v2.2 validation effort published in the ACE special issue of ACP, systematic intercomparisons with v2.2 data targeted by Multi-TASTE have been performed for ozone and temperature (hereafter), as well as for OCS, HF and HCN [Li et al., 2009; Duchatelet et al., 2010, Lejeune et al., 2010, Mahieu et al., 2010]. Validation efforts are ongoing for OCS and HF (manuscripts in preparation) and for the newly available version 3.

III.4.1.1 SCISAT-1 ACE-FTS ozone profile [v2.2]

Validation of ACE-FTS ozone profile data version 2.2 has been the subject of a coordinated international validation effort [Dupuy et al., 2009] involving comparisons with satellite, ground- and balloon-based instruments. Multi-TASTE partners have contributed significantly to this international validation effort with comparisons of the ACE-FTS ozone profiles to the correlative observations from ozonesondes and ozone lidars, and archived in international databases (NDACC, WOUDC). We present in Section III.5 on Multi-mission Studies an update of the validation of ACE-FTS ozone profiles. Monthly statistics of the agreement between SCISAT-1 ACE-FTS v2.2 ozone profile data and correlative measurements from ozonesonde stations contributing to the Multi-TASTE project are provided as an electronic annex.

III.4.1.2 SCISAT-1 ACE-FTS temperature profile [v2.2]

Validation of ACE-FTS temperature profile data version 2.2 has been the subject of a coordinated international validation effort [Sica et al., 2008] involving comparisons with satellite, ground- and balloon-based instruments. Multi-TASTE partners have contributed significantly to this international validation effort with comparisons of the ACE-FTS temperature profiles to the correlative observations from radiosondes and temperature lidars, and archived in international databases (NDACC, WOUDC). We present here an update of the comparison between ACE-FTS temperature profiles (from January 2004 to May 2009) and temperature profiles recorded by 38 balloon-borne radiosondes and by 6 NDACC temperature lidars.

The orbital inclination of the SCISAT-1 platform is such that the solar occultation measurements occur mainly at polar and mid-latitudes. Co-location criteria were chosen as the best compromise between a sufficient amount of comparison pairs and a sufficient co-location of the probed air masses: a maximum distance of 500 km between the ground-based station and the ACE tangent point and a maximum time difference of 12h.

We excluded unreliable correlative and satellite measurements from the analysis. For the correlative data we based ourselves on the evolution in altitude, pressure and temperature to reject individual measurement points. Likewise, ACE-FTS data points with a temperature retrieval error larger than 500% were rejected, and, when more than five grid points satisfied this condition, the entire profile was removed. The correlative profiles were box-averaged to the satellite resolution, before all data (satellite and ground-based) were linearly interpolated to a common altitude grid between 12-120 km.

The statistical study of the vertical structure of the differences between pairs of co-located profiles is presented in Figure 31 for the radiosonde measurements at Ny-Ålesund (Svalbard) and Belgrano (Antarctica) and the lidar measurements at Observatoire Haute Provence (France). The plot shows the median (solid) and 68% inter-percentile (dashed) of the absolute temperature differences between ACE-FTS and correlative measurements. These results are representative for the other ground-based stations.

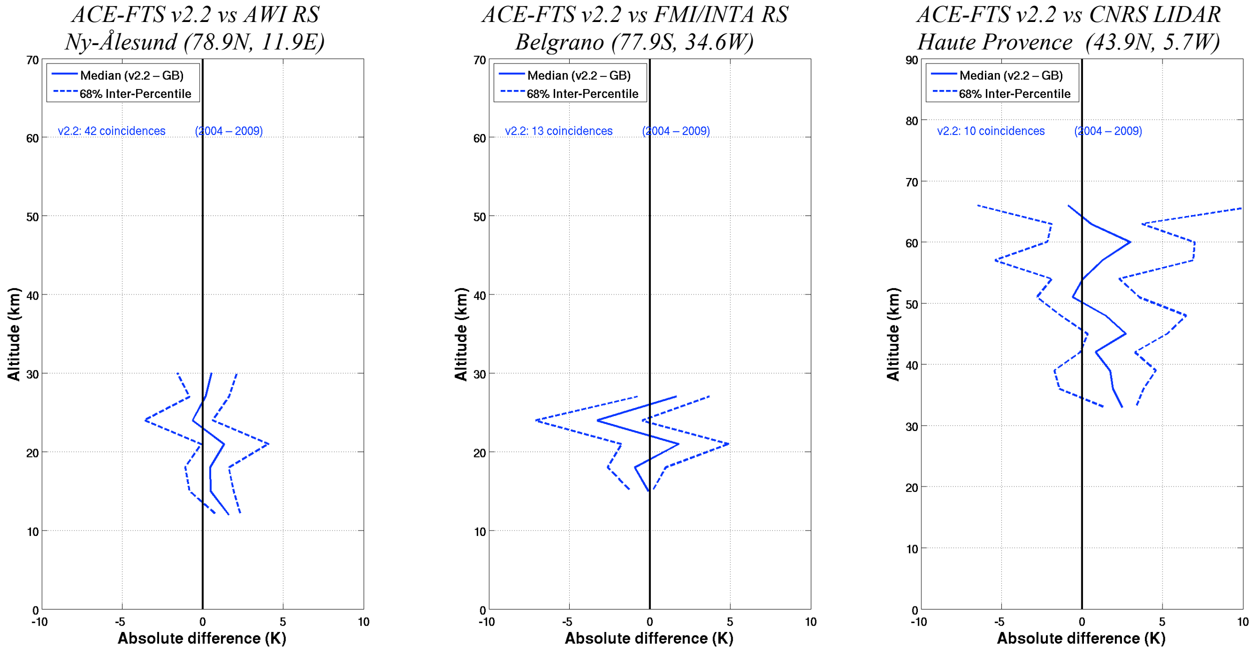

Figure 31: Vertical dependence of median (solid) and 68% inter-percentile (dashed) of the absolute temperature differences between ACE-FTS v2.2 and radiosondes (left, centre) and lidar (right).

This analysis update confirms the conclusions of the previous report. From 10 to 30km, a median difference within ±2K is observed. The previously reported unphysical oscillating structures in the ACE temperature profiles affect the comparisons and result in oscillations with altitude of the median temperature difference. Even though the larger vertical step size (3 km compared to 1 km in previous report) averages this effect more out, it remains clearly visible. The oscillation amplitude and hence the 68% inter-percentile increases with altitude, from ±1K at 10 km to ±2K at 30 km. The apparent +2K median bias with respect to lidar measurements in the higher stratosphere may be explained by the difference in measurement time and atmospheric tides.

Monthly statistics of the agreement between SCISAT-1 ACE-FTS v2.2 temperature profile data and correlative measurements from radiosonde stations contributing to the Multi-TASTE project are provided as an electronic annex.

III.4.2 GOSAT TANSO

Many of the Multi-TASTE partners operating NDACC-affiliated FTIR instruments are expanding their measurement capabilities to the near infrared (NIR), in an effort to join TCCON (http://www.tccon.caltech.edu/), the Total Carbon Column Observatory Network. Some instruments are already working in time sharing between regular NDACC-type measurements and TCCON/GOSAT activities, like the Bruker 120HR operated at Lauder. Developed initially to support the validation of NASA's OCO satellite, TCCON is also intended to support the geophysical validation and algorithm verification of CO_2 column data acquired by GOSAT, successfully launched by JAXA in January 2009. IUP has submitted a proposal in response to the GOSAT Research Announcement, aiming at performing GOSAT validation and exploiting potential synergies with SCIAMACHY SWIR validation. This GOSAT validation project includes the FTIR sites in Spitsbergen and Bremen plus two new sites in Bialystok (Poland) and Orléans (France). IASB-BIRA has also installed a Bruker 125 HR FTIR instrument at La Reunion, to be fully operational by summer 2011 at latest. We hope to contribute with the observations made with this instrument to the validation of CO_2 and CH_4 from SCIAMACHY and GOSAT (and OCO-2).

III.5 Multi-mission studies

III.5.1 Multi-mission consistency of Envisat and TPM limb ozone profilers

III.5.1.1 Introduction

In the framework of the Multi-TASTE project and of external projects like Belgian Science Policy Office/ProDEX SECPEA and EC FP6 IP GEOmon, networks of ozonesonde and lidar stations have been used as a standard transfer to investigate the consistency of Envisat ozone profile data, of data records from historical satellites, and of more contemporary sensors like ACE-FTS and Aura-MLS data. These results have been updated with the latest data available and presented publicly at ESA's Living Planet Symposium held in Bergen, Norway (28 June - 2 July 2010) and reported in the conference proceedings (see Section IV.4 for references). Hereafter we present a summary of the main validation results of ESA Envisat GOMOS v6.0cf / IPF 5.00, MIPAS IPF 4.61/4.62, SCIAMACHY limb SGP 3.01, of CSA SCISAT-1 ACE-FTS v2.2 updated and of NRL/CNES/ONR SPOT-3 POAM-II v5 and SPOT-4 POAM-III v4 ozone profile data.

Monthly statistics of the agreement between ozone profiles from GOMOS, MIPAS, SCIAMACHY and ACE-FTS, and correlative ozonesonde data from stations contributing to Multi-TASTE, are provided as an electronic annex.

III.5.1.2 Description of ozone profile data sets

GOMOS operates successfully since July 2002 except for an anomaly in 2005 that resulted in a gap in the data. Previous validation studies of successive GOMOS ozone profile data versions have shown that only data acquired on dark limb are of sufficient quality for scientific use [Meijer et al., 2004; De Clercq et al., 2004]. Comparisons between dark limb profiles of the latest reprocessed version 6.0cf and ground-based ozonesondes and lidars have shown a typical agreement within 10% from 20 km up to 50 km [De Clercq et al., 2006]. In this report we use GOMOS ozone data from the latest reprocessing (version 6.0cf) and its operational implementation IPF 5.00. Only dark limb data have been selected (including straylight data).

MIPAS operated at full resolution from July 2002 till March 2004, when the instrument experienced a major anomaly. In January 2005 operations were resumed in an optimized resolution mode, not studied here. Latest versions of the profile retrievals at full resolution, IPF 4.61 and 4.62, were the subject of an extensive validation effort. MIPAS profiles were compared to those of several other satellites, balloons and ground-based instruments [Cortesi et al., 2007]. This coordinated study concluded to a typical agreement within ±10% from 20 to 50 km and highlights a significant positive bias of up to +25% in the Upper Troposphere Lower Stratosphere (UTLS). In this study, we used ozone data from both versions IPF 4.61 and IPF 4.62. The results of an initial validation effort of the latest version of the processor (IPF 5.04), which is able to handle both full and optimized resolution scenarios, can be found in Section III.2.3.

Previous SCIAMACHY Ground Processor (SGP) retrievals suffered from pointing errors [De Clercq et al., 2004; De Clercq et al., 2006; von Savigny et al., 2003] and the retrieved ozone profiles exhibited an altitude shift of 0 to 1.5 km. Accordingly, comparisons concluded to an altitude-dependent bias of up to ±20%. SGP version 3.01 retrieves ozone profiles on an altitude grid between 15 and 40 km and includes a pointing correction that should reduce the altitude uncertainty to less than 500 m, and thus the bias. Retrievals from the recently activated processor version, SGP 5.01, are not considered here, the results of an initial validation effort can be found in Section III.3.8.

CSA's Atmospheric Chemistry Experiment Fourier Transform Spectrometer (ACE-FTS) onboard SCISAT-1 uses the infrared solar occultation technique from an orbit at 75° inclination. The latest version of ACE-FTS ozone profiles is version 2.2 updated. This data set has been the subject of a coordinated international validation [Dupuy et al., 2009] involving comparisons with satellite, ground- and balloon-based instruments. The study concluded to a typical agreement of the ACE-FTS profile data within 5% between 15 and 45 km, with a small positive bias in ACE-FTS data with respect to correlative data.

Operating from a polar orbit, NRL's Polar Ozone and Aerosol Measurement II and III (POAM-II and III) aboard the polar orbiting French platforms SPOT-3/4, measured ozone profiles, from 1993 to 1996 and from 1998 to 2005 respectively, with coverage of the polar zones but no measurement at latitudes below about 56°. POAM-II v5 ozone profiles have been compared to measurements from satellites and from ozonesondes [Rusch et al., 1997; Deniel et al., 1997]. The POAM-II data show a typical mean agreement within 5-7% above 22 km, with in general a negative bias of a few percents with respect to correlative measurements. Studies based on the current version 6 show similar results and also depict a negative bias [Danilin et al., 2002]. The current version of POAM-III ozone profile data is v4. The previous version v3 had been extensively validated using observations from aircrafts, balloons and satellite instruments [Randall et al., 2003]. These studies showed a typical agreement of ±5% from 13 to 60 km. Minor changes have been implemented in the current version v4 for ozone retrieval and comparisons with correlative data show a similar agreement than for v3.

For this preliminary study we have adopted basic coincidence criteria based on the maximum distance between the tangent point at the ozone maximum and the location of the ground-based stations. Even though more accurate selection methods do exist, given the horizontal resolutions of the satellite and ground-based measurements, a maximum distance of 500 km was found as the best compromise between a sufficient coincidence of the air masses to be compared and a sufficient amount of co-located pairs of profiles. While the selection of horizontal coincidence criteria can offer some flexibility, temporal distance criteria are constrained directly by the measurement time of the data being compared, which depend on parameters like the radiation source and the orbit inclination. In this exercise, the time difference between ground-based and satellite measurements varies from 0 to maximum 12 hours. Co-locations of satellite and ground-based profiles have been identified according to the above criteria for 50 ozonesonde and 10 lidar stations.

III.5.1.3 Comparison results

III.5.1.3.1 Seasonal and long-term features

In this first part of our study, we analyze time series of the relative differences between satellite and correlative data at selected altitude/pressure levels. In particular, we look for any seasonal feature or long-term drift. To determine if a long-term drift exists, a robust linear regression is undertaken. No regression is done if the standard deviation of the data set exceeds 30 %, or if the time series comprises less than 20 co-located pairs of profiles. The slope of this regression is considered to be significantly different from zero if zero is not in the 95% confidence interval (slope ± 2 * error) of the calculated slope. The error on the calculated slope is obtained using standard statistics, to which the effect of noise autocorrelation is added.

This temporal analysis has been performed for each satellite at each selected ground-based station. Graphs representing the drifts as a function of the latitude, for different altitude levels, are shown in Figures 32-34. Significant drifts are plotted in red (for comparisons with lidar data) or blue (for comparisons with ozonesonde data) while non-significant drifts are plotted in grey. The 95% confidence intervals are also displayed as a bar of the same colour as the drift.

In order for the presence of drifts to be detected, a sufficiently long time series of data and a sufficient number of coincident pairs of profiles is required. For this reason, the analysis is inconclusive for MIPAS, ACE-FTS and POAM-II/III. For these instruments, drifts are indeed detected, but they are not significant and/or not consistent from station to station (see for example Figure 32 for MIPAS). This analysis will probably improve for ACE-FTS when the time series get longer. For MIPAS, the upcoming optimized resolution data will allow a new drift analysis to be undertaken, on a longer time series.

For GOMOS and SCIAMACHY, the analysis revealed significant drifts, even if they are not fully consistent from station to station. GOMOS data (Figure 33) show negative drifts of 1 to 2% per year at Northern mid-latitudes, from 20 to 30 km altitude. SCIAMACHY data (Figure 34) present positive drifts of 1 to 2% per year at 26 km altitude, all latitudes; and negative drifts of 1 to 2% per year at 19 km altitude, high Northern latitudes.

Besides drifts, seasonal features were observed as well in SCIAMACHY comparison data, over the whole altitude range. The relative differences with ground-based data are more positive (or less negative where there is a negative bias) in the summer, and more negative in the winter. The amplitude of the seasonal cycle is about 10%. Both seasonal cycle and drifts might be reduced by the new SGP 5.01 algorithm. Initial SGP 5.01 validation results can be found in Section III.3.8.

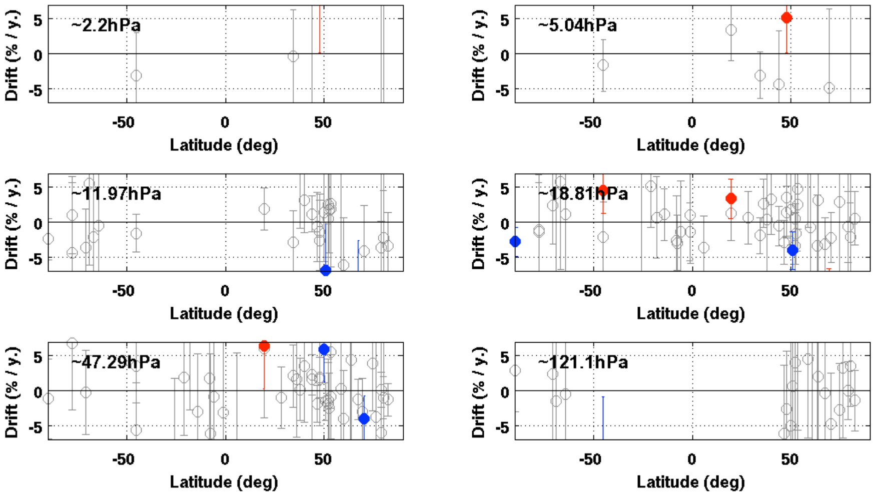

Figure 32: Slope of the multi-year linear trend fitted to time series of the relative differences between MIPAS IPF 4.61/4.62 and ground-based (ozonesonde and lidar) ozone measurements at each station, plotted as a function of latitude and at different pressure levels. Red dots (comparisons vs. lidars) and blue dots (comparisons vs. ozonesondes) represent trends with statistical significance (95% confidence level). Trends with no significance are shown in grey

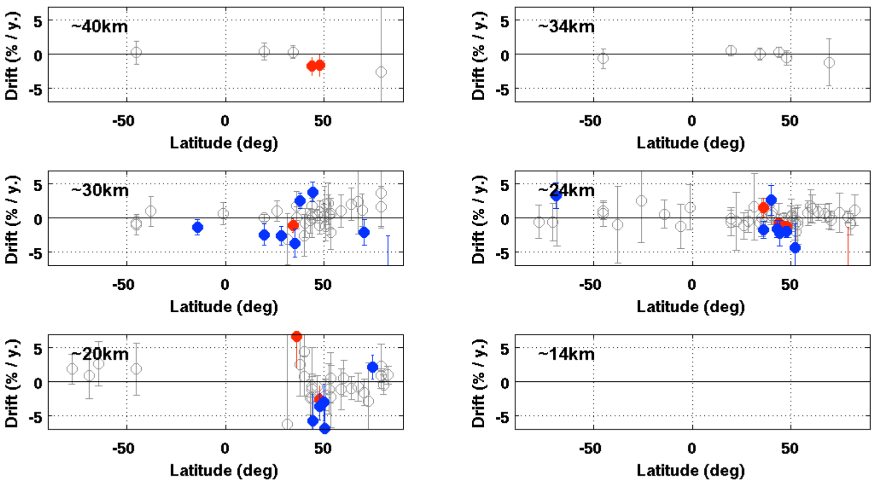

Figure 33: Same as Figure 32 for GOMOS IPF 5.00 / GOPR 6.0cf at different altitude levels.

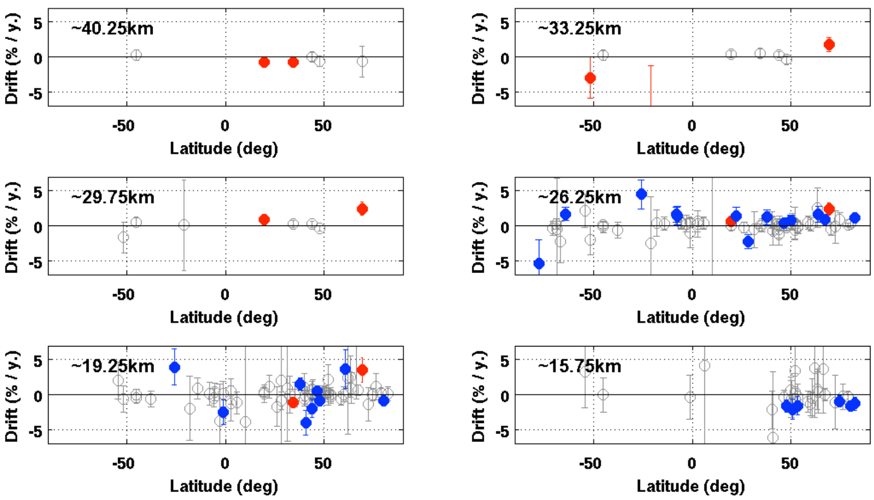

Figure 34: Same as Figure 32 for SCIAMACHY SGP 3.01 at different altitude levels.

III.5.1.3.2 Meridian and vertical structures

While the agreement between satellite and ground-based data varies with altitude and latitude, it does not vary between stations close in latitude and it shows long-term stability for most satellites. These findings allow us to derive multi-year and zonal statistics, which we use hereafter to study meridian and vertical features of the consistency between the various satellites. Figures 35-38 show, as a function of latitude and altitude, the median relative difference between satellite and correlative ground-based data, averaged into 5°-wide latitude bins.

In general, the mean agreement between satellite and ground-based data in the stratosphere is 7% or better, with a standard deviation of about 10%. In the following paragraphs we discuss the features which differ from the general one.

For GOMOS (35), a mean negative bias of 10% is observed at Arctic stations. The GOMOS Quality Working Group (QWG) is investigating possible links between this bias and the contamination of GOMOS spectra by auroral light.

The MIPAS data (Figure 36) show a permanent positive bias of 10 to 15% in the inter-tropical upper troposphere and lower stratosphere.

The SCIAMACHY comparison data (Figure 37) bear a negative bias of about 10% at all altitudes. The stability of this bias with altitude indicates that the altitude pointing correction implemented in SGP 3.01 is working properly.

ACE-FTS data (38) do not show any feature different from those of the satellite datasets described before. The orbital inclination of ACE is such that the amount of collocations with ground-based data at tropical sites is too weak to derive statistics. Consequently, only polar and mid-latitude regions have been considered in this meridian analysis.

Our analysis using the ground-based networks as standard transfer confirms a 5% bias between POAM-II and POAM-III datasets, even though both agree with ground-based data within about 7% like the other instruments.

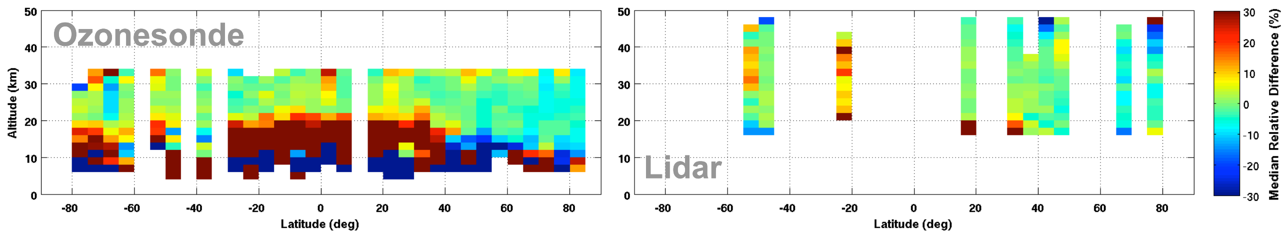

Figure 35: Median relative differences between GOMOS IPF 5.00 / GOPR 6.0cf and ozonesonde (left) or lidar (right) ozone profile data, as a function of altitude and latitude.

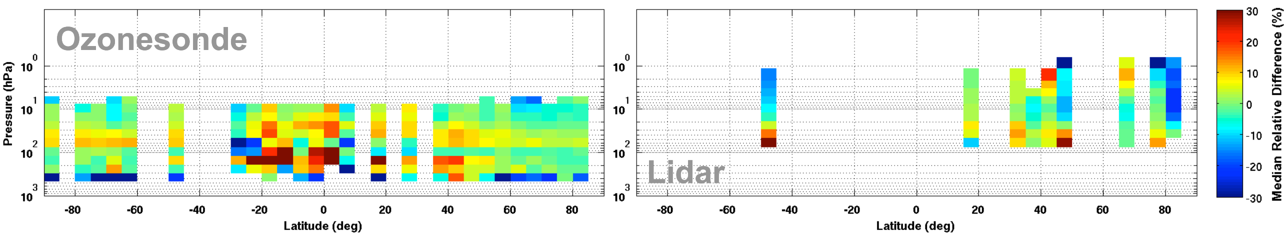

Figure 36: Same as Figure 35, for MIPAS IPF 4.61/4.62 data.

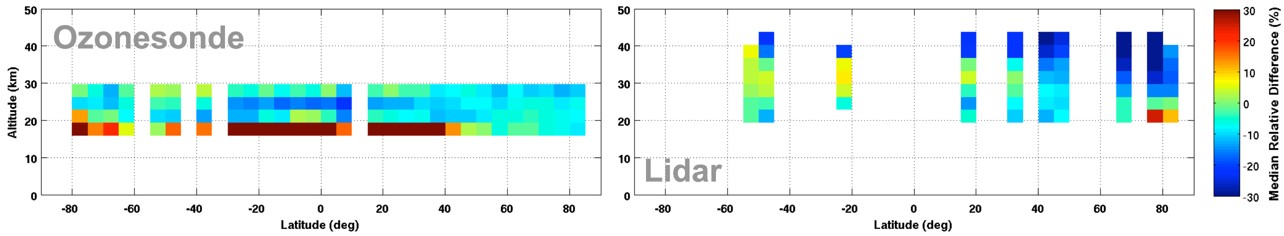

Figure 37: Same as Figure 35, for SCIAMACHY SGP 3.01 data

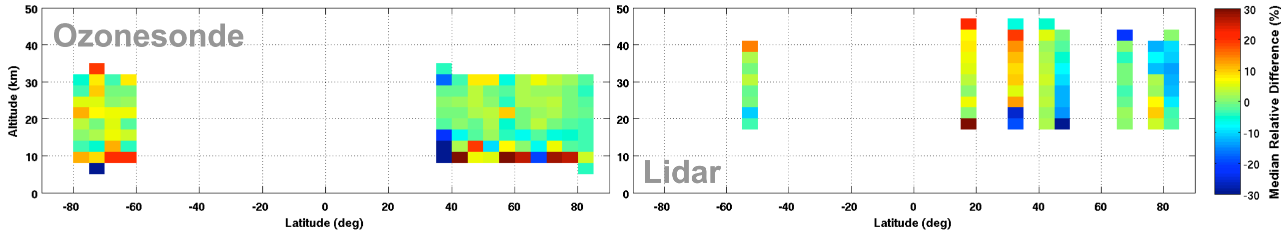

Figure 38: Same as Figure 35, for ACE-FTS v2.2 updated data

III.5.1.3.3 Lowest altitude with statistical quality

Interferences with aerosols and clouds limit the access of limb sounding to accurate information on the UTLS and the troposphere. As a consequence, below an altitude threshold usually varying between 10 and 20 km depending on the instrument measurement technique and the aerosol load, the quality of individual profiles can differ significantly from the quality estimates derived statistically from comparisons with correlative data. Above this threshold altitude the ozone profiles agree statistically with ground-based network data, below this altitude the data quality varies strongly from one profile to another. Using the meridian and vertical analysis results reported above, we estimate here the respective threshold altitude of the limb sounders by two different means. The upper panel of Figure 39 shows the altitude below which the median relative difference exceeds 20%, while the lower panel shows the altitude below which the half 68% inter-percentile exceeds 30%. These two criteria give similar results.

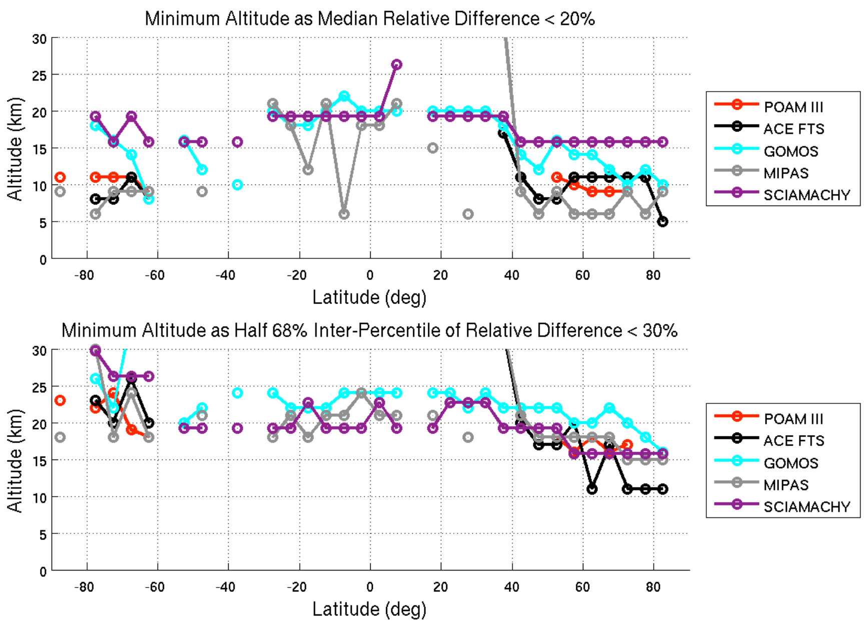

Figure 39: Threshold altitude of satellite measurements, below which median relative differences exceed systematically 20% (top panel) and below which half 68% inter-percentiles exceed systematically 30% (bottom panel).

The threshold altitude is found to vary as a function of latitude, likely following the meridian variation of the tropopause height, from 8 km in the Arctic to 20 km at low latitudes. It varies also primarily with the viewing technique and its radiation source: it is the lowest for infrared sounding (10 to 15 km) and the highest for UV-visible scattering and star occultation (15 to 20 km). In the star occultation case, atmospheric scintillation, which increases as the atmosphere becomes denser, adds to the radiative transfer perturbations caused by aerosols and clouds.

III.5.1.4 Conclusion

In the stratosphere, the analysis concludes to a mutual consistency of the studied ozone profile data records, to within 7% ± 10%. However, a few exceptions and peculiarities have been detected and reported:

- GOMOS IPF 5.00 / GOPR 6.0cf ozone profiles have a negative bias of 10% in the Arctic.
- MIPAS IPF 4.61/4.62 ozone profiles have a positive bias of 10% in the inter-tropical UTLS.
- Over the entire altitude range, SCIAMACHY SGP 3.01 underestimates ozone densities by 10%.
- Although both agree with ground-based data with a mean difference within ±7%, we confirm a 5% bias between POAM-II and POAM-III ozone data.

For most of the data sets, the observed agreement seems to remain stable along the satellite measurement period. However, due to the short time series of the available data and/or the low time sampling, the current non-detection of drifts does not guarantee the temporal stability of the data set. Exceptions to the absence of drifts are GOMOS and SCIAMACHY. GOMOS bears a negative drift of 1 to 2% per year from 20 to 30 km altitude at Northern mid-latitudes. SCIAMACHY, in addition to a seasonal behaviour, shows positive drifts of 1 to 2% per year at 26 km altitude at all latitudes and negative drifts of 1 to 2% per year at 19 km altitude at high Northern latitudes. However, for both GOMOS and SCIAMACHY, the analysis is not fully consistent from station to station and would greatly benefit from the extension of the time series. The use of both datasets for the establishment of long-term ozone profile time series is limited by the presence of drifts.

Below 10-20 km, the ozone profile data quality of any limb sounding instrument degrades rapidly, and should not be used in the establishment of long-term ozone profile records. This study shows that the threshold altitude (defined here as the lowermost altitude below which the mean difference with ground-based data exceeds 20% or the standard deviation exceeds 30%) varies with the latitude and the measurement technique. Lowest altitudes (10 km at the poles and 15 km at the tropics) are reached by infrared sounders like ACE-FTS and MIPAS, while scintillation limits this altitude to 18-20 km for the GOMOS star occultation instrument and scattering limits this altitude to 15-20 km for the SCIAMACHY UV visible instrument.

This work shows that ground-based networks can be used successfully as a standard transfer to investigate the consistency of ozone profile data records from (very) different satellites. However, we should remark that the station-to-station homogeneity of network data sets can depend on a variety of factors, like differences in instrument maintenance, operation, calibration, data retrieval, as well as the range of measured atmospheric states, which also varies from one station to another. Therefore, statistical studies should always be carried out wit the greatest care. Considering the accuracy achieved currently by satellite ozone profilers, the internal consistency of the networks seems to be sufficient for multi-mission analysis, after appropriate selection of ground-based stations.

III.6 References

Cortesi, U., Lambert, J. C., De Clercq, C., Bianchini, G., Blumenstock, T., Bracher, A., Castelli, E., Catoire, V., Chance, K. V., De Mazière, M., Demoulin, P., Godin-Beekmann, S., Jones, N., Jucks, K., Keim, C., Kerzenmacher, T., Kuellmann, H., Kuttippurath, J., Iarlori, M., Liu, G. Y., Liu, Y., McDermid, I. S., Meijer, Y. J., Mencaraglia, F., Mikuteit, S., Oelhaf, H., Piccolo, C., Pirre, M., Raspollini, P., Ravegnani, F., Reburn, W. J., Redaelli, G., Remedios, J. J., Sembhi, H., Smale, D., Steck, T., Taddei, A., Varotsos, C., Vigouroux, C., Waterfall, A., Wetzel, G., and Wood, S.: Geophysical validation of MIPAS-Envisat operational ozone data, Atmos. Chem. Phys., 7, 4807-4867, doi:10.5194/acp-7-4807-2007, 2007.

Danilin, M. Y., M. K. W. Ko, L. Froidevaux, M. L. Santee, L. V. Lyjak, R. M. Bevilacqua, J. M. Zawodny, Y. Sasano, H. Irie, Y. Kondo, J. M. Russell III, C. J. Scott, W. G. Read, Trajectory hunting as an effective technique to validate multiplatform measurements: Analysis of the MLS, HALOE, SAGE-II, ILAS, and POAM-II data in October-November 1996, J. Geophys. Res., 107(D20), 4420-4438, doi:10.1029/2001JD002012, 2002.

De Clercq, C., Lambert, J.-C., Calisesi, Y., Claude, H., Stubi, R., von Savigny, C., et al. (2004), Integrated Characterisation of ENVISAT Ozone Profile Data Using Ground-based Network Data, Proc. ERS-ENVISAT Symposium, Salzburg, ESA SP-572.

De Clercq, C., Gerard, P., Granville, J., Lambert, J., et al. (2006), Geophysical consistency of ENVISAT ozone profile data with Global Atmosphere Watch pole to-pole network measurements, Proc. Atmos. Chem. Validation of Envisat-3 (ACVE-3), Frascati.

Deniel, C., F. Dalaudier, E. Chasseféire, R. Bevilacqua, E. Shettle, K. Hoppel, J. Hornstein, J. Lumpe, D. Rusch, C. Randall, A comparative study of POAMII and electrochemical concentration cell ozonesonde measurements obtained over northern Europe, J. Geophys. Res., 102(D19), 23629-23642, 1997

Dupuy et al., 2009, full reference in Section IV.2.

Hendrick et al., 2007, full reference in Section II.5.

Hendrick et al., 2009, full reference in Section II.5.

Meijer, Y. J., et al., Pole-to-pole validation of Envisat GOMOS ozone profiles using data from ground-based and balloon sonde measurements, J. Geophys. Res., 109, D23305, doi:10.1029/2004JD004834, 2004.

Payan, et al., 2009, full reference in Section.

Randall, C. E., et al., Validation of POAM III ozone: Comparisons with ozonesonde and satellite data, J. Geophys. Res., 108, 4367, doi:10.1029/2002JD002944, 2003.

Ridolfi, M., Blum, U., Carli, B., Catoire, V., Ceccherini, S., Claude, H., De Clercq, C., Fricke, K. H., Friedl-Vallon, F., Iarlori, M., Keckhut, P., Kerridge, B., Lambert, J.-C., Meijer, Y. J., Mona, L., Oelhaf, H., Pappalardo, G., Pirre, M., Rizi, V., Robert, C., Swart, D., von Clarmann, T., Waterfall, A., and Wetzel, G.: Geophysical validation of temperature retrieved by the ESA processor from MIPAS/ENVISAT atmospheric limb-emission measurements, Atmos. Chem. Phys., 7, 4459-4487, doi:10.5194/acp-7-4459-2007, 2007.

Rusch, D., et al., Validation of POAM ozone measurements with coincident MLS, HALOE, and SAGE II observations, J. Geophys. Res., 102(D19), 23615-23627., 1997.

Sica, R.J., M.R.M. Izawa, K.A. Walker, C. Boone, S.V. Petelina, P.S. Argall, P. Bernath, G. B. Burns, V. Catoire, R.L. Collins, W.H. Daffer, C. De Clercq, Z.Y. Fan, B.J. Firanski, W.J.R. French, P. Gerard, M. Gerding, J. Granville, J.L. Innis, P. Keckhut, T. Kerzenmacher, A.R. Klekociuk, E. Kyrö, J.C. Lambert, E.J. Llewellyn, G.L. Manney, I.S. McDermid, K. Mizutani, Y. Murayama, C. Piccolo, P. Raspollini, M. Ridolfi, C. Robert, W. Steinbrecht, K.B. Strawbridge, K. Strong, R. Stübi, B. Thurairajah: Validation of the Atmospheric Chemistry Experiment (ACE) version 2.2 temperature using ground-based and space-borne measurements, Atmos. Chem. Phys., 8, 35-62, 2008, doi:10.5194/acp-8-35-2008.

Sussmann, R., F. Forster, T. Borsdorff, B. Dils, M. De Mazière, C. Vigouroux, T. Blumenstock, M. Buchwitz, J.P. Burrows, P. Duchatelet, C. Frankenberg, J. Hannigan, F. Hase, N. Jones, J. Klyft, E. Mahieu, J. Mellqvist, J. Notholt, K. Petersen, O. Schneising, K. Strong, J. Taylor, Satellite validation of column-averaged methane on global scale: Harmonized data from 13 FTIR ground stations versus last generation ENVISAT/SCIAMACHY retrievals, Verhandl. DPG (VI) 44, 2009, UP 10.5, http://www.dpg-verhandlungen.de/2009/hamburg/up10.pdf (Poster).

von Savigny, C., Rozanov, A., Bovensmann, H., Noël, S., and Kaiser, J. W., SCIAMACHY Limb Pointing Analysis Report, SCIAMACHY Technical Report, University of Bremen, 2003.

Wang, D. Y., Höpfner, M., Mengistu Tsidu, G., Stiller, G. P., von Clarmann, T., Fischer, H., Blumenstock, T., Glatthor, N., Grabowski, U., Hase, F., Kellmann, S., Linden, A., Milz, M., Oelhaf, H., Schneider, M., Steck, T., Wetzel, G., López-Puertas, M., Funke, B., Koukouli, M. E., Nakajima, H., Sugita, T., Irie, H., Urban, J., Murtagh, D., Santee, M. L., Toon, G., Gunson, M. R., Irion, F. W., Boone, C. D., Walker, K., and Bernath, P. F.: Validation of nitric acid retrieved by the IMK-IAA processor from MIPAS/ENVISAT measurements, Atmos. Chem. Phys., 7, 721-738, doi:10.5194/acp-7-721-2007, 2007.

IV ANNEXE 1: MEETINGS, ARTICLES AND PRESENTATIONS

IV.1 Meetings

2009

- NDACC Steering Committee meeting 2009, WMO, Geneva, Switzerland, Sep. 29-Oct. 2, 2009.
- GEOmon Activity 4 (stratosphere) Workshop, Paris, France, October 5-6, 2009.
- IMECC mid-term review meeting, Gembloux, Belgium, 6 October 2009.
- GOMOS Quality Working Group Meeting #21, ESRIN, Frascati, Italy, October 6, 2009.
- Metadata Board meeting, Brussels, Belgium, October 7-8, 2009.
- HYMN workshop and final meeting, Brussels, Belgium, October 12-14, 2009.
- O3M-SAF PT Meeting, Copenhagen, Denmark, October 27-28, 2009.
- PROMOTE Final Meeting, ESRIN, Frascati, Italy, October 29-30, 2009.
- 5th Atmospheric Limb conference, FMI, Helsinki, Finland, November 16-19, 2009.

2010

- 3rd GEOmon General Assembly, London, UK, January 18-20, 2010.
- CEOS WGCV ACSG meeting, February 11-12, 2010.
- CEOS WGCV-31 meeting, NIST at the Bolger Center, Potomac, MD, USA, March 2-4, 2010.
- 2nd CINDI workshop, BIRA-IASB, Brussels, Belgium, March 10-11, 2010.
- Swiss National GAW meeting, MeteoSchweiz, Zürich, Switzerland, April 9, 2010.
- EGU General Assembly, Vienna, Austria, May 2-7, 2010.
- ACE Science team meeting, Waterloo, Canada, May 26-27, 2010.
- NDACC-IRWG annual meeting, Murramarang, Australia, June 2-4, 2010.
- 27th Nordic Meteorologist Meeting, FMI, Helsinki, Finland, June 7-11, 2010.
- MIPAS Quality Working Group meeting #23, KIT, Karlsruhe, Germany, June 16-18, 2010.
- SCIAMACHY Quality Working Group meeting, ESA-ESRIN, Frascati, Italy, June 21-23, 2010.
- ESA Living Planet Symposium, Bergen, Norway, June 28-July 2, 2010.
- 38th COSPAR Scientific Assembly, Bremen, Germany, July 18-24, 2010.
- SCAR XXXI, Buenos Aires, Argentina, July 30 - August 11, 2010.
- WMO Technical Conference on Meteorological and Environmental Instruments and Methods of Observation (TECO-2010), Helsinki, Finland, August 30 - September 1, 2010.
- SCIAMACHY Quick Look Validation meeting, BIRA-IASB, Brussels, Belgium, September 6-7, 2010.
- NDACC Steering Committee meeting 2010, Queenstown, New Zealand, October 5-8, 2010.

IV.2 Peer-reviewed articles

de Laat, A. T. J., Gloudemans, A. M. S., Schrijver, H., Aben, I., Nagahama, Y., Suzuki, K., Mahieu, E., Jones, N. B., Paton-Walsh, C., Deutscher, N. M., Griffith, D. W. T., De Mazière, M., Mittelmeier, R., Fast, H., Notholt, J., Palm, M., Hawat, T., Blumenstock, T., Rinsland, C., Dzhola, A. V., Grechko, E. I., Poberovskii, A. M., Makarova, M. V., Mellqvist, J., Strandberg, A., Sussmann, R., Borsdorff, T., and Rettinger, M.: Validation of five years (2003–2007) of SCIAMACHY CO total column measurements using ground-based spectrometer observations, Atmos. Meas. Tech. Discuss., 3, 2891-2930, doi:10.5194/amtd-3-2891-2010, 2010.

Dupuy, E., Walker, K. A., Kar, J., Boone, C. D., McElroy, C. T., Bernath, P. F., Drummond, J. R., Skelton, R., McLeod, S. D., Hughes, R. C., Nowlan, C. R., Dufour, D. G., Zou, J., Nichitiu, F., Strong, K., Baron, P., Bevilacqua, R. M., Blumenstock, T., Bodeker, G. E., Borsdorff, T., Bourassa, A. E., Bovensmann, H., Boyd, I. S., Bracher, A., Brogniez, C., Burrows, J. P., Catoire, V., Ceccherini, S., Chabrillat, S., Christensen, T., Coffey, M. T., Cortesi, U., Davies, J., De Clercq, C., Degenstein, D. A., De Mazière, M., Demoulin, P., Dodion, J., Firanski, B., Fischer, H., Forbes, G., Froidevaux, L., Fussen, D., Gerard, P., Godin-Beekmann, S., Goutail, F., Granville, J., Griffith, D., Haley, C. S., Hannigan, J. W., Höpfner, M., Jin, J. J., Jones, A., Jones, N. B., Jucks, K., Kagawa, A., Kasai, Y., Kerzenmacher, T. E., Kleinböhl, A., Klekociuk, A. R., Kramer, I., Küllmann, H., Kuttippurath, J., Kyrölä, E., Lambert, J.-C., Livesey, N. J., Llewellyn, E. J., Lloyd, N. D., Mahieu, E., Manney, G. L., Marshall, B. T., McConnell, J. C., McCormick, M. P., McDermid, I. S., McHugh, M., McLinden, C. A., Mellqvist, J., Mizutani, K., Murayama, Y., Murtagh, D. P., Oelhaf, H., Parrish, A., Petelina, S. V., Piccolo, C., Pommereau, J.-P., Randall, C. E., Robert, C., Roth, C., Schneider, M., Senten, C., Steck, T., Strandberg, A., Strawbridge, K. B., Sussmann, R., Swart, D. P. J., Tarasick, D. W., Taylor, J. R., Tétard, C., Thomason, L. W., Thompson, A. M., Tully, M. B., Urban, J., Vanhellemont, F., Vigouroux, C., von Clarmann, T., von der Gathen, P., von Savigny, C., Waters, J. W., Witte, J. C., Wolff, M., and Zawodny, J. M.: Validation of ozone measurements from the Atmospheric Chemistry Experiment (ACE), Atmos. Chem. Phys., 9, 287-343, doi:10.5194/acp-9-287-2009, 2009.

Frankenberg, C., P. Bergamaschi, A. Butz, S. Houweling, J. F. Meirink, J. Notholt, A. K. Petersen, H. Schrijver, T. Warneke, and I. Aben (2008), Tropical methane emissions: A revised view from SCIAMACHY onboard ENVISAT, Geophys. Res. Lett., 35, L15811, doi:10.1029/2008GL034300, 2008.

Frankenberg, C., Warneke, T., Butz, A., Aben, I., Hase, F., Spietz, P., and Brown, L. R.: Pressure broadening in the $2\nu_3$ band of methane and its implication on atmospheric retrievals, Atmos. Chem. Phys., 8, 5061-5075, doi:10.5194/acp-8-5061-2008, 2008.

Frankenberg C., K. Yoshimura, T. Warneke, I. Aben, A. Butz, N. Deutscher, D. Griffith, F. Hase, J. Notholt, M. Schneider, H. Schrijver, T. Rückmann, Dynamic Processes Governing Lower-Tropospheric HDO/H2O Ratios as Observed from Space and Ground, Science, 11 September 2009: Vol. 325, no. 5946, pp. 1374-1377, doi:10.1126/science.1173791.

Hains, J.C., Boersma, F.K., Kroon, M., Dirksen, R.J., Cohen, R.C., Perring, A.E., Bucsela, E., Volten, H., Swart, D.P.J., Richter, A., Wittrock, F., Schoenhardt, A., Wagner, T., Ibrahim, O.W., van Roozendael, M., Pinardi, G., Gleason, J.F., Veefkind, J. P., Levelt, P., Testing and improving OMI DOMINO tropospheric NO2 using observations from the DANDELIONS and INTEX-B validation campaigns, J. Geophys. Res., 115, D05301, doi:10.1029/2009JD012399, 2010.

Hendrick, F., Pommereau, J.-P., Goutail, F., Evans, R. D., Ionov, D., Pazmino, A., Kyrö, E., Held, G., Eriksen, P., Dorokhov, V., Gil, M., and Van Roozendael, M.: NDACC UV-visible total ozone measurements: improved retrieval and comparison with correlative satellite and ground-based observations, Atmos. Chem. Phys. Discuss., 10, 20405-20460, doi:10.5194/acpd-10-20405-2010, 2010.

Höpfner, M., von Clarmann, T., Fischer, H., Funke, B., Glatthor, N., Grabowski, U., Kellmann, S., Kiefer, M., Linden, A., Milz, M., Steck, T., Stiller, G. P., Bernath, P., Blom, C. E., Blumenstock, Th., Boone, C., Chance, K., Coffey, M. T., Friedl-Vallon, F., Griffith, D., Hannigan, J. W., Hase, F., Jones, N., Jucks, K. W., Keim, C., Kleinert, A., Kouker, W., Liu, G. Y., Mahieu, E., Mellqvist, J., Mikuteit, S., Notholt, J., Oelhaf, H., Piesch, C., Reddmann, T., Ruhnke, R., Schneider, M., Strandberg, A., Toon, G., Walker, K. A., Warneke, T., Wetzel, G., Wood, S., and Zander, R.: Validation of MIPAS $ClONO_2$ measurements, Atmos. Chem. Phys., 7, 257-281, doi:10.5194/acp-7-257-2007, 2007.

Kerzenmacher, T., Wolff, M. A., Strong, K., Dupuy, E., Walker, K. A., Amekudzi, L. K., Batchelor, R. L., Bernath, P. F., Berthet, G., Blumenstock, T., Boone, C. D., Bramstedt, K., Brogniez, C., Brohede, S., Burrows, J. P., Catoire, V., Dodion, J., Drummond, J. R., Dufour, D. G., Funke, B., Fussen, D., Goutail, F., Griffith, D. W. T., Haley, C. S., Hendrick, F., Höpfner, M., Huret, N., Jones, N., Kar, J., Kramer, I., Llewellyn, E. J., López-Puertas, M., Manney, G., McElroy, C. T., McLinden, C. A., Melo, S., Mikuteit, S., Murtagh, D., Nichitiu, F., Notholt, J., Nowlan, C., Piccolo, C., Pommereau, J.-P., Randall, C., Raspollini, P., Ridolfi, M., Richter, A., Schneider, M., Schrems, O., Silicani, M., Stiller, G. P., Taylor, J., Tétard, C., Toohey, M., Vanhellemont, F., Warneke, T., Zawodny, J. M., and Zou, J.: Validation of NO_2 and NO from the Atmospheric Chemistry Experiment (ACE), Atmos. Chem. Phys., 8, 5801-5841, doi:10.5194/acp-8-5801-2008, 2008.

Keim, C., Eremenko, M., Orphal, J., Dufour, G., Flaud, J.-M., Höpfner, M., Boynard, A., Clerbaux, C., Payan, S., Coheur, P.-F., Hurtmans, D., Claude, H., Dier, H., Johnson, B., Kelder, H., Kivi, R., Koide, T., López Bartolomé, M., Lambkin, K., Moore, D., Schmidlin, F. J., and Stübi, R.: Tropospheric ozone from IASI: comparison of different inversion algorithms and validation with ozone sondes in the northern middle latitudes, Atmos. Chem. Phys., 9, 9329-9347, doi:10.5194/acp-9-9329-2009, 2009.

Li, Q., Palmer, P. I., Pumphrey, H. C., Bernath, P., and Mahieu, E.: What drives the observed variability of HCN in the troposphere and lower stratosphere?, Atmos. Chem. Phys., 9, 8531-8543, doi:10.5194/acp-9-8531-2009, 2009.

Lindenmaier, R., R. L. Batchelor, K. Strong, H. Fast, F. Goutail, F. Kolonjari, C. T. McElroy, R. L. Mittermeier, K. A. Walker, An evaluation of infrared microwindows for ozone retrievals using the Eureka Bruker 125HR Fourier transform spectrometer, Journal of Quantitative Spectroscopy and Radiative Transfer, 111 (4), 569-585, doi:10.1016/j.jqsrt.2009.10.013, 2010.

Mahieu, E., Duchatelet, P., Demoulin, P., Walker, K. A., Dupuy, E., Froidevaux, L., Randall, C., Catoire, V., Strong, K., Boone, C. D., Bernath, P. F., Blavier, J.-F., Blumenstock, T., Coffey, M., De Mazière, M., Griffith, D., Hannigan, J., Hase, F., Jones, N., Jucks, K. W., Kagawa, A., Kasai, Y., Mebarki, Y., Mikuteit, S., Nassar, R., Notholt, J., Rinsland, C. P., Robert, C., Schrems, O., Senten, C., Smale, D., Taylor, J., Tétard, C., Toon, G. C., Warneke, T., Wood, S. W., Zander, R., and Servais, C.: Validation of ACE-FTS v2.2 measurements of HCl, HF, CCl_3F and CCl_2F_2 using space-, balloon- and ground-based instrument observations, Atmos. Chem. Phys., 8, 6199-6221, doi:10.5194/acp-8-6199-2008, 2008.

Oetjen, H., Wittrock, F., Richter, A., Chipperfield, M. P., Medeke, T., Sheode, N., Sinnhuber, B.-M., Sinnhuber, M., and Burrows, J. P.: Evaluation of stratospheric chlorine chemistry for the Arctic spring 2005 using modelled and measured OClO column densities, Atmos. Chem. Phys. Discuss., 9, 26539-26575, doi:10.5194/acpd-9-26539-2009, 2009.

Paatero, J., P. Vaattovaara, M. Vestenius, O. Meinander, U.Makkonen, R. Kivi, A. Hyvärinen, E. Asmil, M. Tjernström, C. Leck, 2009, Finnish contribution to the Arctic Summer Cloud Ocean Study (ASCOS) expedition, Arctic Ocean 2008, Geophysica, 45(1-2), 119-146, 2009.

Pałm, M., Melsheimer, C., Noël, S., Heise, S., Notholt, J., Burrows, J., and Schrems, O.: Integrated water vapor above Ny Ålesund, Spitsbergen: a multi-sensor intercomparison, Atmos. Chem. Phys., 10, 1215-1226, doi:10.5194/acp-10-1215-2010, 2010.

Parrondo, M. C., Extreme low ozone episodes over the sub-Arctic region of Keflavik, Física de la Tierra, 21, 131-141, 2009.

Payan, S., Camy-Peyret, C., Oelhaf, H., Wetzel, G., Maucher, G., Keim, C., Pirre, M., Huret, N., Engel, A., Volk, M. C., Kuellmann, H., Kuttippurath, J., Cortesi, U., Bianchini, G., Mencaraglia, F., Raspollini, P., Redaelli, G., Vigouroux, C., De Mazière, M., Mikuteit, S., Blumenstock, T., Velazco, V., Notholt, J., Mahieu, E., Duchatelet, P., Smale, D., Wood, S., Jones, N., Piccolo, C., Payne, V., Bracher, A., Glatthor, N., Stiller, G., Grunow, K., Jeseck, P., Te, Y., and Butz, A.: Validation of version-4.61 methane and nitrous oxide observed by MIPAS, Atmos. Chem. Phys., 9, 413-442, doi:10.5194/acp-9-413-2009, 2009.

Roscoe, H. K., Van Roozendael, M., Fayt, C., du Piesanie, A., Abuhassan, N., Adams, C., Akrami, M., Cede, A., Chong, J., Clémer, K., Friess, U., Gil Ojeda, M., Goutail, F., Graves, R., Griesfeller, A., Grossmann, K., Hemerijckx, G., Hendrick, F., Herman, J., Hermans, C., Irie, H., Johnston, P. V., Kanaya, Y., Kreher, K., Leigh, R., Merlaud, A., Mount, G. H., Navarro, M., Oetjen, H., Pazmino, A., Perez-Camacho, M., Peters, E., Pinardi, G., Puentedura, O., Richter, A., Schönhardt, A., Shaiganfar, R., Spinei, E., Strong, K., Takashima, H., Vlemmix, T., Vrekoussis, M., Wagner, T., Wittrock, F., Yela, M., Yilmaz, S., Boersma, F., Hains, J., Kroon, M., and Piters, A.: Intercomparison of slant column measurements of NO_2 and O_4 by MAX-DOAS and zenith-sky UV and visible spectrometers, Atmos. Meas. Tech. Discuss., 3, 3383-3423, doi:10.5194/amtd-3-3383-2010, 2010.

Rozanov, A., Weigel, K., Bovensmann, H., Dhomse, S., Eichmann, K.-U., Kivi, R., Rozanov, V., Vömel, H., Weber, M., and Burrows, J. P.: Retrieval of water vapor vertical distributions in the upper troposphere and the lower stratosphere from SCIAMACHY limb measurements, Atmos. Meas. Tech. Discuss., 3, 4009-4057, doi:10.5194/amtd-3-4009-2010, 2010.

Salau O. R., T. Warneke, J. Notholt, C. Shim, Q. Li and Y. Xiao (2009) Tropospheric trace gases at Bremen measured with FTIR spectrometry, J. Environ. Monit., 2009, 11, 1529-1534, doi:10.1039/b903198g.

Salawitch, R.J.; Canty, T.; Kurosu, T.; Chance, K.; Liang, Q.; da Silva, A.; Pawson, S.; Nielsen, J.E.; Rodriguez, J.M.; Bhartia, P.K.; Liu, X.; Huey, L.G.; Liao, J.; Stickel, R.E.; Tanner, D.J.; Dibb, J.E.; Simpson, W.R.; Donohoue, D.; Weinheimer, A.; Flocke, F.; Knapp, D.; Montzka, D.; Neuman, J.A.; Nowak, J.B.; Ryerson, T.B.; Oltmans, S.; Blake, D.R.; Atlas, E.L.; Kinnison, D.E; Tilmes, S.; Pan, L.L.; Hendrick, F.; Van Roozendael, M.; Kreher, K.; Johnston, P.V.; Gao, R.S.; Bui, T.P.; Chen, G.; Pierce, R.B.; Crawford, J.H.; Jacob D.J., A New Interpretation of Total Column BrO during Arctic Spring, Geophys. Res. Lett., doi:10.1029/2010GL043798, in press.

Schneising, O., Buchwitz, M., Burrows, J. P., Bovensmann, H., Reuter, M., Notholt, J., Macatangay, R., and Warneke, T.: Three years of greenhouse gas column-averaged dry air mole fractions retrieved from satellite – Part 1: Carbon dioxide, Atmos. Chem. Phys., 8, 3827-3853, doi:10.5194/acp-8-3827-2008, 2008.

Strong, K., Wolff, M. A., Kerzenmacher, T. E., Walker, K. A., Bernath, P. F., Blumenstock, T., Boone, C., Catoire, V., Coffey, M., De Mazière, M., Demoulin, P., Duchatelet, P., Dupuy, E., Hannigan, J., Höpfner, M., Glatthor, N., Griffith, D. W. T., Jin, J. J., Jones, N., Jucks, K., Kuellmann, H., Kuttippurath, J., Lambert, A., Mahieu, E., McConnell, J. C., Mellqvist, J., Mikuteit, S., Murtagh, D. P., Notholt, J., Piccolo, C., Raspollini, P., Ridolfi, M., Robert, C., Schneider, M., Schrems, O., Semeniuk, K., Senten, C., Stiller, G. P., Strandberg, A., Taylor, J., Tétard, C., Toohey, M., Urban, J., Warneke, T., and Wood, S.: Validation of ACE-FTS N_2O measurements, Atmos. Chem. Phys., 8, 4759-4786, doi:10.5194/acp-8-4759-2008, 2008.

Vigouroux, C., Hendrick, F., Stavrakou, T., Dils, B., De Smedt, I., Hermans, C., Merlaud, A., Scolas, F., Senten, C., Vanhaelewyn, G., Fally, S., Carleer, M., Metzger, J.-M., Müller, J.-F., Van Roozendael, M., and De Mazière, M.: Ground-based FTIR and MAX-DOAS observations of formaldehyde at Réunion Island and comparisons with satellite and model data, Atmos. Chem. Phys., 9, 9523-9544, doi:10.5194/acp-9-9523-2009, 2009.

IV.3 Book chapters

Lambert, J.-C., C. De Clercq, and T. von Clarmann, Comparing and merging water vapour observations: A multi-dimensional perspective on smoothing and sampling issues, Chapter 9 (23 pp.) of ISSI Book “Ground-based remote sensing and in-situ methods for monitoring atmospheric water vapour”, International Space Science Institute (Ed.), Bern, Switzerland. New status: revised, submitted to the Editor.

Lambert, J.-C., A. Piters, A. Richter, S. Mieruch, H. Bovensmann, M. Buchwitz, and A. Friker, SCIAMACHY Validation, Chapter 9 of “SCIAMACHY, Monitoring the Changing Earth’s Atmosphere”, 2nd Edition, Book edited by M. Gottwald, published by DLR, Institut für Methodik der Fernerkundung (IMF), 167 pp., © DLR/IUP-IFE/SRON/KNMI/BIRA-IASB. New status: in press.

Loyola, D., T. Erbertseder, D. Balis, J-C. Lambert, R. Spurr, M. Van Roozendael, P. Valks, W. Zimmer, J. Meyer-Arnek, and C. Lerot, "Operational Monitoring of the Antarctic Ozone Hole: Transition from GOME and SCIAMACHY to GOME-2", Chapter in Ozone Depletion: From its discovery to Envisat and Aura, Book commemorating the 20th anniversary of the Montreal Protocol, C. Zerefos et al. (eds.), Twenty Years of Ozone Decline, © Springer Science + Business Media B. V., pp. 215-238, 2009.

Piters, A. J. M., B. Buchmann, D. Brunner, R. Cohen, J-C. Lambert, G. de Leeuw, P. Stammes, M. van Weele, and F. Wittrock, Data quality and validation of satellite measurements of atmospheric composition, Chapter 7 of AT-2 Book on "Tropospheric Measurements from Space". New status: in press.

IV.4 Conference proceedings

De Clercq, C., S., Vandenbussche, J. Granville, J.-C. Lambert, and the Multi-TASTE Team, On the consistency of ozone profile data from Envisat, historical satellites and the NDACC network, in Proc. ESA Atmospheric Science Conference 2009, Barcelona, Spain, 7-11 September 2009, ESA Special Publication ESA-SP-676, 2009.

De Maziere, M., H. K. Roscoe, J. C. Lambert, P. Keckhut, C. Textor, and NDACC partners involved for observations, modelling and outreach, Monitoring the stratosphere in GEOmon and NDACC, poster presentation (EGU2009-10636) at the EGU General Assembly 2009, Vienna, April 2-24, 2009.

Kivi, R., Kujanpää, J., Aulamo, O., Heikkinen, P., Hassinen, S., Calbet, X., Montagner, F., Vömel, H., Observations of water vapor profiles over Northern Finland by satellite and balloon borne instruments, In Proceedings: 2009 EUMETSAT Meteorological Satellite Conference, 21-25 September 2009, Bath, UK, EUMETSAT P.55.

Kivi, R. et al., (2010), LAPBIAT Atmospheric Sounding Campaign in 2010: Upper-Air and Remote Sensing Observations of Water Vapor. In Proceeding: WMO Technical Conference on Meteorological and Environmental Instruments and Methods of Observation (TECO-2010), Helsinki, Finland, 30 August - 1 September 2010. Instruments and Observing System Methods Report No. 104, WMO/TD-No. 1546.

Kivi, R., E. Kyrö, J. Pulliainen, P. Heikkinen, P. Ahonen (2010), Carbon dioxide observations over Sodankylä (Finland) using Fourier transform infrared spectroscopy, In: The 27th Nordic Meteorologist Meeting, 7 - 11 June, 2010, Editors S. Haapanala, M. Heinonen, Finnish Meteorological Institute, Helsinki, Finland.

Vandenbussche, S., J.-C. Lambert, C. De Clercq, J. Granville, D. Hubert, and the NDACC Ozone Profiling Team, NDACC network based study of the consistency of ozone profile data from Envisat, third-party missions and historical satellites, in Proc. ESA Living Planet Symposium, Bergen, Norway, 28 June-2 July 2010, ESA Special Publication ESA-SP-686, 2010.

IV.5 Oral presentations

Ciais, P., P. Keckhut, M. Minnock, S. Kirschke, and the GEOmon Coordination Team, Global Earth Observation and Monitoring – GEOmon, oral presentation (EGU2010-13790) at the EGU General Assembly 2010, Vienna, May 2-7, 2010.

De Mazière, M., G. Vanhaelewyn, Comparisons of MIPAS profiles of CH4, N2O and HNO3 with ground-based FTIR data at NDACC stations Kiruna, Jungfraujoch and St Denis (Ile de La Réunion), MIPAS Quality Working Group meeting #23, KIT, Karlsruhe, Germany, June 16-18, 2010.

Dils, B., M. De Mazière, C. Vigouroux, F. Forster, R.Sussmann, T. Borsdorff, P. Bousquet, T. Blumenstock, M. Buchwitz, S. Dalsoren, P. Demoulin, P. Duchatelet, C. Frankenberg, J. Hannigan, F. Hase, I. Isaksen, N. Jones, J.Klyft, I. Kramer, E. Mahieu, J. Mellqvist, L. Neef, J. Notholt, K. Petersen, I. Pison, O. Schneising, A.Strandberg, K. Strong, S. Szopa, J. Taylor, P. van Velthoven, M. van Weele, S. Wood, Validation of methane data products from chemistry transport models and SCIAMACHY satellite retrievals, using FTIR data from a quasi-global network, oral presentation at the 5th International Symposium on Non-CO_2 greenhouse gases (NCGG-5), Science, Reduction Policy and Implementation, Wageningen, The Netherlands, June 30-July 3, 2009.

Dils, B., M. De Mazière, C. Vigouroux, F. Forster, R. Sussmann, T. Borsdorff, P. Bousquet, T. Blumenstock, M. Buchwitz, S. Dalsoren, P. Demoulin, P. Duchatelet, C.Frankenberg, J. Hannigan, F. Hase, I. Isaksen, N. Jones, J.Klyft, I. Kramer, E. Mahieu, J. Mellqvist, L. Neef, J. Notholt, K. Petersen, I. Pison, O. Schneising, A.Strandberg, K. Strong, S. Szopa, J. Taylor, P. van Velthoven, M. van Weele, S. Wood, Validation of methane data products from chemistry transport models and SCIAMACHY satellite retrieval algorithms, using a quasi-global network of FTIR stations, oral presentation at the HYMN Open Science & Policy Workshop, BIRA-IASB, Brussels, Oct. 13, 2009.

Dils, B., M. De Mazière, C. Vigouroux, F. Forster, R.Sussmann, T. Borsdorff, P. Bousquet, T. Blumenstock, M. Buchwitz, S. Dalsoren, P. Demoulin, P. Duchatelet, C.Frankenberg, J. Hannigan, F. Hase, I. Isaksen, N. Jones, J.Klyft, I. Kramer, E. Mahieu, J. Mellqvist, L. Neef, J. Notholt, K. Petersen, I. Pison, O. Schneising, A.Strandberg, K. Strong, S. Szopa, J. Taylor, P. van Velthoven, M. van Weele, S. Wood, A comparison between Methane data products from 3D Chemistry Transport Models, SCIAMACHY and FTIR data from a quasi-global network, oral presentation (EGU2010-4593) at the EGU General Assembly 2010, Vienna, May 2-7, 2010.

Dils, B., et al., Initial validation of operational L2 SCIAMACHY CO, SCIAMACHY Quality Working Group meeting, ESA-ESRIN, Frascati, Italy, June 21-23, 2010.

Dils, B., M. Palm, E. Mahieu, M. De Mazière, Initial validation of total column CO, SCIAMACHY Quality Working Group meeting, ESA-ESRIN, Frascati, Italy, June 21-23, 2010.

Goutail, F., D. Ionov', A. Pazmino, J.-P. Pommereau, F. Hendrick, M. van Roozendael, M. Pastel, A. Griesfeller' Validation of satellite total ozone and NO2 data with ground-based SAOZ network, Envisat atmospheric science conference, Sept. 2009.

Goutail, F., A. Pazmino, A. Griesfeller, D. Ionov, Tropospheric NO_2 from SAOZ, CINDI workshop, Brussels, March 2010.

Hay, T.W; Johnston, P.V., Lauder NO_2 Profiles from CINDI Campaign, June-July 2009, CINDI Workshop, Brussels, March 2010.

Hendrick, F., M. De Mazière, N. Theys, and M. Van Roozendael, A. Rozanov, B.-M. Sinnhuber, and H. Bovensmann, P. V. Johnston and K. Kreher, O. Puentedura and M. Gil. Trend Analysis of stratospheric BrO: Comparison between SCIAMACHY Limb and Ground-Based UV- visible observations, ESA Atmospheric Science Conference, Madrid, 7-11 September 2009.

Hendrick, F., J. Granville, J.-C. Lambert, M. Van Roozendael, SCIAMACHY delta-validation 2010: BrO results, SCIAMACHY Quality Working Group meeting, ESA-ESRIN, Frascati, Italy, June 21-23, 2010.

Hendrick, F., J. Granville, J.-C. Lambert, M. Van Roozendael, Verification of the ESA SCIAMACHY limb and nadir BrO products using ground-based UVvis BrO Profiling, SCIAVALIG Quick Look Validation meeting, BIRA-IASB, Brussels, Belgium, September 6-7, 2010.

Hubert, D., S. Vandenbussche, J. Granville, J.-C. Lambert, Ground-Based Network Verification of MIPAS ORM 1.000 versus IPF 4.61/2: O3 profile and T profile, MIPAS Quality Working Group meeting #23, KIT, Karlsruhe, Germany, June 16-18, 2010.

Hubert, D., S. Vandenbussche, J. Granville, J.-C. Lambert, Ground-Based Network Verification of SCIAMACHY SGP 5.01 versus SGP 3.01: O3 profile, SCIAMACHY Quality Working Group meeting, ESA-ESRIN, Frascati, Italy, June 21-23, 2010.

Hubert, D., J.-C. Lambert, J. Granville, and S. Vandenbussche, Delta validation of SCIAMACHY SGP upgrade to v5.01: Ozone profile SCIAVALIG Quick Look Validation meeting, BIRA-IASB, Brussels, Belgium, September 6-7, 2010.

Johnston, P.V., Lauder's Formaldehyde measurements at the CINDI Campaign, June-July 2009, CINDI Workshop, Brussels, March 2010.

Kreher, K., Johnston, P.V.; Thomas, A.; Hay, T.; J.B. Liley, M. Aviles-Martinez, U. Friess, F. Hendrick, M. Van Roozendael, G.E. Bodeker, R. Schofield, R.J. Salawitch, T. Canty, Techniques for analysing ground-based UV-visible long-term BrO and NO_2 observations for satellite validation and trend analysis, 38th COSPAR Scientific Assembly, Bremen, Germany, July 2010.

Lambert, J.-C., On the integration of NDACC and satellite data: satellite validation issues, GEOmon Activity 4 (Stratospheric Ozone) workshop, Paris, France, 5-6 October 2009.

Lambert, J.-C., C. De Clercq, S. Vandenbussche, and Q. Errera, On the multi-mission validation of ozone limb sounders using NDACC network data, 5th Atmospheric Limb Workshop, Helsinki, Finland, 16-19 November 2009.

Lambert, J.-C., S. Vandenbussche, C. De Clercq, and T. von Clarmann, Pragmatic observation operators for remotely sensed data, GEOmon GEOmon Third General Assembly, London, UK, 18-20 January 2010.

Lambert, J.-C., J. Granville, D. Hubert, C. Lerot, M. Van Roozendael, Ground-Based Verification of Nadir O3 and NO2 Columns, SCIAMACHY Quality Working Group meeting, ESA-ESRIN, Frascati, Italy, June 21-23, 2010.

Lambert, J.-C., and B. R. Bojkov, Development of reference practices for the calibration and validation of atmospheric composition satellites, 38th COSPAR Scientific Assembly, Bremen, Germany, July 17-25, 2010.

Lambert, J.-C., J. Granville, D. Hubert, C. Lerot, M. Van Roozendael, Delta validation of SCIAMACHY SGP upgrade to v5.01: Nadir O3 Column, SCIAVALIG Quick Look Validation meeting, BIRA-IASB, Brussels, Belgium, September 6-7, 2010.

Lejeune, B., P. Demoulin, P. Duchatelet, E. Mahieu, G. Roland, C. Servais, R. Zander, Jungfraujoch FTIR activities, GAW-CH meeting, 9 April 2010, Zürich, Switzerland, 2010.

Mahieu, E., B. Lejeune, R. Zander, P. Demoulin, P. Duchatelet, C.P. Rinsland, P.F. Bernath, C.D. Boone and K.A. Walker, Some topics under investigations at ULg using ground-based Jungfraujoch FTIR solar spectra, and planned interactions with ACE-FTS data products (v2.2 and v3), oral presentation at the ACE Science Team Meeting, May 2010, Waterloo, Canada, 2010.

Vandenbussche, S., C. De Clercq, J. Granville, J.-C. Lambert, Ground-based network verification of GOMOS ozone profile data v 7.0cd versus 6.0cf, GOMOS Quality Working Group Meeting #21, ESRIN, Frascati, Italy, October 6, 2009.

Vandenbussche, S., C. De Clercq, J. Granville, and J.-C. Lambert, NDACC-based detection of long-term drifts in satellite ozone data: methodology and some results, GEOmon Activity 4 (Stratospheric Ozone) workshop, Paris, France, 5-6 October 2009.

Vandenbussche, S., J.-C. Lambert, C. De Clercq, R.J.D. Spurr, Multi-dimensional issues of the comparison of remotely sensed atmospheric composition data, 38th COSPAR Scientific Assembly, Bremen, Germany, July 17-25, 2010.

IV.6 Posters

Dils, B., M. De Mazière, C. Vigouroux, F. Forster, R. Sussmann, T. Borsdorff, P. Bousquet, T. Blumenstock, M. Buchwitz, S. Dalsoren, P. Demoulin, P. Duchatelet, C. Frankenberg, J. Hannigan, F. Hase, I. Isaksen, N. Jones, J. Klyft, I. Kramer, E. Mahieu, J. Mellqvist, L. Neef, J. Notholt, K. Petersen, I. Pison, O. Schneising, A. Strandberg, K. Strong, S. Szopa, J. Taylor, P. van Velthoven, M. van Weele, S. Wood and M. Coffey, A Comparison of methane data products from Chemistry Transport Models, SCIAMACHY, and a quasi-global network of FTIR stations, poster presentation at the ESA Atmospheric Science Conference, Barcelona, Sept. 7-11, 2009.

Dils, B., M. De Mazière, C. Vigouroux, F. Forster, R.Sussmann, T.Borsdorff, P. Bousquet, T. Blumenstock, M. Buchwitz, S. Dalsoren, P.Demoulin, P. Duchatelet, C.Frankenberg, J. Hannigan, F. Hase, I.Isaksen, N. Jones, J.Klyft, I. Kramer, E. Mahieu, J. Mellqvist, L. Neef, J.Notholt, K. Petersen, I. Pison, O. Schneising, A.Strandberg, K. Strong,S. Szopa, J. Taylor, P. van Velthoven, M. van Weele, S. Wood, A comparison of Methane data products from Chemistry Transport Models, SCIAMACHY and a quasi-global network of FTIR stations, poster presentation at the NDACC-IRWG annual meeting, Murramarang, Australia, June 2-4, 2010.

Dils, B., M. De Mazière, C. Vigouroux, F. Forster, R.Sussmann, T.Borsdorff, P. Bousquet, T. Blumenstock, M. Buchwitz, S. Dalsoren, P.Demoulin, P. Duchatelet, C.Frankenberg, J. Hannigan, F. Hase, I.Isaksen, N. Jones, J.Klyft, I. Kramer, E. Mahieu, J. Mellqvist, L. Neef, J.Notholt, K. Petersen, I. Pison, O. Schneising, A.Strandberg, K. Strong,S. Szopa, J. Taylor, P. van Velthoven, M. van Weele, S. Wood, A Comparison of Methane Data Products from Chemistry Transport Models, SCIAMACHY and a Network of FTIR Stations, poster presentation at the ESA Living Planet Symposium, Bergen, Norway, June 28-July 2, 2010.

Duchatelet, P., P. Demoulin, F. Hase, E. Mahieu, P.F. Bernath, C.D. Boone, and K.A. Walker, Updating hydrogen fluoride (HF) FTIR time series above the Jungfraujoch: comparison of two retrieval algorithms and impact of line shape models, poster presentation (EGU2010-1354) at the EGU General Assembly 2010, Vienna, May 2-7, 2010.

Goutail ,F., A. Pazmiño, J. P. Pommereau, M. Pastel, D. Ionov, F. Hendrick, M. Van Roozendael, E. Kyrö, P. Eriksen, V. Dorokhov, G. Held, Validation of nadir viewing satellite total ozone and NO_2 column with ground-based SAOZ network, GEOmon annual meeting, London, UK, Jan. 2010.

Goutail, F., A. Pazmino, A. Griesfeller, D. Ionov, K. Clemer, M. Van Roozendael, Monitoring pollution using a SAOZ zenith sky spectrometer, GEOmon annual meeting, London, UK, Jan. 2010.

Goutail, F., A. Pazmino, A. Griessfeller, D. Ionov, K. Clemer, M. Van Roozendael, Tropospheric columns using SAOZ zenith sky spectrometer, poster presentation (EGU2010-5177) at the EGU General Assembly 2010, Vienna, May 2-7, 2010.

Hay, T.; Kreher, K.; Johnston, P.V.; Bodeker, G.; Schofield, R.; Thomas, A.; McDonald, A.; Martinez-Aviles, M.; Profiling of MAX-DOAS BrO measurements from Antarctica and NO_2 measurements from CINDI, poster presentation (EGU2010-8141) at the EGU General Assembly 2010, Vienna, May 2-7, 2010.

Pazmino, A., F. Goutail, J. P. Pommereau, M. Pastel, D. Ionov, F. Hendrick, M. Van Roozendael, R. Evans, V. Dorokhov, E. Kyro, P. Heikkinen, P. Eriksen, G. Held, Homogenization of UV-Visible NDACC spectrometers reprocessing for ozone and NO2, poster presentation (EGU2010-5044) at the EGU General Assembly 2010, Vienna, May 2-7, 2010.

Kivi, R., E. Kyrö, H. Vömel, F. Immler, N. Kämpfer, C. Straub, V. Yushkov, S. Khaykin, T. Christensen, and F. G. Wienhold (2010), Polar stratospheric cloud, water vapor and ozone observations at Sodankylä, poster presentation (EGU2010-13701) at the EGU General Assembly 2010, Vienna, May 2-7, 2010.

Kyrö, E., J. Pulliainen, P. Heikkinen, P. Ahonen, R. Kivi, J. Hatakka (2010), Early results on the validation of GOSAT/TANSO GHG observations at the Sodankylä-Pallas satellite pixel (67N, 27E), poster presentation (EGU2010-9252) at the EGU General Assembly 2010, Vienna, May 2-7, 2010.

Lejeune, B., E. Mahieu, C. Servais, P. Duchatelet, and P. Demoulin, Optimized approach to retrieve information on the tropospheric and stratospheric carbonyl sulfide (OCS) vertical distributions above Jungfraujoch from high-resolution FTIR solar spectra, poster presentation (EGU2010-3513) at the EGU General Assembly 2010, Vienna, May 2-7, 2010.

Parrondo M. C., M. Yela, M. Gil, H. Ochoa, Ozone variability over Antarctic Continent, poster presentation (EGU2010-10158) at the EGU General Assembly 2010, Vienna, May 2-7, 2010.

Parrondo, M.C., M. Yela, M. Gil, and H. Ochoa, Analysis of ozonesonde measurements at Belgrano Station, SCAR XXXI meeting, Buenos Aires, July 30 – August 11, 2010.

Petersen, K., T. Blumenstock, B. Dils, F. Hase , C. Hermans, M. De Mazière, J. Notholt, M. Schneider, T. Warneke, Ground-based FTIR observations at the tropical and subtropical NDACC stations Paramaribo, Tenerife Is. and Ile de La Reunion, poster presentation at SCOUT-O_3 final meeting, Schliersee, Germany, June 15-17, 2009.

Rozanov, A., B.-M. Sinnhuber, H. Bovensmann, M. Gil, P. V. Johnston, K.Kreher, J. Orphal, O. Puentedura, M. Van Roozendael, and J. P. Burrows, Seven years of stratospheric BrO observations from SCIAMACHY, 5th Limb Conference and workshop, 16-19 November, Helsinki, 2009.

Vandenbussche, S., C. De Clercq, J. Granville, and J.-C. Lambert, NDACC-based detection of long-term drifts in nine satellite ozone data records, GEOmon Third General Assembly, London, UK, 18-20 January 2010.

Vanhaelewyn, G., P. Duchatelet, C. Vigouroux, B. Dils, N. Kumps, C. Hermans, P. Demoulin, E. Mahieu. R. Sussmann, and M. De Mazière, Comparison of the error budgets associated with ground-based FTIR measurements of atmospheric CH4 profiles at Ile de la Réunion and Jungfraujoch, poster presentation (EGU2010-15537) at the EGU General Assembly 2010, Vienna, May 2-7, 2010.

Vigouroux, C., F. Hendrick, T. Stavrakou, B. Dils, I. De Smedt, C. Hermans, A. Merlaud, F. Scolas, C. Senten, G. Vanhaelewyn, S. Fally, M. Carleer, J.-M. Metzger, J.-F. Müller, M. Van Roozendael, and M. De Mazière, Ground-based FTIR and MAXDOAS observations of HCHO at Reunion Island and comparions with SCIAMACHY and the CTM IMAGES, poster presentation at the ESA Atmospheric Science Conference, Barcelona, Sept. 7-11, 2009.

V ANNEXE 2: CORRELATIVE DATABASE STATUS

This Annexe presents an overview of the correlative data delivered to the Envisat Cal/Val Data Centre operated at NILU on behalf of ESA. To get a consistent overview despite the wide variety of ground-based techniques, numbers reported in the following tables represent the amount of days for which there is at least one measurement suitable for Envisat and TPM validation. It should be noted that the actual amount of individual measurements stored on Cal/Val may vary with:

- The type of ground-based instrument: e.g. the feasibility of direct sun observations (Brewer, Dobson, FTIR) depend on weather conditions while scattered-light UVVIS observations are feasible virtually in all weather;
- The latitude: standard techniques requiring sunlight do not provide measurements during polar night; zenith-sky spectrometers measuring during twilight can not measure – at latitudes well above the polar circles – in the heart of the polar night and of the polar day where there is by definition no twilight.
- The actual presence of the molecule: OClO is a product of one of the channels of the coupling between ClO and BrO; therefore the presence of this molecule is highly dependent on the level of chlorine activation by heterogeneous reactions on polar stratospheric clouds (PSCs);
- The data type and file format adopted by the Data Submitter: some stations store data in monthly files, others in daily files, and others by individual measurement; some Brewer or microwave data files report one measurement every 30 min (reaching sometimes several thousands a month) while others provide only daily averages (thus a maximum of 31 values a month);
- The type of data processing: SAOZ/UVVIS data at remote stations processed in real-time by the built-in software and transmitted to CNRS via the ARGOS satellite system include only one average value for each twilight, while reprocessing at the central laboratory of all the recorded spectra yields one value for every individual measurement.

In the following tables, grey shaded cells highlight periods during which measurements are simply not possible, due e.g. to the absence of light source (no sunlight during polar night, no twilight near the poles at the solstices) or absence of the target species (no stratospheric OClO if no chlorine activation).

V.1 Monthly Data Distribution for O_3 Column Data

2006

Brewer	Inst.	Lat	Long	J	F	M	A	M	J	J	A	S	O	N	D	#
Sodankylä	FMI	67N	27E	8	18	31	30	31	23	31	31	30	22	4	0	259
Jokioinen	FMI	61N	23E	14	23	27	30	30	28	28	30	30	30	16	5	291
De Bilt	KNMI	52N	5E	31	28	31	30	31	30	31	31	30	31	30	31	365
Uccle	RMI	51N	4E	30	28	31	30	31	30	31	31	29	31	30	31	363
Hohenpeißenberg	DWD	48N	11E	24	21	26	24	29	30	31	30	27	30	25	27	324
Arosa	MCH	47N	10E	25	28	26	28	26	27	27	25	25	26	27	23	313
Paramaribo	KNMI	6N	55W	31	26	15	30	31	29	25	31	24	29	27	28	326

Dobson	Inst.	Lat	Long	J	F	M	A	M	J	J	A	S	O	N	D	#
Hohenpeißenberg	DWD	48N	11E	14	12	19	11	16	17	20	13	18	21	14	17	192
Arosa	MCH	47N	10E	25	23	16	21	21	27	25	22	26	26	24	24	280
Lauder	NIWA	45S	170E	0	0	0	0	0	0	0	0	0	21	20	15	56
Vernadsky	BAS/KTSU	65S	64W	31	28	31	20	0	0	0	31	30	12	0	0	183
Halley	BAS	76S	27W	31	27	31	15	0	0	0	6	29	31	30	7	207
Arrival Heights	NIWA	78S	167E	0	0	0	0	0	0	0	0	0	2	15	13	30

FTIR	Inst.	Lat	Long	J	F	M	A	M	J	J	A	S	O	N	D	#
Ny-Ålesund	IUP/IFE	79N	12E	0	0	2	3	5	0	1	0	0	0	0	0	11

Kiruna	FZK/IMK	68N	21E	0	9	13	7	10	12	6	13	6	7	5	0	88
Bremen	IUP/IFE	53N	9E	2	2	3	3	6	5	6	3	9	3	0	1	43
Izaña	FZK	28N	16W	4	5	14	7	9	17	14	14	13	11	11	10	129
Lauder	NIWA	45S	170E	8	11	4	9	11	8	5	11	7	11	6	3	94
Arrival Heights	NIWA	78S	167E	9	4	3	2	0	0	0	0	2	4	5	0	29

M124	Inst.	Lat	Long	J	F	M	A	M	J	J	A	S	O	N	D	#
Murmansk	MGO	69N	33E	0	0	0	29	27	29	31	29	25	0	0	0	170
Pechora	MGO	65N	57E	11	27	30	30	31	28	28	31	30	25	0	0	271
Arkhangel'sk	MGO	65N	40E	0	0	0	0	0	0	0	0	29	25	0	0	54
Yakutsk	MGO	62N	130E	9	14	22	29	30	30	30	27	28	26	10	0	255
St Petersburg	MGO	60N	31E	0	27	30	30	30	28	30	31	30	28	26	0	290
Magadan	MGO	60N	151E	24	22	26	26	23	24	28	23	27	26	16	25	290
Vitim	MGO	59N	113E	15	19	21	22	27	24	26	28	28	26	19	0	255
Krasnoyarsk	MGO	56N	93E	0	0	0	0	0	0	0	0	29	23	19	17	88
Omsk	MGO	55N	73E	28	26	30	29	31	30	28	30	30	30	26	28	346
Samara	MGO	53N	50E	21	18	28	28	30	30	30	28	30	28	24	18	313
Nikolaevsk	MGO	53N	141E	15	19	17	18	27	0	0	28	25	20	20	27	216
Irkutsk	MGO	52N	104E	28	25	31	30	30	27	28	30	30	29	24	30	342
Voronezh	MGO	52N	39E	28	24	26	30	31	29	31	30	28	28	0	0	285
Vladivostok	MGO	43N	132E	30	25	29	28	28	0	0	0	29	31	30	30	260

UV-Vis DOAS	Inst.	Lat	Long	J	F	M	A	M	J	J	A	S	O	N	D	#
Ny-Ålesund	IUP/IFE	79N	12E	0	10	31	30	31	25	31	31	28	24	0	0	241
Thule	DMI	77N	69W	0	18	31	30	5	0	0	21	30	31	0	0	166
Scoresbysund	CNRS/DMI	70N	22W	14	28	31	30	31	30	31	31	30	31	23	0	310
Sodankylä	CNRS/FMI	67N	27E	31	28	30	30	31	26	30	31	30	31	30	31	359
Zhigansk	CNRS/CAO	67N	123E	26	11	30	26	29	28	29	31	30	31	30	27	328
Salekhard	CNRS/CAO	67N	67E	26	28	31	30	31	30	31	31	30	31	28	28	355
Harestua	BIRA.IASB	60N	11E	10	23	31	30	31	30	28	31	30	30	25	30	329
Bremen	IUP/IFE	53N	9E	29	12	24	28	30	23	18	24	0	22	30	29	269
Jungfraujoch	BIRA.IASB	47N	8E	31	28	28	2	16	21	18	0	2	31	30	31	238
OHP	CNRS	44N	6E	31	28	31	30	31	30	31	31	30	31	30	31	365
Izaña	INTA	28N	16W	31	28	31	30	31	28	28	29	30	31	30	31	358
Mérida	IUP/IFE	8N	71W	27	23	25	26	18	24	20	28	0	26	17	31	265
St Denis	CNRS	21S	55E	31	28	30	30	31	30	31	28	30	31	29	31	360
Bauru	CNRS/UNESP	22S	49W	14	28	31	30	31	30	31	31	30	31	29	27	343
Kerguelen	CNRS	49S	70E	31	28	31	30	31	30	31	31	30	31	30	31	365
Dumont d'Urville	CNRS	67S	140E	31	28	31	30	31	30	30	31	30	31	29	31	363
Rothera	BAS	68S	68W	31	28	31	29	31	30	30	27	10	0	0	0	247

2007

Brewer	Inst.	Lat	Long	J	F	M	A	M	J	J	A	S	O	N	D	#
Sodankylä	FMI	67N	27E	2	16	30	30	29	30	31	31	30	23	6	5	263
Jokioinen	FMI	61N	23E	14	22	28	30	29	30	31	31	29	28	29	8	309
De Bilt	KNMI	52N	5E	30	28	31	19	31	25	28	31	30	29	28	22	332
Uccle	RMI	51N	4E	31	26	30	0	0	0	0	0	0	0	0	0	87
Hohenpeißenberg	DWD	48N	11E	19	24	29	29	29	28	29	27	25	24	20	21	304
Arosa	MCH	47N	10E	22	26	26	30	26	28	30	25	27	29	24	27	320
Paramaribo	KNMI	6N	55W	31	27	31	30	31	29	27	30	28	30	28	31	353

Dobson	Inst.	Lat	Long	J	F	M	A	M	J	J	A	S	O	N	D	#
Hohenpeißenberg	DWD	48N	11E	9	13	17	17	15	19	19	15	11	16	13	10	174
Arosa	MCH	47N	10E	22	19	25	28	20	25	27	21	14	26	17	25	269
Lauder	NIWA	45S	170E	19	18	20	16	20	15	16	20	20	20	24	16	224
Vernadsky	BAS/KTSU	65S	64W	31	28	31	30	0	0	0	31	30	31	30	31	273
Halley	BAS	76S	27W	31	28	31	3	0	0	0	4	30	31	30	30	218
Arrival Heights	NIWA	78S	167E	10	5	7	0	0	0	0	0	6	13	6	7	54

FTIR	Inst.	Lat	Long	J	F	M	A	M	J	J	A	S	O	N	D	#
Ny-Ålesund	IUP/IFE	79N	12E	0	0	1	0	7	6	4	3	4	0	0	0	25
Kiruna	FZK/IMK	68N	21E	4	9	16	11	7	0	1	11	9	11	3	0	82
Bremen	IUP/IFE	53N	9E	1	1	7	6	4	2	4	2	2	1	3	1	34
Izaña	FZK	28N	16W	10	14	5	12	12	10	16	20	10	8	3	10	130
Lauder	NIWA	45S	170E	5	4	8	4	8	7	8	10	10	8	7	7	86
Arrival Heights	NIWA	78S	167E	4	3	7	2	0	0	0	0	6	10	1	8	41

M124	Inst.	Lat	Long	J	F	M	A	M	J	J	A	S	O	N	D	#
Murmansk	MGO	69N	33E	0	0	30	28	28	26	27	31	28	25	0	0	223
Igarka	MGO	67N	87E	0	0	0	0	0	0	0	0	0	0	11	0	11
Pechora	MGO	65N	57E	0	27	31	28	0	0	0	0	0	0	20	0	106
Markovo	MGO	65N	170E	0	0	0	0	0	0	0	0	0	0	17	0	17
Arkhangel'sk	MGO	65N	40E	0	0	27	25	0	0	0	0	27	26	20	0	125
Tura	MGO	64N	100E	0	0	0	0	0	0	0	0	0	0	19	0	19
Yakutsk	MGO	62N	130E	0	0	26	29	30	30	30	30	26	20	10	5	236
Hanty-Mansiysk	MGO	61N	69E	0	0	0	0	0	0	0	0	0	0	0	27	27
St Petersburg	MGO	60N	31E	0	27	27	30	30	27	31	31	29	27	24	26	309
Magadan	MGO	60N	151E	24	20	22	25	22	24	27	30	28	24	27	26	299
Vitim	MGO	59N	113E	0	0	0	0	28	29	30	31	26	17	13	12	186
Ekaterinburg	MGO	57N	61E	0	0	0	0	0	0	0	0	0	0	26	27	53
Krasnoyarsk	MGO	56N	93E	0	0	0	0	0	0	0	0	0	0	17	17	34
Omsk	MGO	55N	73E	31	27	31	30	25	30	31	31	29	31	25	24	345
Samara	MGO	53N	50E	0	22	27	28	0	0	0	0	0	0	0	22	99
Nikolaevsk	MGO	53N	141E	0	0	0	0	23	22	20	23	28	23	21	23	183
Petropavlovsk	MGO	53N	159E	0	0	0	0	0	0	0	27	30	30	0	0	87
Irkutsk	MGO	52N	104E	27	28	31	30	31	28	29	31	29	29	25	28	346
Voronezh	MGO	52N	39E	27	19	28	28	31	30	31	31	28	30	24	20	327
Karaganda	MGO	50N	73E	24	20	28	0	30	29	30	31	30	28	23	26	299
Yuzhno-Sahalinsk	MGO	47N	143E	27	19	24	27	30	29	30	27	26	30	27	24	320
Vladivostok	MGO	43N	132E	29	27	27	26	0	0	0	0	0	0	0	29	138

UV-Vis DOAS	Inst.	Lat	Long	J	F	M	A	M	J	J	A	S	O	N	D	#
Ny-Ålesund	IUP/IFE	79N	12E	0	0	28	30	31	0	28	30	29	22	0	0	198
Thule	DMI	77N	69W	0	19	29	29	1	0	0	23	24	31	0	0	156
Scoresbysund	CNRS/DMI	70N	22W	8	28	31	30	31	27	26	20	2	28	23	0	254
Sodankylä	CNRS/FMI	67N	27E	31	26	31	30	31	30	31	31	30	31	30	30	362
Zhigansk	CNRS/CAO	67N	123E	31	26	30	29	25	25	29	30	29	21	30	26	331
Salekhard	CNRS/CAO	67N	67E	26	26	31	30	31	30	23	31	30	31	30	26	345
Harestua	BIRA.IASB	60N	11E	30	28	31	30	31	30	30	31	30	31	30	27	359
Bremen	IUP/IFE	53N	9E	31	27	28	29	30	30	29	31	27	29	29	31	351
Jungfraujoch	BIRA.IASB	47N	8E	31	6	30	30	17	10	0	0	0	0	0	0	124
OHP	CNRS	44N	6E	21	27	31	30	31	28	30	31	30	31	30	24	344
Izaña	INTA	28N	16W	31	28	31	29	31	26	30	31	29	31	30	31	358
Mérida	IUP/IFE	8N	71W	14	13	6	13	7	27	18	28	25	22	21	25	219
St Denis	CNRS	21S	55E	31	28	31	24	31	27	24	31	29	30	30	30	346
Bauru	CNRS/UNESP	22S	49W	28	27	31	30	31	30	31	30	30	30	27	20	345
Kerguelen	CNRS	49S	70E	31	28	31	30	31	30	31	31	30	30	29	31	363
Dumont d'Urville	CNRS	67S	140E	31	27	31	30	31	30	31	31	30	31	30	31	364
Rothera	BAS	68S	68W	27	16	31	30	31	23	0	0	0	0	0	0	158
Dome Concorde	CNRS	75S	123E	0	0	31	29	25	0	10	0	0	0	0	0	95

2008

Brewer	Inst.	Lat	Long	J	F	M	A	M	J	J	A	S	O	N	D	#
Sodankylä	FMI	67N	27E	5	20	31	30	31	22	31	31	29	26	8	0	264
Jokioinen	FMI	61N	23E	9	23	30	30	30	28	31	31	30	30	30	6	308
De Bilt	KNMI	52N	5E	29	23	28	27	31	30	31	31	0	0	0	0	230
Hohenpeißenberg	DWD	48N	11E	26	27	27	25	24	27	28	28	25	23	27	16	303
Arosa	MCH	47N	10E	27	28	28	23	28	26	28	31	28	28	25	20	320
Paramaribo	KNMI	6N	55W	31	29	31	30	31	28	31	31	30	31	30	29	362

Dobson	Inst.	Lat	Long	J	F	M	A	M	J	J	A	S	O	N	D	#
Hohenpeißenberg	DWD	48N	11E	18	18	7	10	16	12	18	18	17	12	15	12	173
Arosa	MCH	47N	10E	25	28	21	17	24	24	27	26	24	26	23	19	284
Lauder	NIWA	45S	170E	21	19	18	19	16	17	18	21	20	26	21	19	235
Vernadsky	BAS/KTSU	65S	64W	31	29	31	2	0	0	0	31	30	31	30	31	246
Halley	BAS	76S	27W	27	25	23	9	0	0	0	3	29	29	25	27	197
Arrival Heights	NIWA	78S	167E	6	5	1	0	0	0	0	0	6	12	15	20	65

FTIR	Inst.	Lat	Long	J	F	M	A	M	J	J	A	S	O	N	D	#
Ny-Ålesund	IUP/IFE	79N	12E	0	0	3	6	0	0	2	4	3	0	0	0	18
Kiruna	FZK/IMK	68N	21E	2	5	9	9	1	1	9	2	7	3	6	0	54
Bremen	IUP/IFE	53N	9E	1	4	0	1	0	0	2	0	0	0	1	0	9
Izaña	FZK	28N	16W	6	3	10	6	5	7	11	5	8	4	3	5	73
Lauder	NIWA	45S	170E	9	5	6	10	7	8	7	6	6	8	8	5	85
Arrival Heights	NIWA	78S	167E	7	4	1	1	0	0	0	0	5	0	0	5	23

M124	Inst.	Lat	Long	J	F	M	A	M	J	J	A	S	O	N	D	#
Tiksi	MGO	72N	129E	0	10	0	0	0	0	0	0	0	0	0	0	10
Murmansk	MGO	69N	33E	0	21	27	0	0	0	0	0	0	0	0	0	48
Olenek	MGO	68N	112E	0	23	29	0	0	0	0	0	0	0	0	0	52
Igarka	MGO	67N	87E	0	9	0	0	0	0	0	0	0	0	0	0	9
Pechora	MGO	65N	57E	8	24	30	0	0	0	0	0	0	0	0	0	62
Markovo	MGO	65N	170E	6	27	0	0	0	0	0	0	0	0	0	0	33
Arkhangel'sk	MGO	65N	40E	6	18	25	0	0	0	0	0	0	0	0	0	49
Tura	MGO	64N	100E	10	23	0	0	0	0	0	0	0	0	0	0	33
Yakutsk	MGO	62N	130E	6	9	25	0	0	0	0	0	0	0	0	0	40
Hanty-Mansiysk	MGO	61N	69E	22	22	0	0	0	0	0	0	0	0	0	0	44
St Petersburg	MGO	60N	31E	28	24	30	0	0	0	0	0	0	0	0	0	82
Magadan	MGO	60N	151E	25	20	29	0	0	0	0	0	0	0	0	0	74
Vitim	MGO	59N	113E	16	16	0	0	0	0	0	0	0	0	0	0	32
Ekaterinburg	MGO	57N	61E	27	26	28	0	0	0	0	0	0	0	0	0	81
Krasnoyarsk	MGO	56N	93E	19	18	24	0	0	0	0	0	0	0	0	0	61
Omsk	MGO	55N	73E	26	28	31	0	0	0	0	0	0	0	0	0	85
Samara	MGO	53N	50E	21	19	23	0	0	0	0	0	0	0	0	0	63
Nikolaevsk	MGO	53N	141E	24	20	19	0	0	0	0	0	0	0	0	0	63
Petropavlovsk	MGO	53N	159E	27	25	25	0	0	0	0	0	0	0	0	0	77
Irkutsk	MGO	52N	104E	27	28	30	0	0	0	0	0	0	0	0	0	85
Voronezh	MGO	52N	39E	26	28	29	0	0	0	0	0	0	0	0	0	83
Karaganda	MGO	50N	73E	27	23	28	0	0	0	0	0	0	0	0	0	78
Yuzhno-Sahalinsk	MGO	47N	143E	26	25	30	0	0	0	0	0	0	0	0	0	81
Vladivostok	MGO	43N	132E	31	28	0	0	0	0	0	0	0	0	0	0	59

UV-Vis DOAS	Inst.	Lat	Long	J	F	M	A	M	J	J	A	S	O	N	D	#
Ny-Ålesund	IUP/IFE	79N	12E	0	9	31	30	30	17	24	27	29	21	0	0	218
Scoresbysund	CNRS/DMI	70N	22W	13	29	0	0	0	0	27	28	29	28	23	0	177
Sodankylä	CNRS/FMI	67N	27E	31	29	31	0	0	0	24	31	30	31	30	30	267
Zhigansk	CNRS/CAO	67N	123E	25	21	29	0	0	0	10	6	30	28	25	20	194
Salekhard	CNRS/CAO	67N	67E	24	28	29	0	0	0	31	31	30	31	30	0	234
Harestua	BIRA.IASB	60N	11E	31	26	31	30	23	30	29	29	20	26	29	25	329
Bremen	IUP/IFE	53N	9E	25	17	31	28	26	29	31	31	17	27	24	31	317
Jungfraujoch	BIRA.IASB	47N	8E	0	0	0	0	0	0	0	0	0	27	30	30	87
OHP	CNRS	44N	6E	28	29	30	0	0	0	31	30	29	31	30	30	268
Izaña	INTA	28N	16W	31	29	31	30	31	30	31	31	30	31	30	31	366
Mérida	IUP/IFE	8N	71W	29	22	14	0	0	0	0	0	0	0	0	0	65
St Denis	CNRS	21S	55E	30	29	31	0	0	0	31	28	30	30	28	30	267
Bauru	CNRS/UNESP	22S	49W	28	23	24	0	0	0	28	30	25	27	25	30	240
Kerguelen	CNRS	49S	70E	0	28	29	0	0	0	31	30	29	27	29	30	233
Rio Gallegos	CNRS	52S	69W	0	0	0	29	30	23	31	31	29	29	27	20	249
Dumont d'Urville	CNRS	67S	140E	31	29	30	30	31	26	31	31	0	0	0	0	239
Rothera	BAS	68S	68W	31	26	30	6	0	0	0	0	0	0	0	0	93
Dome Concorde	CNRS	75S	123E	0	0	28	27	23	0	13	31	30	31	30	30	243

2009

Brewer	Inst.	Lat	Long	J	F	M	A	M	J	J	A	S	O	N	D	#
Sodankylä	FMI	67N	27E	1	19	30	30	31	29	31	30	28	24	0	0	253
Jokioinen	FMI	61N	23E	14	23	31	30	30	26	30	31	30	30	29	9	313
Hohenpeißenberg	DWD	48N	11E	19	17	23	28	29	28	0	0	28	30	23	16	241
Arosa	MCH	47N	10E	27	19	28	27	30	25	28	29	30	30	23	23	319
Paramaribo	KNMI	6N	55W	6	18	16	22	31	30	28	26	30	31	29	30	297

Dobson	Inst.	Lat	Long	J	F	M	A	M	J	J	A	S	O	N	D	#
Hohenpeißenberg	DWD	48N	11E	10	13	14	17	15	13	0	0	18	17	12	7	136
Arosa	MCH	47N	10E	24	16	25	24	29	23	24	25	26	25	20	19	280
Lauder	NIWA	45S	170E	23	18	19	18	15	18	18	14	25	25	26	17	236
Vernadsky	BAS/KTSU	65S	64W	31	28	31	30	0	0	9	31	30	31	30	31	282
Halley	BAS	76S	27W	31	27	25	13	0	0	0	3	29	29	27	31	215
Arrival Heights	NIWA	78S	167E	14	9	5	0	0	0	0	0	11	15	15	0	69

FTIR	Inst.	Lat	Long	J	F	M	A	M	J	J	A	S	O	N	D	#
Ny-Ålesund	IUP/IFE	79N	12E	0	0	3	8	5	6	7	2	0	0	0	0	31
Kiruna	FZK/IMK	68N	21E	0	10	8	1	1	2	1	4	6	4	1	0	38
Bremen	IUP/IFE	53N	9E	0	0	0	1	5	4	1	3	3	0	0	0	17
Izaña	FZK	28N	16W	9	4	9	16	12	12	1	14	5	8	1	3	94
Lauder	NIWA	45S	170E	4	4	2	4	7	10	4	9	8	9	9	4	74
Arrival Heights	NIWA	78S	167E	11	5	7	1	0	0	0	0	6	10	12	7	59

UV-Vis DOAS	Inst.	Lat	Long	J	F	M	A	M	J	J	A	S	O	N	D	#
Ny-Ålesund	IUP/IFE	79N	12E	0	0	26	29	31	18	22	31	30	22	0	0	209
Scoresbysund	CNRS/DMI	70N	22W	14	28	31	30	30	22	24	31	29	31	23	0	293
Sodankylä	CNRS/FMI	67N	27E	31	28	31	30	31	30	30	30	30	31	30	29	361
Zhigansk	CNRS/CAO	67N	123E	16	26	11	29	29	29	30	31	28	30	21	20	300
Salekhard	CNRS/CAO	67N	67E	29	25	31	30	30	27	22	5	8	31	30	29	297
Harestua	BIRA.IASB	60N	11E	25	27	29	29	29	20	16	15	24	18	21	30	283
Bremen	IUP/IFE	53N	9E	30	28	30	25	22	29	31	31	28	31	30	31	346
Jungfraujoch	BIRA.IASB	47N	8E	31	28	31	30	28	30	17	4	0	0	21	31	251
OHP	CNRS	44N	6E	31	28	31	29	31	8	31	31	30	31	20	21	322
Izaña	INTA	28N	16W	31	28	25	27	27	30	31	31	27	27	28	30	342
St Denis	CNRS	21S	55E	31	28	31	30	29	30	31	31	30	31	25	29	356
Bauru	CNRS/UNESP	22S	49W	31	24	31	30	31	30	31	28	16	2	6	7	267
Kerguelen	CNRS	49S	70E	30	28	31	29	12	29	29	29	30	30	30	28	335
Rio Gallegos	CNRS	52S	69W	27	24	21	27	12	21	28	30	23	23	16	25	277
Dumont d'Urville	CNRS	67S	140E	27	27	30	28	31	27	27	28	30	28	29	26	338
Rothera	BAS	68S	68W	31	26	27	29	31	30	31	31	10	0	0	0	246
Dome Concorde	CNRS	75S	123E	31	28	30	30	13	0	4	30	27	31	30	27	281

2010

Brewer	Inst.	Lat	Long	J	F	M	A	M	J	J	A	S	O	N	D	#
Sodankylä	FMI	67N	27E	1	16	30	30	21	30	28	30					214
Jokioinen	FMI	61N	23E	19	23	28	30	31	29	30	29					246
Hohenpeißenberg	DWD	48N	11E	0	0	27	28	22	17	29	27					150
Arosa	MCH	47N	10E	26	26	29	25	23	25	28	29					211

Dobson	Inst.	Lat	Long	J	F	M	A	M	J	J	A	S	O	N	D	#
Hohenpeißenberg	DWD	48N	11E	0	0	17	20	9	13	19	13					91
Arosa	MCH	47N	10E	25	21	26	23	18	20	25	22					180
Lauder	NIWA	45S	170E	22	22	23	20	17	11	18						133
Vernadsky	BAS/KTSU	65S	64W	7	0	0	0	0	0	0						7
Halley	BAS	76S	27W	31	25	16	0	0	0	0						72
Arrival Heights	NIWA	78S	167E	0	3	6	0	0	0	0						9

FTIR	Inst.	Lat	Long	J	F	M	A	M	J	J	A	S	O	N	D	#
Bremen	IUP/IFE	53N	9E	1	1	5	10	2	6	4						29
Lauder	NIWA	45S	170E	5	6	4	7	7	5	4						38
Arrival Heights	NIWA	78S	167E	6	7	4	0	0	0	0						17

UV-Vis DOAS	Inst.	Lat	Long	J	F	M	A	M	J	J	A	S	O	N	D	#
Ny-Ålesund	IUP/IFE	79N	12E	0	0	19	19	28	23	26	29					144
Scoresbysund	CNRS/DMI	70N	22W	14	28	31	30	10	30	28	27					198
Sodankylä	CNRS/FMI	67N	27E	29	23	22	30	10	30	30	27					201
Zhigansk	CNRS/CAO	67N	123E	24	19	26	24	8	28	17	22					168
Salekhard	CNRS/CAO	67N	67E	31	28	31	30	10	5	10	31					176
Harestua	BIRA.IASB	60N	11E	31	27	31	29	23	16	29						186
Bremen	IUP/IFE	53N	9E	31	28	31	30	22	28	22						192
Jungfraujoch	BIRA.IASB	47N	8E	31	28	30	30	29	8	16						172
OHP	CNRS	44N	6E	31	28	31	30	10	30	31	31					222
Izaña	INTA	28N	16W	31	25	25	17	20	23	24						165
St Denis	CNRS	21S	55E	31	28	31	27	10	30	28	31					216
Bauru	CNRS/UNESP	22S	49W	31	27	30	28	10	30	30	31					217
Kerguelen	CNRS	49S	70E	31	27	31	30	9	30	31	31					220
Rio Gallegos	CNRS	52S	69W	18	18	30	30	10	26	28	26					186
Dumont d'Urville	CNRS	67S	140E	23	24	31	30	10	30	29	31					208
Rothera	BAS	68S	68W	14	0	0	0	0	0	0						14
Dome Concorde	CNRS	75S	123E	31	27	31	28	8	0	3	24					152

V.2 Monthly Data Distribution for O_3 Profile Data

2006

FTIR	Inst.	Lat	Long	J	F	M	A	M	J	J	A	S	O	N	D	#
Kiruna	FZK/IMK	68N	21E	0	9	13	7	10	12	6	13	6	7	5	0	88
Izaña	FZK	28N	16W	4	5	14	7	9	17	14	14	13	11	11	10	129

Microwave	Inst.	Lat	Long	J	F	M	A	M	J	J	A	S	O	N	D	#
Ny-Ålesund	IUP/IFE	79N	12E	0	0	0	0	0	0	0	0	0	0	0	26	26
Kiruna	FZK/IMK	68N	21E	31	28	30	0	20	12	0	0	20	30	30	31	232
Bremen	IUP/IFE	53N	9E	0	0	0	0	0	0	0	0	0	0	0	17	17
Payerne	UBERN	46N	7E	30	28	31	30	24	30	25	29	30	31	30	29	347
Mérida	FZK/IMK	8N	71W	0	4	0	22	1	18	13	26	26	19	21	3	153

Ozonesonde	Inst.	Lat	Long	J	F	M	A	M	J	J	A	S	O	N	D	#
Ny-Ålesund	AWI	79N	12E	9	8	10	5	5	4	4	4	4	3	4	6	66
Thule	DMI	77N	69W	1	1	1	0	0	0	0	0	0	0	0	3	6
Scoresbysund	DMI	70N	22W	4	3	4	3	4	5	4	3	4	4	3	0	41
Sodankylä	FMI	67N	27E	3	4	13	13	4	4	4	5	4	4	5	4	67
Keflavik	INTA	64N	23W	3	4	0	0	0	0	0	0	0	0	0	0	7
Legionowo	IMWM	52N	21E	6	4	5	5	8	6	7	6	4	1	0	0	52
De Bilt	KNMI	52N	5E	4	3	4	4	4	4	4	5	6	3	5	4	50
Uccle	RMI	51N	4E	12	12	14	11	12	11	11	12	13	13	11	9	141
Hohenpeißenberg	DWD	48N	11E	10	12	13	11	10	7	9	9	8	8	12	11	120
Payerne	MCH	46N	7E	15	12	14	10	12	12	12	14	12	12	13	12	150
Paramaribo	KNMI	6N	55W	4	4	5	4	3	3	3	3	4	3	4	3	43
Lauder	NIWA	45S	170E	3	4	4	2	4	6	7	5	4	5	3	4	51
Marambio	FMI	64S	57W	2	2	3	2	2	6	7	6	4	8	9	5	56
Dumont d'Urville	CNRS	67S	140E	1	1	0	1	1	1	2	2	3	3	3	3	21
Belgrano	INTA	78S	35W	3	1	3	2	4	2	2	5	5	5	4	3	39

2007

FTIR	Inst.	Lat	Long	J	F	M	A	M	J	J	A	S	O	N	D	#
Kiruna	FZK/IMK	68N	21E	4	9	16	11	7	0	1	11	9	11	3	0	82
Izaña	FZK	28N	16W	10	14	5	12	12	10	16	20	10	8	3	10	130

Microwave	Inst.	Lat	Long	J	F	M	A	M	J	J	A	S	O	N	D	#
Ny-Ålesund	IUP/IFE	79N	12E	26	22	25	17	0	0	0	0	0	0	0	15	105
Kiruna	FZK/IMK	68N	21E	28	26	1	0	0	0	0	0	0	11	25	31	122
Payerne	UBERN	46N	7E	29	28	29	25	28	29	31	27	27	30	25	30	338
Mérida	FZK/IMK	8N	71W	0	6	0	0	0	0	23	6	9	29	22	27	122

Ozonesonde	Inst.	Lat	Long	J	F	M	A	M	J	J	A	S	O	N	D	#
Thule	DMI	77N	69W	3	4	5	4	0	0	0	0	0	0	0	0	16
Scoresbysund	DMI	70N	22W	4	3	3	4	3	5	3	5	4	4	3	1	42
Sodankylä	FMI	67N	27E	10	28	9	5	5	4	4	5	3	5	4	4	86
Salekhard	CAO	67N	67E	6	6	6	0	0	0	0	0	0	0	0	0	18
Keflavik	INTA	64N	23W	6	7	5	0	0	0	0	0	0	0	0	0	18
Jokioinen	FMI	61N	23E	7	6	1	0	0	0	0	0	0	0	0	0	14
De Bilt	KNMI	52N	5E	6	5	4	4	4	4	4	5	4	4	5	4	53
Uccle	RMI	51N	4E	12	11	13	11	11	8	0	2	4	6	6	1	85
Hohenpeißenberg	DWD	48N	11E	13	11	11	10	9	7	9	9	8	10	11	10	118
Payerne	MCH	46N	7E	14	11	13	11	13	12	14	14	12	13	14	11	152
Paramaribo	KNMI	6N	55W	4	4	2	2	3	2	1	3	2	3	2	4	32
Lauder	NIWA	45S	170E	3	8	4	7	7	2	6	4	4	5	6	5	61
Marambio	FMI	64S	57W	3	2	1	1	3	5	7	15	8	10	7	5	67
Dumont d'Urville	CNRS	67S	140E	1	0	0	0	0	0	0	0	0	0	0	0	1
Belgrano	INTA	78S	35W	2	3	1	2	2	3	9	10	9	5	3	1	50

2008

FTIR	Inst.	Lat	Long	J	F	M	A	M	J	J	A	S	O	N	D	#
Kiruna	FZK/IMK	68N	21E	2	5	9	9	1	1	9	2	7	3	6	0	54
Izaña	FZK	28N	16W	6	3	10	6	5	7	11	5	8	4	3	5	73

Microwave	Inst.	Lat	Long	J	F	M	A	M	J	J	A	S	O	N	D	#
Ny-Ålesund	IUP/IFE	79N	12E	27	21	7	3	0	0	0	0	0	20	19	26	123
Kiruna	FZK/IMK	68N	21E	25	26	29	15	0	0	0	0	0	0	0	0	95
Payerne	UBERN	46N	7E	29	24	22	23	30	30	30	21	20	23	23	23	298
Mérida	FZK/IMK	8N	71W	27	23	27	0	0	0	0	0	0	0	0	0	77

Ozonesonde	Inst.	Lat	Long	J	F	M	A	M	J	J	A	S	O	N	D	#
Sodankylä	FMI	67N	27E	4	5	5	5	4	4	5	4	4	4	4	3	51
Keflavik	INTA	64N	23W	5	7	4	0	0	0	0	0	0	0	0	3	19
Jokioinen	FMI	61N	23E	2	7	1	0	0	0	0	0	0	0	0	0	10
De Bilt	KNMI	52N	5E	5	6	4	5	4	4	5	6	4	5	4	5	57
Hohenpeißenberg	DWD	48N	11E	13	12	11	13	7	8	9	8	9	7	11	12	120
Payerne	MCH	46N	7E	14	13	11	13	12	12	14	14	14	14	12	13	156
Paramaribo	KNMI	6N	55W	3	0	2	3	0	0	0	0	0	0	0	0	8
Lauder	NIWA	45S	170E	6	4	4	5	5	6	7	4	5	6	5	6	63
Marambio	FMI	64S	57W	2	2	2	2	2	3	7	9	8	9	9	10	65
Belgrano	INTA	78S	35W	2	2	2	3	1	2	3	4	6	7	4	4	40

2009

FTIR	Inst.	Lat	Long	J	F	M	A	M	J	J	A	S	O	N	D	#
Kiruna	FZK/IMK	68N	21E	0	10	8	1	1	2	1	4	6	4	1	0	38
Izaña	FZK	28N	16W	9	4	9	16	12	12	1	14	5	8	1	3	94

Microwave	Inst.	Lat	Long	J	F	M	A	M	J	J	A	S	O	N	D	#
Ny-Ålesund	IUP/IFE	79N	12E	10	23	19	29	14	6	0	1	1	0	2	0	105
Payerne	UBERN	46N	7E	20	17	11	0	0	0	0	1	0	0	0	0	49

Ozonesonde	Inst.	Lat	Long	J	F	M	A	M	J	J	A	S	O	N	D	#
Sodankylä	FMI	67N	27E	4	3	4	4	2	4	5	4	4	3	4	5	46
Keflavik	INTA	64N	23W	5	4	4	0	0	0	0	0	0	0	0	0	13
Jokioinen	FMI	61N	23E	1	0	0	0	0	0	0	0	0	0	0	0	1
Hohenpeißenberg	DWD	48N	11E	13	12	12	12	8	9	9	9	8	8	12	12	124
Payerne	MCH	46N	7E	12	12	12	11	13	13	13	14	14	12	13	11	150
Lauder	NIWA	45S	170E	6	6	3	4	6	6	5	2	3	1	2	3	47
Marambio	FMI	64S	57W	2	2	2	4	2	2	1	1	1	0	3	8	28
Belgrano	INTA	78S	35W	4	2	2	3	3	3	3	4	5	5	5	2	41

2010

Microwave	Inst.	Lat	Long	J	F	M	A	M	J	J	A	S	O	N	D	#
Ny-Ålesund	IUP/IFE	79N	12E	13	28	31	28	4	0	0						104
Payerne	MCH	46N	7E	0	0	0	1	0	16	23	26					69

Ozonesonde	Inst.	Lat	Long	J	F	M	A	M	J	J	A	S	O	N	D	#
Sodankylä	FMI	67N	27E	5	5	5	4	4	4	4	3					38
Keflavik	INTA	64N	23W	4	5	4	0	0	0	0						13
Jokioinen	FMI	61N	23E	1	2	0	0	0	0	0						3
Hohenpeißenberg	DWD	48N	11E	12	12	14	18	0	0	0						56
Payerne	MCH	46N	7E	13	11	14	12	12	14	13	12					113
Lauder	NIWA	45S	170E	2	3	6	6	3	2	2	2					26
Ushuaia	INTA	55S	68W	2	1	2	1	2	2	2						12
Marambio	FMI	64S	57W	6	2	1	2	1	7	8	8					43
Belgrano	INTA	78S	35W	2	1	3	2	2	2	2						14

V.3 Monthly Data Distribution for NO_2 Column Data

2006

FTIR	Inst.	Lat	Long	J	F	M	A	M	J	J	A	S	O	N	D	#
Ny-Ålesund	IUP/IFE	79N	12E	0	0	2	3	5	0	1	0	0	0	0	0	11
Kiruna	FZK/IMK	68N	21E	0	8	14	7	8	10	7	13	6	6	4	0	83
Bremen	IUP/IFE	53N	9E	2	2	3	5	6	6	7	3	9	4	1	1	49
Izaña	FZK	28N	16W	4	5	14	7	8	17	14	13	13	10	11	10	126

UV-Vis DOAS	Inst.	Lat	Long	J	F	M	A	M	J	J	A	S	O	N	D	#
Ny-Ålesund	IUP/IFE	79N	12E	0	9	25	30	28	19	31	31	28	26	0	0	227
Thule	DMI	77N	69W	0	18	31	30	5	0	0	21	30	31	0	0	166
Scoresbysund	CNRS/DMI	70N	22W	14	28	31	30	31	30	31	31	30	31	23	0	310
Kiruna	NIWA	68N	21E	23	26	31	30	31	1	22	18	20	31	30	3	266
Sodankylä	CNRS/FMI	67N	27E	31	28	30	30	31	26	30	31	30	31	30	31	359
Zhigansk	CNRS/CAO	67N	123E	26	11	30	26	29	28	29	31	30	31	30	27	328
Salekhard	CNRS/CAO	67N	67E	26	28	31	30	31	30	31	31	30	31	28	28	355
Harestua	BIRA.IASB	60N	11E	12	23	31	30	31	30	28	31	30	30	25	31	332
St Petersburg	SPBSU	60N	31E	31	28	31	30	31	30	31	30	30	31	30	30	363
Bremen	IUP/IFE	53N	9E	29	12	29	30	31	29	23	22	0	24	29	30	288
Jungfraujoch	BIRA.IASB	47N	8E	31	28	28	2	16	21	18	0	3	31	30	31	239
OHP	CNRS	44N	6E	31	28	31	30	31	30	31	31	30	31	30	31	365
Issyk Kul	KSNU	43N	77E	31	26	29	30	31	30	31	31	29	31	30	31	360
Izaña	INTA	28N	16W	31	28	31	30	31	28	28	29	30	31	30	31	358
Mauna Loa	NIWA	20N	156W	31	28	31	30	30	30	31	31	29	26	28	31	356
Mérida	IUP/IFE	8N	71W	27	23	25	25	17	23	18	27	0	26	17	31	259
St Denis	CNRS	21S	55E	31	28	30	30	31	30	31	28	30	31	29	31	360
Bauru	CNRS/UNESP	22S	49W	14	28	31	30	31	30	31	31	30	31	29	27	343
Lauder	NIWA	45S	170E	31	28	31	30	24	30	31	31	30	31	30	21	348
Kerguelen	CNRS	49S	70E	31	28	31	30	31	30	31	31	30	31	30	31	365
Macquarie	NIWA	54S	159E	31	27	31	28	30	30	31	31	30	31	30	31	361
Marambio	INTA	64S	57W	30	28	31	30	30	29	31	31	30	31	30	31	362
Dumont d'Urville	CNRS	67S	140E	31	28	31	30	31	30	30	31	30	31	29	31	363
Rothera	BAS	68S	68W	31	28	31	29	31	27	23	27	10	0	0	0	237
Arrival Heights	NIWA	78S	167E	0	12	31	22	0	0	0	11	30	25	0	0	131
Belgrano	INTA	78S	35W	0	14	29	22	0	0	0	0	18	31	0	0	114

2007

FTIR	Inst.	Lat	Long	J	F	M	A	M	J	J	A	S	O	N	D	#
Ny-Ålesund	IUP/IFE	79N	12E	0	0	1	0	7	6	4	3	4	0	0	0	25
Kiruna	FZK/IMK	68N	21E	3	7	15	11	9	4	6	9	8	9	3	0	84
Bremen	IUP/IFE	53N	9E	2	1	7	9	2	0	0	0	0	0	0	0	21
Izaña	FZK	28N	16W	10	13	5	12	12	10	16	18	10	8	3	9	126

UV-Vis DOAS	Inst.	Lat	Long	J	F	M	A	M	J	J	A	S	O	N	D	#
Ny-Ålesund	IUP/IFE	79N	12E	0	0	15	30	31	0	27	31	29	22	0	0	185
Thule	DMI	77N	69W	0	19	29	29	1	0	0	23	24	31	0	0	156
Scoresbysund	CNRS/DMI	70N	22W	8	28	31	30	31	27	26	20	2	28	23	0	254
Kiruna	NIWA	68N	21E	23	16	30	30	31	1	21	31	6	23	30	3	245
Sodankylä	CNRS/FMI	67N	27E	31	26	31	30	31	30	31	31	30	31	30	30	362
Zhigansk	CNRS/CAO	67N	123E	31	26	30	29	25	25	29	30	29	21	30	26	331
Salekhard	CNRS/CAO	67N	67E	26	26	31	30	31	30	23	31	30	31	30	26	345
Harestua	BIRA.IASB	60N	11E	29	28	30	30	31	30	30	31	30	31	30	27	357
St Petersburg	SPBSU	60N	31E	31	28	29	27	31	30	29	31	27	30	26	31	350
Bremen	IUP/IFE	53N	9E	30	27	31	30	26	28	11	8	30	31	29	29	310
Paris	CNRS	49N	2E	31	28	31	30	29	30	31	31	30	31	30	31	363
Jungfraujoch	BIRA.IASB	47N	8E	31	6	30	30	17	11	0	0	0	0	0	0	125
OHP	CNRS	44N	6E	21	27	31	30	31	28	30	31	30	31	30	24	344
Issyk Kul	KSNU	43N	77E	30	28	30	27	31	29	30	30	30	31	30	31	357
Izaña	INTA	28N	16W	31	28	31	29	31	26	30	31	29	31	30	31	358
Mauna Loa	NIWA	20N	156W	30	24	27	30	30	29	31	31	28	28	30	31	349
Mérida	IUP/IFE	8N	71W	15	14	6	13	9	23	19	29	26	26	19	25	224
St Denis	CNRS	21S	55E	31	28	31	24	31	27	24	31	29	30	30	30	346
Bauru	CNRS/UNESP	22S	49W	28	27	31	30	31	30	31	30	30	30	27	20	345
Lauder	NIWA	45S	170E	29	28	31	30	31	30	29	31	30	31	28	31	359
Kerguelen	CNRS	49S	70E	31	28	31	30	31	30	31	31	30	30	29	31	363
Macquarie	NIWA	54S	159E	31	28	30	29	31	30	31	31	30	31	30	31	363
Ushuaia	INTA	55S	68W	31	25	28	30	28	30	30	17	28	27	9	29	312
Marambio	INTA	64S	57W	31	27	31	30	31	30	31	31	30	30	30	31	363
Dumont d'Urville	CNRS	67S	140E	31	27	31	30	31	30	31	31	30	31	30	31	364
Rothera	BAS	68S	68W	27	16	31	30	31	19	0	0	0	0	0	0	154
Dome Concorde	CNRS	75S	123E	0	0	31	29	25	0	10	0	0	0	0	0	95
Arrival Heights	NIWA	78S	167E	0	12	31	22	0	0	0	10	30	25	0	0	130
Belgrano	INTA	78S	35W	0	16	31	22	0	0	0	14	29	30	0	0	142

2008

FTIR	Inst.	Lat	Long	J	F	M	A	M	J	J	A	S	O	N	D	#
Ny-Ålesund	IUP/IFE	79N	12E	0	0	3	6	0	0	2	4	3	0	0	0	18
Kiruna	FZK/IMK	68N	21E	1	4	9	7	1	1	9	2	7	4	5	0	50
Izaña	FZK	28N	16W	6	3	9	6	5	7	11	5	8	4	2	5	71

UV-Vis DOAS	Inst.	Lat	Long	J	F	M	A	M	J	J	A	S	O	N	D	#
Ny-Ålesund	IUP/IFE	79N	12E	0	6	31	29	30	24	30	27	29	17	0	0	223
Scoresbysund	CNRS/DMI	70N	22W	13	29	0	0	0	0	27	28	29	28	23	0	177
Kiruna	NIWA	68N	21E	23	29	28	30	31	0	22	31	30	30	30	2	286
Sodankylä	CNRS/FMI	67N	27E	31	29	31	0	0	0	24	31	30	31	30	30	267
Zhigansk	CNRS/CAO	67N	123E	25	21	29	0	0	0	10	6	30	28	25	20	194
Salekhard	CNRS/CAO	67N	67E	24	28	29	0	0	0	31	31	30	31	30	0	234
Harestua	BIRA.IASB	60N	11E	29	26	31	30	23	30	29	29	20	26	29	26	328
St Petersburg	SPBSU	60N	31E	30	27	31	0	0	0	0	0	0	0	0	0	88
Bremen	IUP/IFE	53N	9E	28	11	30	27	26	30	31	31	30	29	23	30	326
Paris	CNRS	49N	2E	12	12	12	12	12	12	12	12	12	12	12	12	144
Jungfraujoch	BIRA.IASB	47N	8E	0	0	0	0	0	0	0	0	0	27	30	30	87
OHP	CNRS	44N	6E	28	29	30	0	0	0	31	30	29	31	30	30	268
Issyk Kul	KSNU	43N	77E	30	29	29	0	0	0	0	0	0	0	0	0	88
Izaña	INTA	28N	16W	31	29	31	30	31	30	31	31	30	31	30	31	366
Mauna Loa	NIWA	20N	156W	31	24	0	0	0	0	0	0	0	0	0	0	55
Mérida	IUP/IFE	8N	71W	31	22	16	0	0	0	0	0	0	0	0	0	69
St Denis	CNRS	21S	55E	30	29	31	0	0	0	31	28	30	30	28	30	267
Bauru	CNRS/UNESP	22S	49W	28	23	24	0	0	0	28	30	25	27	25	30	240
Lauder	NIWA	45S	170E	30	29	29	30	31	30	31	31	30	31	23	31	356
Kerguelen	CNRS	49S	70E	0	28	29	0	0	0	31	30	29	27	29	30	233
Rio Gallegos	CNRS	52S	69W	0	0	0	29	30	23	31	31	29	29	27	20	249
Macquarie	NIWA	54S	159E	31	29	31	30	31	30	31	28	27	31	30	24	353
Ushuaia	INTA	55S	68W	22	29	31	30	28	30	30	30	23	30	28	31	342
Marambio	INTA	64S	57W	31	29	30	30	31	30	31	31	30	31	30	30	364
Dumont d'Urville	CNRS	67S	140E	31	29	30	30	31	26	31	31	0	0	0	0	239
Rothera	BAS	68S	68W	31	26	30	6	0	0	0	0	0	0	0	0	93
Dome Concorde	CNRS	75S	123E	0	0	28	27	23	0	13	31	30	31	30	30	243
Arrival Heights	NIWA	78S	167E	0	13	31	22	0	0	0	11	30	24	0	0	131
Belgrano	INTA	78S	35W	0	16	30	19	0	0	0	15	29	30	0	0	139

2009

FTIR	Inst.	Lat	Long	J	F	M	A	M	J	J	A	S	O	N	D	#
Ny-Ålesund	IUP/IFE	79N	12E	0	0	3	8	5	6	7	1	0	0	0	0	30
Kiruna	FZK/IMK	68N	21E	0	10	7	1	0	0	0	0	0	0	0	0	18
Izaña	FZK	28N	16W	9	4	8	15	12	8	0	0	0	0	0	0	56

UV-Vis DOAS	Inst.	Lat	Long	J	F	M	A	M	J	J	A	S	O	N	D	#
Ny-Ålesund	IUP/IFE	79N	12E	0	0	23	29	31	21	26	31	30	22	0	0	213
Scoresbysund	CNRS/DMI	70N	22W	14	28	31	30	30	22	24	31	29	31	23	0	293
Kiruna	NIWA	68N	21E	23	28	31	30	31	0	22	31	30	31	30	3	290
Sodankylä	CNRS/FMI	67N	27E	31	28	31	30	31	30	30	30	30	31	30	29	361
Zhigansk	CNRS/CAO	67N	123E	16	26	11	29	29	29	30	31	28	30	21	20	300
Salekhard	CNRS/CAO	67N	67E	29	25	31	30	30	27	22	5	8	31	30	29	297
Harestua	BIRA.IASB	60N	11E	25	27	29	29	29	20	16	15	24	18	19	30	281
Bremen	IUP/IFE	53N	9E	31	15	31	28	9	11	31	31	30	31	30	31	309
Paris	CNRS	49N	2E	4	4	4	5	5	0	0	0	0	0	0	0	22
Jungfraujoch	BIRA.IASB	47N	8E	31	28	31	30	28	30	17	8	8	0	21	31	263
OHP	CNRS	44N	6E	31	28	31	29	31	8	31	31	30	31	20	21	322
Izaña	INTA	28N	16W	31	28	25	27	27	30	31	31	27	27	28	30	342
St Denis	CNRS	21S	55E	31	28	31	30	29	30	31	31	30	31	25	29	356
Bauru	CNRS/UNESP	22S	49W	31	24	31	30	31	30	31	28	16	2	6	7	267
Lauder	NIWA	45S	170E	31	28	31	27	31	30	31	31	30	31	30	30	361
Kerguelen	CNRS	49S	70E	30	28	31	29	12	29	29	29	30	30	30	28	335
Rio Gallegos	CNRS	52S	69W	27	24	21	27	12	21	28	30	23	23	16	25	277
Macquarie	NIWA	54S	159E	30	28	31	30	31	30	31	31	30	30	8	17	327
Ushuaia	INTA	55S	68W	27	28	26	30	31	30	28	26	30	30	30	30	346
Marambio	INTA	64S	57W	30	28	31	30	29	28	15	31	30	30	29	30	341
Dumont d'Urville	CNRS	67S	140E	27	27	30	28	31	27	27	28	30	28	29	26	338
Rothera	BAS	68S	68W	31	26	27	29	31	30	31	31	10	0	0	0	246
Dome Concorde	CNRS	75S	123E	31	28	30	30	13	0	4	30	27	31	30	27	281
Arrival Heights	NIWA	78S	167E	0	12	31	21	0	0	0	11	30	24	0	0	129
Belgrano	INTA	78S	35W	0	16	31	22	0	0	0	15	28	30	0	0	142

2010

UV-Vis DOAS	Inst.	Lat	Long	J	F	M	A	M	J	J	A	S	O	N	D	#
Ny-Ålesund	IUP/IFE	79N	12E	0	0	19	19	29	22	26	29					144
Scoresbysund	CNRS/DMI	70N	22W	14	28	31	30	10	30	28	27					198
Kiruna	NIWA	68N	21E	23	28	0	0	0	0	0						51
Sodankylä	CNRS/FMI	67N	27E	29	23	22	30	10	30	30	27					201
Zhigansk	CNRS/CAO	67N	123E	24	19	26	24	8	28	17	22					168
Salekhard	CNRS/CAO	67N	67E	31	28	31	30	10	5	10	31					176
Harestua	BIRA.IASB	60N	11E	31	27	31	29	23	16	29						186
Bremen	IUP/IFE	53N	9E	26	27	31	30	22	28	27						191
Jungfraujoch	BIRA.IASB	47N	8E	31	28	30	30	31	10	20						180
OHP	CNRS	44N	6E	31	28	31	30	10	30	31	31					222
Izaña	INTA	28N	16W	31	25	25	17	20	23	24						165
St Denis	CNRS	21S	55E	31	28	31	27	10	30	28	31					216
Bauru	CNRS/UNESP	22S	49W	31	27	30	28	10	30	30	31					217
Lauder	NIWA	45S	170E	31	28	31	30	31	30	31						212
Kerguelen	CNRS	49S	70E	31	27	31	30	9	30	31	31					220
Rio Gallegos	CNRS	52S	69W	18	18	30	30	10	26	28	26					186
Macquarie	NIWA	54S	159E	31	28	31	30	30	30	29						209
Ushuaia	INTA	55S	68W	30	24	30	29	31	28	31						203
Marambio	INTA	64S	57W	31	23	31	30	25	30	31						201
Dumont d'Urville	CNRS	67S	140E	23	24	31	30	10	30	29	31					208
Rothera	BAS	68S	68W	14	0	0	0	0	0	0						14
Dome Concorde	CNRS	75S	123E	31	27	31	28	8	0	3	24					152
Arrival Heights	NIWA	78S	167E	0	12	31	22	0	0	0						65
Belgrano	INTA	78S	35W	0	17	31	25	0	0	0						73

V.4 Monthly Data Distribution for NO_2 Profile Data

2006

FTIR	Inst.	Lat	Long	J	F	M	A	M	J	J	A	S	O	N	D	#
Kiruna	FZK/IMK	68N	21E	0	0	0	0	0	0	0	0	6	6	4	0	16
Izaña	FZK	28N	16W	4	5	14	7	8	17	14	13	13	10	11	10	126

2007

FTIR	Inst.	Lat	Long	J	F	M	A	M	J	J	A	S	O	N	D	#
Kiruna	FZK/IMK	68N	21E	3	7	15	11	9	4	6	9	8	9	3	0	84
Izaña	FZK	28N	16W	10	13	5	12	12	10	16	18	10	8	3	9	126

2008

FTIR	Inst.	Lat	Long	J	F	M	A	M	J	J	A	S	O	N	D	#
Kiruna	FZK/IMK	68N	21E	1	4	9	7	1	1	9	2	7	4	5	0	50
Izaña	FZK	28N	16W	6	3	9	6	5	7	11	5	8	4	2	5	71

2009

FTIR	Inst.	Lat	Long	J	F	M	A	M	J	J	A	S	O	N	D	#
Kiruna	FZK/IMK	68N	21E	0	10	7	1	0	0	0	0	0	0	0	0	18
Izaña	FZK	28N	16W	9	4	8	15	12	8	0	0	0	0	0	0	56

V.5 Monthly Data Distribution for BrO Column Data

2006

UV-Vis DOAS	Inst.	Lat	Long	J	F	M	A	M	J	J	A	S	O	N	D	#
Harestua	BIRA.IASB	60N	11E	20	24	31	30	30	29	30	31	30	31	29	31	346

2007

UV-Vis DOAS	Inst.	Lat	Long	J	F	M	A	M	J	J	A	S	O	N	D	#
Harestua	BIRA.IASB	60N	11E	31	28	31	30	31	30	30	31	25	21	2	0	290

2008

UV-Vis DOAS	Inst.	Lat	Long	J	F	M	A	M	J	J	A	S	O	N	D	#
Harestua	BIRA.IASB	60N	11E	1	10	29	30	27	30	31	30	28	26	24	28	294

2009

UV-Vis DOAS	Inst.	Lat	Long	J	F	M	A	M	J	J	A	S	O	N	D	#
Harestua	BIRA.IASB	60N	11E	20	27	29	29	28	21	28	24	24	19	22	31	302

2010

UV-Vis DOAS	Inst.	Lat	Long	J	F	M	A	M	J	J	A	S	O	N	D	#
Harestua	BIRA.IASB	60N	11E	28	26	31	30	23	10	28						176

V.6 Monthly Data Distribution for OClO Column Data

2006

UV-Vis DOAS	Inst.	Lat	Long	J	F	M	A	M	J	J	A	S	O	N	D	#
Harestua	BIRA.IASB	60N	11E	17	24	31	30	0	0	0	0	0	0	28	31	161

2007

UV-Vis DOAS	Inst.	Lat	Long	J	F	M	A	M	J	J	A	S	O	N	D	#
Harestua	BIRA.IASB	60N	11E	27	28	31	30	0	0	0	0	0	0	1	0	117

2008

UV-Vis DOAS	Inst.	Lat	Long	J	F	M	A	M	J	J	A	S	O	N	D	#
Harestua	BIRA.IASB	60N	11E	0	0	28	28	0	0	0	0	0	0	24	25	105

2009

UV-Vis DOAS	Inst.	Lat	Long	J	F	M	A	M	J	J	A	S	O	N	D	#
Harestua	BIRA.IASB	60N	11E	19	27	29	29	0	0	0	0	0	0	22	30	156

2010

UV-Vis DOAS	Inst.	Lat	Long	J	F	M	A	M	J	J	A	S	O	N	D	#
Harestua	BIRA.IASB	60N	11E	17	23	31	29	0	0	0						100

V.7 Monthly Data Distribution for CO Column Data

2006

FTIR	Inst.	Lat	Long	J	F	M	A	M	J	J	A	S	O	N	D	#
Ny-Ålesund	IUP/IFE	79N	12E	0	0	2	3	5	3	2	0	0	0	0	0	15
Kiruna	FZK/IMK	68N	21E	0	8	13	5	6	9	4	11	4	5	4	0	69
St Petersburg	SPBSU	60N	31E	6	10	14	4	2	11	10	4	9	0	0	0	70
Zvenigorod	SPBSU	55N	36E	4	9	13	10	10	13	10	8	2	0	1	0	80
Bremen	IUP/IFE	53N	9E	2	2	3	3	6	5	7	3	9	5	1	1	47
Jungfraujoch	ULg-GIRPAS	47N	8E	7	9	1	8	5	10	18	4	6	6	7	6	87
Izaña	FZK	28N	16W	4	5	13	7	8	17	14	13	12	9	11	10	123
Lauder	NIWA	45S	170E	6	11	4	9	11	8	4	11	7	10	5	4	90
Arrival Heights	NIWA	78S	167E	10	3	3	2	0	0	0	0	2	7	6	0	33

2007

FTIR	Inst.	Lat	Long	J	F	M	A	M	J	J	A	S	O	N	D	#
Ny-Ålesund	IUP/IFE	79N	12E	0	0	2	0	8	6	5	4	4	0	0	0	29
Kiruna	FZK/IMK	68N	21E	0	6	14	7	7	3	4	7	6	4	2	0	60
St Petersburg	SPBSU	60N	31E	4	11	6	11	10	14	8	7	7	2	1	2	83
Zvenigorod	SPBSU	55N	36E	1	10	8	8	11	12	8	16	13	1	0	0	88
Bremen	IUP/IFE	53N	9E	2	1	7	9	2	2	2	4	1	2	3	1	36
Jungfraujoch	ULg-GIRPAS	47N	8E	3	0	9	13	8	0	12	7	18	8	10	6	94
Izaña	FZK	28N	16W	10	14	5	12	12	10	16	16	10	8	3	9	125
Lauder	NIWA	45S	170E	4	4	9	4	9	7	8	10	10	8	7	3	83
Arrival Heights	NIWA	78S	167E	4	3	4	2	0	0	0	0	6	10	1	8	38

2008

FTIR	Inst.	Lat	Long	J	F	M	A	M	J	J	A	S	O	N	D	#
Ny-Ålesund	IUP/IFE	79N	12E	0	0	3	8	3	3	4	5	4	0	0	0	30
Kiruna	FZK/IMK	68N	21E	1	3	8	6	1	1	9	1	6	2	6	0	44
St Petersburg	SPBSU	60N	31E	5	3	3	0	0	0	0	0	0	0	0	0	11
Bremen	IUP/IFE	53N	9E	1	4	2	7	6	2	2	0	1	0	1	1	27
Jungfraujoch	ULg-GIRPAS	47N	8E	11	13	0	3	8	14	12	3	15	8	3	6	96
Izaña	FZK	28N	16W	6	3	10	6	5	7	11	5	8	4	3	5	73
Lauder	NIWA	45S	170E	8	5	5	9	7	7	7	5	5	6	3	2	69
Arrival Heights	NIWA	78S	167E	7	4	1	1	0	0	0	0	5	0	0	5	23

2009

FTIR	Inst.	Lat	Long	J	F	M	A	M	J	J	A	S	O	N	D	#
Ny-Ålesund	IUP/IFE	79N	12E	0	0	4	9	6	6	8	3	4	0	0	0	40
Kiruna	FZK/IMK	68N	21E	0	5	7	0	0	0	0	0	0	0	0	0	12
Bremen	IUP/IFE	53N	9E	0	0	1	2	6	4	1	5	5	0	0	0	24
Jungfraujoch	ULg-GIRPAS	47N	8E	12	6	5	8	10	9	12	21	10	13	4	6	116
Izaña	FZK	28N	16W	9	4	8	16	12	7	0	0	0	0	0	0	56
Lauder	NIWA	45S	170E	0	2	2	4	6	9	3	9	8	9	5	1	58
Arrival Heights	NIWA	78S	167E	12	3	4	1	0	0	0	0	7	12	12	7	58

2010

FTIR	Inst.	Lat	Long	J	F	M	A	M	J	J	A	S	O	N	D	#
Ny-Ålesund	IUP/IFE	79N	12E	0	0	3	9	3	2	3						20
Bremen	IUP/IFE	53N	9E	1	2	6	9	2	7	4						31
Jungfraujoch	ULg-GIRPAS	47N	8E	9	2	6	11	6	14	0						48
Lauder	NIWA	45S	170E	3	3	3	7	7	5	4						32
Arrival Heights	NIWA	78S	167E	6	7	4	0	0	0	0						17

V.8 Monthly Data Distribution for CO Profile Data

2006

FTIR	Inst.	Lat	Long	J	F	M	A	M	J	J	A	S	O	N	D	#
Kiruna	FZK/IMK	68N	21E	0	8	13	5	6	9	4	11	4	5	4	0	69
Jungfraujoch	ULg-GIRPAS	47N	8E	7	9	1	8	5	10	18	4	6	6	7	6	87
Izaña	FZK	28N	16W	4	5	13	7	8	17	14	13	12	9	11	10	123

2007

FTIR	Inst.	Lat	Long	J	F	M	A	M	J	J	A	S	O	N	D	#
Kiruna	FZK/IMK	68N	21E	0	6	14	7	7	3	4	7	6	4	2	0	60
Jungfraujoch	ULg-GIRPAS	47N	8E	3	0	9	13	8	0	12	7	18	8	10	6	94
Izaña	FZK	28N	16W	10	14	5	12	12	10	16	16	10	8	3	9	125

2008

FTIR	Inst.	Lat	Long	J	F	M	A	M	J	J	A	S	O	N	D	#
Kiruna	FZK/IMK	68N	21E	1	3	8	6	1	1	9	1	6	2	6	0	44
Jungfraujoch	ULg-GIRPAS	47N	8E	11	13	0	3	8	14	12	3	15	8	3	6	96
Izaña	FZK	28N	16W	6	3	10	6	5	7	11	5	8	4	3	5	73

2009

FTIR	Inst.	Lat	Long	J	F	M	A	M	J	J	A	S	O	N	D	#
Kiruna	FZK/IMK	68N	21E	0	5	7	0	0	0	0	0	0	0	0	0	12
Jungfraujoch	ULg-GIRPAS	47N	8E	12	6	5	8	10	9	12	21	10	13	4	6	116
Izaña	FZK	28N	16W	9	4	8	16	12	7	0	0	0	0	0	0	56

2010

FTIR	Inst.	Lat	Long	J	F	M	A	M	J	J	A	S	O	N	D	#
Jungfraujoch	ULg-GIRPAS	47N	8E	9	2	6	11	6	14	0						48

V.9 Monthly Data Distribution for CO_2 Column Data

2006

FTIR	Inst.	Lat	Long	J	F	M	A	M	J	J	A	S	O	N	D	#
Ny-Ålesund	IUP/IFE	79N	12E	0	0	2	3	5	3	2	0	0	0	0	0	15

2007

FTIR	Inst.	Lat	Long	J	F	M	A	M	J	J	A	S	O	N	D	#
Ny-Ålesund	IUP/IFE	79N	12E	0	0	2	0	8	6	5	4	4	0	0	0	29

2008

FTIR	Inst.	Lat	Long	J	F	M	A	M	J	J	A	S	O	N	D	#
Ny-Ålesund	IUP/IFE	79N	12E	0	0	3	8	3	3	4	5	4	0	0	0	30

2009

FTIR	Inst.	Lat	Long	J	F	M	A	M	J	J	A	S	O	N	D	#
Ny-Ålesund	IUP/IFE	79N	12E	0	0	4	9	6	6	8	1	0	0	0	0	34

V.10 Monthly Data Distribution for CH_4 Column Data

2006

FTIR	Inst.	Lat	Long	J	F	M	A	M	J	J	A	S	O	N	D	#
Ny-Ålesund	IUP/IFE	79N	12E	0	0	2	3	5	3	2	0	0	0	0	0	15
Kiruna	FZK/IMK	68N	21E	0	8	14	7	8	10	7	13	6	6	4	0	83
St Petersburg	SPBSU	60N	31E	4	7	12	6	3	12	15	8	13	1	0	0	81
Zvenigorod	SPBSU	55N	36E	3	8	9	2	1	6	4	4	1	0	0	0	38
Bremen	IUP/IFE	53N	9E	2	2	3	5	6	6	7	3	9	4	1	1	49
Jungfraujoch	ULg-GIRPAS	47N	8E	11	10	1	7	6	10	18	4	6	6	8	6	93
Izaña	FZK	28N	16W	4	5	14	7	8	17	14	13	13	10	11	10	126
Lauder	NIWA	45S	170E	6	8	4	7	8	1	2	10	7	10	5	3	71
Arrival Heights	NIWA	78S	167E	4	0	1	1	0	0	0	0	2	5	5	0	18

2007

FTIR	Inst.	Lat	Long	J	F	M	A	M	J	J	A	S	O	N	D	#
Ny-Ålesund	IUP/IFE	79N	12E	0	0	2	0	8	6	5	4	4	0	0	0	29
Kiruna	FZK/IMK	68N	21E	3	7	15	11	9	4	6	9	8	9	3	0	84
St Petersburg	SPBSU	60N	31E	5	13	8	8	12	16	6	9	7	2	0	2	88
Zvenigorod	SPBSU	55N	36E	1	8	7	5	11	5	4	12	11	2	0	0	66
Bremen	IUP/IFE	53N	9E	2	1	7	9	2	2	2	4	1	2	3	1	36
Jungfraujoch	ULg-GIRPAS	47N	8E	2	0	9	14	8	0	14	7	20	11	11	7	103
Izaña	FZK	28N	16W	10	13	5	12	12	10	16	18	10	8	3	9	126
Lauder	NIWA	45S	170E	5	4	9	3	2	4	7	10	10	10	9	9	82
Arrival Heights	NIWA	78S	167E	3	3	7	2	0	0	0	0	7	9	1	4	36

2008

FTIR	Inst.	Lat	Long	J	F	M	A	M	J	J	A	S	O	N	D	#
Ny-Ålesund	IUP/IFE	79N	12E	0	0	3	8	3	3	4	5	4	0	0	0	30
Kiruna	FZK/IMK	68N	21E	1	4	9	7	1	1	9	2	7	3	5	0	49
St Petersburg	SPBSU	60N	31E	5	3	3	0	0	0	0	0	0	0	0	0	11
Bremen	IUP/IFE	53N	9E	1	4	2	7	6	2	2	0	1	2	1	1	29
Jungfraujoch	ULg-GIRPAS	47N	8E	12	14	0	3	7	15	12	2	14	9	3	8	99
Izaña	FZK	28N	16W	6	3	9	6	5	7	11	5	8	4	3	5	72
Lauder	NIWA	45S	170E	12	8	9	10	6	6	7	3	6	7	8	5	87
Arrival Heights	NIWA	78S	167E	7	2	1	1	0	0	0	0	5	0	0	1	17

2009

FTIR	Inst.	Lat	Long	J	F	M	A	M	J	J	A	S	O	N	D	#

Ny-Ålesund	IUP/IFE	79N	12E	0	0	4	9	6	6	8	2	0	0	0	0	35
Kiruna	FZK/IMK	68N	21E	0	10	7	1	0	2	1	3	5	4	1	0	34
Bremen	IUP/IFE	53N	9E	0	0	1	2	8	4	3	5	5	0	0	0	28
Jungfraujoch	ULg-GIRPAS	47N	8E	12	7	5	10	13	11	13	9	11	14	4	8	117
Izaña	FZK	28N	16W	9	4	8	16	12	11	1	13	5	8	1	4	92
Lauder	NIWA	45S	170E	3	1	3	4	4	3	3	8	7	7	9	3	55
Arrival Heights	NIWA	78S	167E	10	5	8	1	0	0	0	0	5	11	8	5	53

2010

FTIR	Inst.	Lat	Long	J	F	M	A	M	J	J	A	S	O	N	D	#
Ny-Ålesund	IUP/IFE	79N	12E	0	0	0	0	2	1	1						4
Bremen	IUP/IFE	53N	9E	1	2	6	9	2	7	4						31
Jungfraujoch	ULg-GIRPAS	47N	8E	10	8	8	12	0	0	0						38
Lauder	NIWA	45S	170E	5	7	5	6	5	4	4						36
Arrival Heights	NIWA	78S	167E	7	7	4	0	0	0	0						18

V.11 Monthly Data Distribution for CH_4 Profile Data

2006

FTIR	Inst.	Lat	Long	J	F	M	A	M	J	J	A	S	O	N	D	#
Kiruna	FZK/IMK	68N	21E	0	0	0	0	0	0	0	0	6	6	4	0	16
Jungfraujoch	ULg-GIRPAS	47N	8E	11	10	1	7	6	10	18	4	6	6	8	6	93
Izaña	FZK	28N	16W	4	5	14	7	8	17	14	13	13	10	11	10	126
Lauder	NIWA	45S	170E	6	8	4	7	8	1	2	10	7	10	5	3	71
Arrival Heights	NIWA	78S	167E	4	0	1	1	0	0	0	0	2	5	5	0	18

2007

FTIR	Inst.	Lat	Long	J	F	M	A	M	J	J	A	S	O	N	D	#
Kiruna	FZK/IMK	68N	21E	3	7	15	11	9	4	6	9	8	9	3	0	84
Jungfraujoch	ULg-GIRPAS	47N	8E	2	0	9	14	8	0	14	7	20	11	11	7	103
Izaña	FZK	28N	16W	10	13	5	12	12	10	16	18	10	8	3	9	126
Lauder	NIWA	45S	170E	5	4	9	3	2	4	7	10	10	10	9	9	82
Arrival Heights	NIWA	78S	167E	3	3	7	2	0	0	0	0	7	9	1	4	36

2008

FTIR	Inst.	Lat	Long	J	F	M	A	M	J	J	A	S	O	N	D	#
Kiruna	FZK/IMK	68N	21E	1	4	9	7	1	1	9	2	7	3	5	0	49
Jungfraujoch	ULg-GIRPAS	47N	8E	12	14	0	3	7	15	12	2	14	9	3	8	99
Izaña	FZK	28N	16W	6	3	9	6	5	7	11	5	8	4	3	5	72
Lauder	NIWA	45S	170E	12	8	9	10	6	6	7	3	6	7	8	5	87
Arrival Heights	NIWA	78S	167E	7	2	1	1	0	0	0	0	5	0	0	1	17

2009

FTIR	Inst.	Lat	Long	J	F	M	A	M	J	J	A	S	O	N	D	#
Kiruna	FZK/IMK	68N	21E	0	10	7	1	0	2	1	3	5	4	1	0	34
Jungfraujoch	ULg-GIRPAS	47N	8E	12	7	5	10	13	11	13	9	11	14	4	8	117
Izaña	FZK	28N	16W	9	4	8	16	12	11	1	13	5	8	1	4	92
Lauder	NIWA	45S	170E	3	1	3	4	4	3	3	8	7	7	9	3	55
Arrival Heights	NIWA	78S	167E	10	5	8	1	0	0	0	0	5	11	8	5	53

2010

FTIR	Inst.	Lat	Long	J	F	M	A	M	J	J	A	S	O	N	D	#
Jungfraujoch	ULg-GIRPAS	47N	8E	10	8	8	12	0	0	0						38
Lauder	NIWA	45S	170E	5	7	5	6	5	4	4						36
Arrival Heights	NIWA	78S	167E	7	7	4	0	0	0	0						18

V.12 Monthly Data Distribution for HCl Column Data

2006

FTIR	Inst.	Lat	Long	J	F	M	A	M	J	J	A	S	O	N	D	#
Bremen	IUP/IFE	53N	9E	2	2	3	5	6	6	7	3	9	4	1	1	49
Lauder	NIWA	45S	170E	7	14	4	7	10	8	3	10	7	10	7	4	91
Arrival Heights	NIWA	78S	167E	9	3	4	2	0	0	0	0	2	7	6	0	33

2007

FTIR	Inst.	Lat	Long	J	F	M	A	M	J	J	A	S	O	N	D	#
Bremen	IUP/IFE	53N	9E	2	1	7	9	2	0	0	0	0	0	0	0	21
Lauder	NIWA	45S	170E	5	4	10	4	6	6	8	10	10	10	8	10	91
Arrival Heights	NIWA	78S	167E	4	2	7	2	0	0	0	0	7	8	1	6	37

2008

FTIR	Inst.	Lat	Long	J	F	M	A	M	J	J	A	S	O	N	D	#
Lauder	NIWA	45S	170E	10	8	9	9	7	6	7	4	6	8	9	4	87
Arrival Heights	NIWA	78S	167E	6	4	2	1	0	0	0	0	5	0	0	5	23

2009

FTIR	Inst.	Lat	Long	J	F	M	A	M	J	J	A	S	O	N	D	#
Lauder	NIWA	45S	170E	4	3	2	4	5	8	3	8	7	7	9	3	63
Arrival Heights	NIWA	78S	167E	12	5	9	0	0	0	0	0	6	10	8	8	58

2010

FTIR	Inst.	Lat	Long	J	F	M	A	M	J	J	A	S	O	N	D	#
Lauder	NIWA	45S	170E	5	7	5	5	4	4	3						33
Arrival Heights	NIWA	78S	167E	6	7	4	0	0	0	0						17

V.13 Monthly Data Distribution for HNO_3 Column Data

2006

FTIR	Inst.	Lat	Long	J	F	M	A	M	J	J	A	S	O	N	D	#
Ny-Ålesund	IUP/IFE	79N	12E	0	0	2	3	5	0	1	0	0	0	0	0	11
Kiruna	FZK/IMK	68N	21E	0	9	13	7	10	12	6	13	6	7	5	0	88
Bremen	IUP/IFE	53N	9E	2	2	3	3	6	5	6	3	9	3	0	1	43
Jungfraujoch	ULg-GIRPAS	47N	8E	11	10	1	8	5	10	17	4	6	6	8	8	94
Izaña	FZK	28N	16W	4	5	14	7	9	17	14	14	13	11	11	10	129
Lauder	NIWA	45S	170E	5	8	4	9	10	9	8	10	5	11	7	5	91
Arrival Heights	NIWA	78S	167E	9	3	3	0	0	0	0	0	0	7	6	0	28

2007

FTIR	Inst.	Lat	Long	J	F	M	A	M	J	J	A	S	O	N	D	#
Ny-Ålesund	IUP/IFE	79N	12E	0	0	1	0	7	5	3	2	3	0	0	0	21
Kiruna	FZK/IMK	68N	21E	4	9	16	11	7	0	1	11	9	11	3	0	82
Bremen	IUP/IFE	53N	9E	1	1	7	6	4	2	4	2	2	1	3	1	34
Jungfraujoch	ULg-GIRPAS	47N	8E	3	0	9	13	8	0	14	7	20	11	10	7	102
Izaña	FZK	28N	16W	10	14	5	12	12	10	16	20	10	8	3	10	130
Lauder	NIWA	45S	170E	4	5	7	4	7	10	10	11	9	8	6	7	88
Arrival Heights	NIWA	78S	167E	5	3	9	2	0	0	0	0	4	10	1	9	43

2008

FTIR	Inst.	Lat	Long	J	F	M	A	M	J	J	A	S	O	N	D	#
Ny-Ålesund	IUP/IFE	79N	12E	0	0	3	6	0	0	2	2	2	0	0	0	15
Kiruna	FZK/IMK	68N	21E	2	5	9	9	1	1	9	2	7	4	6	0	55
Bremen	IUP/IFE	53N	9E	1	4	0	1	0	0	2	0	0	0	1	0	9
Jungfraujoch	ULg-GIRPAS	47N	8E	12	14	0	3	8	15	12	3	15	9	4	8	103
Izaña	FZK	28N	16W	6	3	10	6	5	7	11	5	8	4	3	5	73
Lauder	NIWA	45S	170E	9	5	5	10	7	9	8	7	5	5	5	4	79
Arrival Heights	NIWA	78S	167E	6	4	5	1	0	0	0	0	3	0	0	8	27

2009

FTIR	Inst.	Lat	Long	J	F	M	A	M	J	J	A	S	O	N	D	#
Ny-Ålesund	IUP/IFE	79N	12E	0	0	3	7	5	6	6	2	3	0	0	0	32
Kiruna	FZK/IMK	68N	21E	0	10	8	1	1	2	1	4	6	4	1	0	38
Bremen	IUP/IFE	53N	9E	0	0	0	1	5	4	1	3	3	0	0	0	17
Jungfraujoch	ULg-GIRPAS	47N	8E	13	6	9	10	10	9	13	22	11	14	4	6	127
Izaña	FZK	28N	16W	9	4	9	16	12	12	1	14	5	8	1	3	94
Lauder	NIWA	45S	170E	3	2	3	5	6	11	4	9	10	6	6	2	67
Arrival Heights	NIWA	78S	167E	11	5	11	2	0	0	0	0	4	13	12	8	66

2010

FTIR	Inst.	Lat	Long	J	F	M	A	M	J	J	A	S	O	N	D	#
Ny-Ålesund	IUP/IFE	79N	12E	0	0	3	9	3	2	2						19
Bremen	IUP/IFE	53N	9E	1	1	5	10	2	6	4						29
Jungfraujoch	ULg-GIRPAS	47N	8E	8	6	7	12	6	14	0						53
Lauder	NIWA	45S	170E	6	4	3	6	6	3	4						32
Arrival Heights	NIWA	78S	167E	7	7	4	0	0	0	0						18

V.14 Monthly Data Distribution for HNO_3 Profile Data

2006

FTIR	Inst.	Lat	Long	J	F	M	A	M	J	J	A	S	O	N	D	#
Jungfraujoch	ULg-GIRPAS	47N	8E	11	10	1	8	5	10	17	4	6	6	8	8	94

2007

FTIR	Inst.	Lat	Long	J	F	M	A	M	J	J	A	S	O	N	D	#
Jungfraujoch	ULg-GIRPAS	47N	8E	3	0	9	13	8	0	14	7	20	11	10	7	102

2008

FTIR	Inst.	Lat	Long	J	F	M	A	M	J	J	A	S	O	N	D	#
Kiruna	FZK/IMK	68N	21E	2	5	9	9	1	1	9	2	7	4	6	0	55
Jungfraujoch	ULg-GIRPAS	47N	8E	12	14	0	3	8	15	12	3	15	9	4	8	103
Izaña	FZK	28N	16W	6	3	10	6	5	7	11	5	8	4	3	5	73

2009

FTIR	Inst.	Lat	Long	J	F	M	A	M	J	J	A	S	O	N	D	#
Kiruna	FZK/IMK	68N	21E	0	10	8	1	1	2	1	4	6	4	1	0	38
Jungfraujoch	ULg-GIRPAS	47N	8E	13	6	9	10	10	9	13	22	11	14	4	6	127
Izaña	FZK	28N	16W	9	4	9	16	12	12	1	14	5	8	1	3	94

2010

FTIR	Inst.	Lat	Long	J	F	M	A	M	J	J	A	S	O	N	D	#
Jungfraujoch	ULg-GIRPAS	47N	8E	8	6	7	12	6	14	0						53

V.15 Monthly Data Distribution for N_2O Column Data

2006

FTIR	Inst.	Lat	Long	J	F	M	A	M	J	J	A	S	O	N	D	#
Ny-Ålesund	IUP/IFE	79N	12E	0	0	2	3	5	0	1	0	0	0	0	0	11
Kiruna	FZK/IMK	68N	21E	0	8	14	7	8	10	7	13	6	6	4	0	83
Bremen	IUP/IFE	53N	9E	2	2	3	5	6	6	7	3	9	5	1	1	50
Jungfraujoch	ULg-GIRPAS	47N	8E	9	9	1	7	6	10	15	4	6	6	7	6	86
Izaña	FZK	28N	16W	4	5	14	7	8	17	14	13	13	10	11	10	126
Lauder	NIWA	45S	170E	6	12	4	7	8	0	2	9	7	10	5	3	73
Arrival Heights	NIWA	78S	167E	4	1	1	1	0	0	0	0	1	2	2	0	12

2007

FTIR	Inst.	Lat	Long	J	F	M	A	M	J	J	A	S	O	N	D	#
Ny-Ålesund	IUP/IFE	79N	12E	0	0	1	0	7	6	4	3	4	0	0	0	25
Kiruna	FZK/IMK	68N	21E	3	7	15	11	9	4	6	9	8	9	3	0	84
Bremen	IUP/IFE	53N	9E	2	1	7	9	2	2	2	4	1	2	3	1	36
Jungfraujoch	ULg-GIRPAS	47N	8E	2	0	9	13	8	0	14	7	19	11	11	6	100
Izaña	FZK	28N	16W	10	13	5	12	12	10	16	18	10	8	3	9	126
Lauder	NIWA	45S	170E	5	4	7	3	2	2	2	6	9	9	9	9	67
Arrival Heights	NIWA	78S	167E	5	3	7	2	0	0	0	0	1	7	1	4	30

2008

FTIR	Inst.	Lat	Long	J	F	M	A	M	J	J	A	S	O	N	D	#
Ny-Ålesund	IUP/IFE	79N	12E	0	0	3	6	0	0	2	4	3	0	0	0	18
Kiruna	FZK/IMK	68N	21E	1	4	9	7	1	1	9	2	7	4	5	0	50
Bremen	IUP/IFE	53N	9E	1	4	2	7	6	2	2	0	1	2	1	1	29
Jungfraujoch	ULg-GIRPAS	47N	8E	12	13	0	3	7	15	12	2	14	8	4	8	98
Izaña	FZK	28N	16W	6	3	9	6	5	7	11	5	8	4	3	5	72
Lauder	NIWA	45S	170E	11	8	7	9	1	2	3	3	6	7	7	2	66
Arrival Heights	NIWA	78S	167E	7	2	1	1	0	0	0	0	4	0	0	4	19

2009

FTIR	Inst.	Lat	Long	J	F	M	A	M	J	J	A	S	O	N	D	#
Ny-Ålesund	IUP/IFE	79N	12E	0	0	3	8	5	6	7	3	4	0	0	0	36
Kiruna	FZK/IMK	68N	21E	0	10	7	1	0	2	1	3	5	4	1	0	34
Bremen	IUP/IFE	53N	9E	0	0	1	2	8	4	3	5	5	0	0	0	28
Jungfraujoch	ULg-GIRPAS	47N	8E	12	6	10	10	11	10	13	9	9	14	4	8	116
Izaña	FZK	28N	16W	9	4	8	16	12	12	1	13	5	8	1	4	93
Lauder	NIWA	45S	170E	3	1	0	2	0	0	0	8	7	7	9	3	40
Arrival Heights	NIWA	78S	167E	12	5	8	0	0	0	0	0	1	5	5	8	44

2010

FTIR	Inst.	Lat	Long	J	F	M	A	M	J	J	A	S	O	N	D	#
Ny-Ålesund	IUP/IFE	79N	12E	0	0	4	9	4	2	4						23
Bremen	IUP/IFE	53N	9E	1	2	6	9	2	7	4						31
Jungfraujoch	ULg-GIRPAS	47N	8E	8	8	7	12	0	0	0						35
Lauder	NIWA	45S	170E	5	7	5	6	5	4	4						36
Arrival Heights	NIWA	78S	167E	7	7	4	0	0	0	0						18

V.16 Monthly Data Distribution for N_2O Profile Data

2006

FTIR	Inst.	Lat	Long	J	F	M	A	M	J	J	A	S	O	N	D	#
Kiruna	FZK/IMK	68N	21E	0	0	0	0	0	0	0	0	6	6	4	0	16
Jungfraujoch	ULg-GIRPAS	47N	8E	9	9	1	7	6	10	15	4	6	6	7	6	86
Izaña	FZK	28N	16W	4	5	14	7	8	17	14	13	13	10	11	10	126
Lauder	NIWA	45S	170E	6	12	4	7	8	0	2	9	7	10	5	3	73
Arrival Heights	NIWA	78S	167E	4	1	1	1	0	0	0	0	1	2	2	0	12

2007

FTIR	Inst.	Lat	Long	J	F	M	A	M	J	J	A	S	O	N	D	#
Kiruna	FZK/IMK	68N	21E	3	7	15	11	9	4	6	9	8	9	3	0	84
Jungfraujoch	ULg-GIRPAS	47N	8E	2	0	9	13	8	0	14	7	19	11	11	6	100
Izaña	FZK	28N	16W	10	13	5	12	12	10	16	18	10	8	3	9	126
Lauder	NIWA	45S	170E	5	4	7	3	2	2	2	6	9	9	9	9	67
Arrival Heights	NIWA	78S	167E	5	3	7	2	0	0	0	0	1	7	1	4	30

2008

FTIR	Inst.	Lat	Long	J	F	M	A	M	J	J	A	S	O	N	D	#
Kiruna	FZK/IMK	68N	21E	1	4	9	7	1	1	9	2	7	4	5	0	50
Jungfraujoch	ULg-GIRPAS	47N	8E	12	13	0	3	7	15	12	2	14	8	4	8	98
Izaña	FZK	28N	16W	6	3	9	6	5	7	11	5	8	4	3	5	72
Lauder	NIWA	45S	170E	11	8	7	9	1	2	3	3	6	7	7	2	66
Arrival Heights	NIWA	78S	167E	7	2	1	1	0	0	0	0	4	0	0	4	19

2009

FTIR	Inst.	Lat	Long	J	F	M	A	M	J	J	A	S	O	N	D	#
Kiruna	FZK/IMK	68N	21E	0	10	7	1	0	2	1	3	5	4	1	0	34
Jungfraujoch	ULg-GIRPAS	47N	8E	12	6	10	10	11	10	13	9	9	14	4	8	116
Izaña	FZK	28N	16W	9	4	8	16	12	12	1	13	5	8	1	4	93
Lauder	NIWA	45S	170E	3	1	0	2	0	0	0	8	7	7	9	3	40
Arrival Heights	NIWA	78S	167E	12	5	8	0	0	0	0	0	1	5	5	8	44

2010

FTIR	Inst.	Lat	Long	J	F	M	A	M	J	J	A	S	O	N	D	#
Jungfraujoch	ULg-GIRPAS	47N	8E	8	8	7	12	0	0	0						35
Lauder	NIWA	45S	170E	5	7	5	6	5	4	4						36
Arrival Heights	NIWA	78S	167E	7	7	4	0	0	0	0						18

VI ANNEXE 3: GUIDELINES FOR VALIDATION METADATA

To ensure traceability of the validation process – a QA4EO requirement – we propose hereafter guidelines for validation metadata, that is, brief but unambiguous documentation of the validation process leading to a validation graph of a comparison data file. They are illustrated with an example text that could accompany any validation graph (attached to the graph as a readme.file.text) and any comparison data file (e.g. included in the file as a header or simply attached externally to the file). In a later stage, when GEOMS becomes available and operational, it might be interesting to extend it with a format for validation results.

VI.1 General information

The header should provide a short, high level description of the content of the related file or graph.

```
# ENVISAT SCIAMACHY VALIDATION STATISTICS
# VALIDATED DATA: LIMB OZONE VERTICAL PROFILE SGP5.01
# CORRELATIVE DATA: MCH OZONESONDE AT PAYERNE, SWITZERLAND
# VALIDATION ANALYSIS BY IASB-BIRA, BELGIUM
# LAST UPDATE: 29-Oct-2010 15:20:27
#
# This file contains ground-based validation results of Envisat SCIAMACHY limb ozone
# profile data retrieved with version 5.01 of the off-line processor SGP. The
# validation process is documented hereafter in the header. Monthly statistics of the
# percent relative difference between satellite and correlative observations are reported
# as a function of the vertical coordinate.
```

or

```
# This file accompanies graphs providing visualisation of ground-based validation
# results of Envisat SCIAMACHY limb ozone profile data retrieved with version 5.01
#  of the off-line processor SGP. The validation process is documented hereafter.
# The associated graph presents monthly statistics of the relative difference between satellite
# and correlative observations, plotted as a function of altitude and time.
```

VI.2 Traceability of satellite data

The metadata on satellite data should be a short description of the satellite data used to obtain the validation results. Without proper information on the producer/provider of the satellite data and the data processing version, validation results are not traceable and can not be trusted.

```
# SATELLITE OBSERVATIONS
# Data processing/archiving: D-PAC
# Data processor/version: SGP 5.01 Off-Line
# Data file name (optional; not relevant when a large number of data files are analysed)
# Retrieved parameter: ozone number density (molec.cm-3)
# Vertical coordinate: altitude (km)
```

VI.3 Traceability of correlative data

The metadata on correlative data should be a short, unambiguous description of the correlative measurements used to obtain the validation results. Accurate information on the data calibration/processing version and the data archiving centre is particularly crucial.

```
# CORRELATIVE OBSERVATIONS
# Station: Payerne / Switzerland / 46.82N / 6.95E / 491m asl
# Instrument: ECC ozonesonde
# Resp. institute: MCH
# Data archiving: Envisat Cal/Val
# Data processor/version: WMO/GAW Standard Operation Procedure
```

Measured parameter: ozone partial pressure (mPa)
Vertical coordinate: pressure (hPa)/altitude (km)

VI.4 Traceability of correlative analysis process

The metadata on correlative analysis should be a short, unambiguous description of the comparison manipulations undertaken to obtain the validation results. From this information one should be able to check if the validation process complies with agreed standards and best practices. The step-by-step description of the data manipulations should also allow proper interpretation of the comparison results and further investigation of the satellite and correlative data quality.

CORRELATIVE ANALYSIS
Cal/Val system (if any): Multi-TASTE
Data filtering: none
(note: could be a filter on the error given in the data file, on the GOMOS star magnitude etc.)
Conversion of units: none (e.g., from VMR to number density)
Time span: 2002-2009
Temporal co-location: max. 12h difference
(or e.g. use of a photochemical model to account for diurnal cycle effects)
Vertical co-location: see vertical smoothing
(another possibility could be e.g. a cross-correlation of the profiles to reduce altitude pointing uncertainties)
Horizontal co-location: DOVP, max. 300km distance
Temporal smoothing: none
(e.g., correlative data averaged over a time window around the satellite overpass)
Vertical smoothing: ozonesonde data box-averaged at satellite resolution
(other possibilities: e.g., smoothed using the averaging kernels and a priori of the satellite retrieval)
Horizontal smoothing: none
Relative difference calculated as (SATELLITE - GROUND)/GROUND
Statistics: monthly mean/standard deviation and median/inter-percentile of the relative difference

VI.5 Format description of the validation results

The validation results contained in the related file or visualised in the related graph should be clearly described.

CONTENT OF THIS DATA FILE or INFORMATION DISPLAYED ON THIS GRAPH
Altitude (km, in column)
Month (in row)
Amount of comparison events by month and by altitude
Relative difference: median (%)
Relative difference: inter-percentile interval at 68% level (%)

VI.6 Credit (and responsibilities)

The metadata file should identify by whom the validation were produced and reported. Information on who to contact might be useful.

CREDIT
Analysis carried out at the Belgian Institute for Space Aeronomy (IASB-BIRA)
Validation scientists: D. Hubert and S. Vandenbussche
Data processing scientists: J. Granville and D. Pieroux
Contact: xxx@aeronomy.be

VII ANNEXE 4: ACRONYMS AND ABBREVIATIONS

BIRA-IASB	Belgian Institute for Space Aeronomy
CCI	Climate Change Initiative
CEOS	Committee on Earth Observation Satellites
CINDI	Cabauw Intercomparison Campaign of Nitrogen Dioxide measuring Instruments
CNRS	Centre National de la Recherche Scientifique
CSA	Canadian Space Agency
DOAS	Differential Optical Absorption Spectroscopy
DSCD	differential slant column density
EC	European Commission
ECV	Essential Climate Variable
Envisat	ESA's Environmental Satellite
ERS-2	ESA's Remote Sensing Satellite
EVDC	Envisat Validation Data Centre
FMI-ARC	Finnish Meteorological Institute - Arctic Research Centre
FP	Framework Programme
FTIR	Fourier Transform Infrared spectrometer
GAS	GMES Atmospheric Service
GAW	WMO's Global Atmosphere Watch
GECA	Generic Environment for Cal/Val Analysis
GEO	Group on Earth Observation
GEOSS	Global Earth Observation System of Systems
GMES	Global Monitoring of Environment and Security
GOMOS	Global Ozone Monitoring by Occultation of Stars
GOSAT	Greenhouse Gases Observing Satellite
HRTP	High Resolution Temperature Profile (GOMOS)
IFE	Institute of Environmental Physics
IMK/FZK	Institute for Meteorology and Climate Research/Forschungszentrum Karlsruhe
INSPIRE	EC Directive "Infrastructure for Spatial Information in the European Community"
INTA	Instituto Nacional de Técnica Aeroespacial
IP	Integrated Project
IPF	Instrument Processing Facility
JAXA	Japan Aerospace Exploration Agency
JRC	EC Joint Research Centre
LATMOS	Laboratoire Atmosphères, Milieux, Observations Spatiales
MACC	Monitoring Atmospheric Composition and Climate (EC FP7 IP)
MIPAS	Fourier transform spectrometer for the detection of limb emission spectra in the middle and upper atmosphere
NDACC	Network for the Detection of Atmospheric Composition Change
NDSC	Network for the Detection of Stratospheric Change
NIES	National Institute for Environmental Studies
NIR	Near InfraRed
NIWA	National Institute of Water and Atmospheric Research (New Zealand)
NR	Nominal Resolution (MIPAS)
PASODOBLE	Promote Air quality Services integrating Observations – Development Of Basic Localised Information for Europe
PROMOTE	PROtocol MOniToring for the GMES Service Element: Atmosphere
PTU	pressure/temperature/humidity sonde
QA4EO	Quality Assurance framework for Earth Observation
QWG	Quality Working Group
RR	Reduced Resolution (MIPAS)
SCD	Slant Column Density
SCIAMACHY	SCanning Imaging Absorption SpectroMeter for Atmospheric CartograpHY

SHADOZ	Southern Hemisphere Additional Ozonesondes
TANSO	Thermal ANd short wave infra-red Sensor for Observing greenhouse gases
ULg	Université de Liège
WaVaCS	Atmospheric Water Vapour in the Climate System (COST Action ES0604)
WMO	World Meteorological Organization
WOUDC	World Ozone and Ultraviolet Radiation Data Center

[end of document]